A Quantum Dot – Based Diagnostic Immunoassay for Biomarker Detection in Gastrointestinal Inflammatory Diseases

A Thesis

Submitted to the Faculty

of

Drexel University

By

David Richard Hansberry

in partial fulfillment of the

requirements for the degree

of

Doctor of Philosophy

August 2011

DEDICATIONS

This thesis is dedicated to the memory of my advisor, Elisabeth Papazoglou. She was truly an unbelievable teacher, mentor and an even better person. The lessons she has taught me extended well beyond the classroom and will be with me forever.

ACKNOWLEDGEMENTS

First of all I'd like to thank my advisor, Elisabeth Papazoglou, for without her, none of this would have been possible. When I joined her lab as a Ph.D. student I was always given the freedom, encouragement, and guidance to pursue my academic and professional goals. Dr. Papazoglou's tireless work effort, passion and unwavering commitment to her students was always evident. This has left a strong impression and much to aspire towards. I couldn't thank Dr. Papazoglou enough for all that she has taught me and will miss her greatly.

I also want to thank the other distinguished members of my thesis committee: Donald McEachron, Margaret Wheatley, Sree Murthy, and James Reynolds for their guidance through my Ph.D. studies. Their leadership qualities are impressive and certainly something to emulate. It's been a pleasure and privilege to work with them.

There are many students from Dr. Papazoglou's lab that have been extremely helpful throughout the course of my Ph.D. research. Perhaps none more so than fellow Ph.D. student Peter Clark who I had the opportunity to work alongside on the QLISA project. His efforts have been extraordinarily helpful in advancing much of this research. Additionally, I'd like to thank my fellow, past and present, lab members including Rosemary Bastian, Zhenyu Haung, Xiang Mao, Sakya Mohaparta, Mike Neidrauer, An Nguyen, Josh Samuels, Venkat Sundaram, Chetna Sunkari, Chengjie Yu. Each of these lab members has been more than willing to help me and I've absolutely appreciated it. I'd also like to thank Nanda Kanagarajan, Thomas Coyne and Scott Naples from the Department of Medicine for, among other things, facilitating the transfer of human samples. Optic expert, Lenoid Zubkov has been tremendously supportive and willing to share his knowledge on the QLISA project.

I'd also like to thank my parents, Brian and Denise, for their continued support in my academic, professional and personal pursuits. My brothers James, Timothy, Mark, and sister Jeanine, deserve a special thanks for all their unconditional support. A particular thanks to, my soon to be wife, Paige for her inspiration and encouragement. The other members of my family, as well as my friends, have also been extraordinarily supportive of my academic endeavors.

Also I would like to acknowledge my M.S. thesis advisors, Ari Brooks and Zach Forbes for laying the foundation for me to pursue my Ph.D. research. Additionally I'd like to thank Greg Kopia, who offered me an internship following my undergraduate education working with drug-eluting stents at

Cordis Corporation. My relationship with Cordis continued over parts of the next 4 years, and undoubtedly Dr. Kopia's encouragement influenced my pursuit of further graduate studies.

Additionally I'd like to acknowledge Drexel University and the School of Biomedical Engineering for providing a truly world class atmosphere to learn. Banu Onaral and the Biomed staff have made my Drexel experience a very rewarding one. The better part of the past 6 years I've spent here have been memorable and it is an honor to be awarded both M.S. and Ph.D. degrees from this institution.

TABLE OF CONTENTS

LIST OF TABLES

LIST OF FIGURES

ABSTRACT

A QUANTUM DOT – BASED DIAGNOSTIC IMMUNOASSAY FOR BIOMARKER DETECTION IN GASTROINTENSTINAL INFLAMMATORY DISEASES

David Richard Hansberry

Elisabeth S. Papazoglou, Ph.D.

Advances and integration in the fields of molecular biology, nanotechnology, bioanalytical chemistry, nanofluidics, and electrochemistry have paved the way for more sensitive, specific and robust biosensors with wide ranging applications from bioterrorism to clinical medicine. In this thesis, we optimize a novel, in-house developed poly(methyl methacrylate), microcapillary immunoassay known as QLISA, in an attempt to quantify fecal levels of myeloperoxidase and lactoferrin to aid in differentiating inflammatory bowel disease (ulcerative colitis and Crohn's disease) from irritable bowel syndrome. Noninvasive specimen collection and analysis to help physicians distinguish these two similarly presenting diseases would allow more rapid and appropriate treatment. Given the similar clinical presentations and drastically different treatments, there is the potential to improve quality patient care while reducing both direct and indirect associated cost through the elimination of unnecessary procedures and more efficient medical treatment.

Using a crosslinking strategy of branched, di-amino polyethylene glycol polymer and glutaraldehyde following wet chemical treatment with sodium hydroxide, we demonstrated significant increase in primary antibody capture on a PMMA substrate, as used in QLISA, over traditional passive adsorption methods typically used in commercial ELISA kits. This unique crosslinking approach provides potential for improved immunoassay performance and is not limited to QLISA or even PMMA-based biosensors. QLISA was validated against commercial ELISA kits when testing for myeloperoxidase and lactoferrin in human fecal samples of patients with an inflammatory bowel disease or healthy control. We found that myeloperoxidase levels were elevated from about 80 to over 12,000 times that of our healthy control patients. Similarly we found lactoferrin levels were elevated from about 265 to almost 9,000 times that of the control patients. Further analysis shows that levels of greater than 1ug/g of myeloperoxidase suggested inflammatory bowel disease – ulcerative colitis or Crohn's disease. This measure was 100% accurate in differentiating the two, however it couldn't differentiate between healthy control and the other inflammatory bowel diseases (ischemic colitis, infectious diarrhea, clostridium difficile) with a myeloperoxidase level below 1ug/g. Lactoferrin in healthy patients have extremely low levels in their stool (0.01ug/g), but a cutoff lactoferrin level is less obvious. Average lactoferrin concentrations for

inflammatory bowel disease (ulcerative colitis and Crohn's disease) and other inflammatory bowel disease (ischemic colitis, infectious diarrhea and clostridium difficile) patients are 28.91ug/g and 2.23ug/g, respectively. Neither myeloperoxidase or lactoferrin were capable of differentiating types of inflammatory bowel disease within this limited sample size. Results were encouraging and suggest the use of QLISA for myeloperoxidase and lactoferrin analysis to increase differential diagnosis when evaluating patients who may have inflammatory bowel disease. These diagnostic biomarkers can help provide an earlier diagnosis and allow quicker, appropriate treatment, potentially bypassing costly, discomforting diagnostic procedures that are time-consuming for both the patient and the physician.

CHAPTER 1: INTRODUCTION

1.1 BIOSENSORS AND BIOMARKERS BACKGROUND

Effective clinical medicine requires reliable diagnostic equipment to help physicians formulate accurate diagnoses to better treat patients. Medical device companies are investing significant resources to create next generation diagnostic equipment that enhances the accuracy and speed of physicians' diagnostic ability. This is especially true for biosensor development.

Biosensor development is a rapidly advancing field because of the wide-variety of biosensor platforms and applications. Advances and integration in the fields of molecular biology, nanotechnology, surface chemistry, fluidics, and electrochemistry are producing faster, more sensitive, and easier to use biosensors that have applications ranging from nanomedicine to bioterrorism (Mohanty & Kougianos, 2006). The versatility of biosensors allows developers to customize their design to meet the specific need of their application. The biosensor field is motivated to detect biomarkers rapidly and more accurately at significantly lower levels. In medicine, we are interested in determining biomarker levels to provide physicians with critical information that leads to

timely clinical decision making. Accuracy, speed, sensitivity and specificity are of paramount importance in medical biosensors.

Some well-known examples of medical biosensors include the early pregnancy test or a glucose monitoring device used by diabetics. Both exemplify how knowing the biomarker levels, human chorionic gonadtropin and glucose, respectively, give valuable information that the clinician (or patient) can then use to evaluate the patient (or themselves). Other biosensor applications include biomarker detection to help diagnose cancer pathologies. This situation demonstrates the need to detect low levels of biomarkers to help physicians make an earlier diagnosis to improve patient prognosis through earlier treatment. During a suspected myocardial infarction, it is routine for patients to have blood drawn to evaluate the level of several biomarkers, like C-reactive protein and troponins, which have diagnostic and prognostic value of a myocardial damage. Here it is important to have the ability to detect very low levels of biomarkers since sub-nanomolar increases of these biomarkers are indicative of myocardial damage. Additionally the results are needed immediately as diagnosis and treatment timeline become critical to these patients and can be life-saving. As alluded to above, biosensors are necessary to more than just helping diagnose earlier, but also in determining disease progression,

patient prognosis, and treatment efficacy. These are just a few of the many applications of biosensors that demonstrate a vital role in medicine. Not surprisingly the biosensor applications to medicine have implications in many other disease pathologies, including differentiating inflammatory bowel disease (IBD) from health patients, as we will discuss in this dissertation.

Biosensors are virtually meaningless if there are not appropriate biomarkers being detected with known significance. In other words, knowing that molecule A has a concentration X is not terribly useful if you don't know the significance of molecule A's concentration when at X. Therefore when using a biosensor, in medicine or other field, it is important to understand the biomarker's significance. To use the glucose monitor example discussed earlier, we can measure blood glucose levels and determine if the body is out of normal homeostatic range. Baseline fasting levels of blood glucose above 125mg/dL would indicate diabetes while below 50mg/dL would be considered hypoglycemic. The point of mention this example is to underline the importance of understanding the biomarkers that the biosensor is detecting. A branch of science is devoted solely to biomarkers and focuses on their discovery and validation using genomic and proteomic approaches such as gene expression, SAGE, DNA or tissue microarray technology, amongst others.

As briefly mentioned above, this dissertation will discuss differentiating irritable bowel syndrome and inflammatory bowel disease through biomarker detection using a novel biosensor. The next section will discuss the significance of these two gastrointestinal diseases and why this technology would translate into improved patient care.

1.2 GASTROINTESTINAL DISEASE

Despite the progress that has been made in biomarker detection technology, challenges remain for improved detection, screening and tailoring treatment of many intractable diseases. In the biomarker research continuum, important steps include identification of reproducible patterns of disease and response to therapy, capacity to distinguish between health and disease or differentiating diseases when they have overlapping symptoms, challenges in collection of specimens often minute in nature, and technology platforms that can accurately measure single or multiple markers (automated, rapid, reliable and reproducible). All of these challenges are inherent to many diseases including inflammatory bowel disease and irritable bowel syndrome.

1.2.1 Inflammatory Bowel Disease (IBD)

Inflammatory Bowel Disease refers to two chronic diseases of intestinal inflammation (ulcerative colitis (UC) and Crohn's disease (CD)) and it affects approximately 4 million people worldwide (1 million Americans), with estimated medical costs in the USA at over $2 billion/yr when adjusted for loss of productivity. There are other kinds of inflammatory bowel disease like ischemic colitis, infectious diarrhea, collagenous colitis and clostridium difficile. It is hard to diagnose ulcerative colitis from Crohn's disease and diagnosis requires medical history, blood tests, X-rays, endoscopy, tissue histopathology and testing of stool samples. Still, early detection is difficult and it represents a dilemma for physicians to manage these patients.

Ulcerative colitis affects the colon and presents in continuous inflammatory lesions involving the mucosa and superficial mucosa (not transmural). The disease begins in the rectum and travels proximally, but does not involve the small intestines. There are also crypt abscesses and ulcers, loss of haustra, and no granulomas. Gastrointestinal manifestations include generalized abdominal pain, bloody diarrhea, anorexia, weakness, fever if severe,

dehydration, abdominal bloating, and increased intestinal gas. Other manifestations of ulcerative colitis include primary sclerosing cholangitis, which can lead to liver disease and pyoderma gangrenosum that can progress to severe chronic wounds. The most serious complications are colon cancer, toxic megacolon, and malnutrition.

Crohn's disease is a distinct inflammatory bowel disease from ulcerative colitis that can affect any portion of the gastrointestinal tract, from mouth to anus. Unlike the continuous inflammatory pattern seen in ulcerative colitis, Crohn's disease presents with portions of diseased gastrointestinal tract with alternating normal portions in between; these are sometimes called skip lesions. Additionally there is granuloma formation, transmural inflammation with linear ulcers, fissures, and fistulas. Gastrointestinal symptoms are similar to ulcerative colitis and include generalized abdominal pain (colitis), right lower quadrant pain (enteritis), diarrhea (not necessarily bloody), anorexia, low fever, weight loss, dehydration, abdominal bloating, and increased intestinal gas. Complications from Crohn's disease include increased risk for colon cancer, strictures, fistulas, perianal disease, malabsorption, and nutritional depletion.

Neither ulcerative colitis nor Crohn's disease has a known etiology. There have been many hypotheses for their etiology, which include immune, microbe, environmental, and / or genetic factors. These are widely debated with scientific evidence supporting vary depending on the study.

Treatment strategies for both ulcerative colitis and Crohn's disease differ based on the severity and current activity of the disease. Generally speaking the goal of treatment is to induce remission of the inflammatory bowel disease and prevent reoccurrences. Some typical treatments include sulfasalazine, which is poorly absorbed in the intestine and consequently acts as an inflammatory drug; infliximab, a monoclonal antibody that targets tumor necrosis factor and frequently used in Crohn's disease treatment; colectomy, which is more effective for ulcerative colitis treatment; and corticosteroids to reduce inflammation. Other treatments include lifestyle modifications, particularly diet changes and smoking cessation as well as antibiotics.

There are other inflammatory bowel diseases like collagenous colitis and ischemic colitis. Although relatively less common than Crohn's or ulcerative colitis, they both can be very severe if untreated.

Collagenous colitis is a microscopic colitis that is caused by frequent watery diarrhea and is commonly seen in women. This disease typically presents normally on colonoscopies but does have elevated lymphocyte activity with characteristic histopathology. Prognosis is good and treatment may include anti-diarrheal and anti-inflammatory therapeutics.

Ischemic colitis can be separated into two varieties: occlusive and non-occlusive. Both result in inadequate blood reaching the large intestine. Occlusive refers to something like a thromboembolic event in the inferior mesentery artery or one of its branches, while non-occlusive may be caused by a hemodynamic instability. Regardless of the cause, ischemic colitis can be very severe. Although prognosis may be considered relatively good, the more severe cases of ischemic colitis can lead to complications resulting in death.

1.2.2 Irritable Bowel Syndrome (IBS)

Irritable bowel syndrome is also associated with abdominal pain or discomfort, altered bowel habits (diarrhea and/or constipation), but without an underlying structural disease. irritable bowel syndrome is a functional disorder of the gut with unclear or multiple etiologies and the syndrome is not commonly

associated with underlying gut inflammation. Patients typically have pain relief upon defecation, changes in stool frequency, and/or changes in the appearance of their stool. It affects a much larger population (10 – 15% prevalence) in most industrialized countries with a worldwide incidence of 1 – 2%. There is no cure for irritable bowel syndrome and treatment is aimed at alleviating symptoms.

To briefly summarize, irritable bowel syndrome is a distinct disease from inflammatory bowel disease despite overlapping clinical symptoms. The underlying differences in pathology lead to different treatment strategies which is critical for the patient. The next section further discusses these differences.

1.2.3 Current Diagnostics - IBD / IBS

Thus, because of symptoms common to both irritable bowel syndrome and inflammatory bowel disease, it is a major challenge for physicians to distinguish inflammatory bowel disease patients from irritable bowel syndrome. Consequently irritable bowel syndrome is a condition typically diagnosed by exclusion signs and symptoms using elaborate, time consuming and expensive laboratory, radiological and endoscopic tests.

Both populations of patients experience significant reduction in their quality of life. In 2004 alone there were approximately 3.1 million ambulatory care visits directly associated with both medical conditions (Everhart & Ruhl, 2009). The number of such patients is expected to increase annually. The prevalence is 2 to 4 times higher among women (Chang & Heitkemper, 2002). The estimate of prevalence for inflammatory bowel disease is between 1-1.5 million patients in the US. In the 7 major economic markets, the estimated inflammatory bowel disease / irritable bowel syndrome population is an astounding 90 million people. Though the prevalence and incidence of inflammatory bowel disease is lower, the morbidity associated with inflammatory bowel disease and the economic loss is far greater. Diagnosing and differentiating inflammatory bowel disease from irritable bowel syndrome at an early stage without recourse to invasive and expensive diagnostic procedures would help patients to avoid intrusive tests and would save millions of dollars in health care costs. The financial costs associated (direct and indirect), though it is a difficult undertaking, it is on excess of $200B annually in the US (McFarland, 2008). For Crohn's Disease alone in 2004, we estimated that approximately $512M was spent for the non-treatment aspects of the disease (i.e. office visits, endoscopy, lab, pathology and radiology (Kappelman et al., 2008). A recent

estimate of direct financial cost of irritable bowel syndrome in the US is around $30 billion dollars per year (Hulisz, 2004).

Treatment for both inflammatory bowel disease and irritable bowel syndrome is available, but there are no cures- only relief is lowering symptoms in irritable bowel syndrome (Mayer, 2008) or suppression of inflammatory response or maintaining remission in inflammatory bowel disease (Baumgart & Sandborn, 2007). Patients with inflammatory bowel disease are currently treated with costly biologics, like Remicade and Humira. On the contrary, patients with irritable bowel syndrome are in a heterogeneous group and have to be managed and treated very individually, i.e. irritable bowel syndrome patients are symptomatically treated. Most patients of inflammatory bowel disease and irritable bowel syndrome present themselves at the physician having endured symptoms for an extended period of time prior to the initial visit. Consequently, they have an increased probability of presenting with more established disease given the delays in seeking medical attention. We believe the faster a patient is correctly diagnosed, the quicker the correct treatment can be initiated especially in an intractable, chronic, debilitative disease such as inflammatory bowel disease. This will improve their health and save the health system from unnecessary expenses.

Therefore the QLISA technology we developed will be tested to illustrate its application for the differential diagnosis of these diseases and to detect biomarkers for disease diagnosis and therapeutic decision making. Due to lack of irritable bowel syndrome patients volunteering to provide stool samples during office visits, we were unable to test any irritable bowel syndrome patients at this time. This is of limited consequence since there is no theoretical reason for myeloperoxidase or lactoferrin levels to be increased in irritable bowel syndrome patients and scientific literature confirms this. However, future work for this project includes analysis of irritable bowel syndrome stool samples.

1.3 QLISA TECHNOLOGY

QLISA is an acronym for Quantum-dot Linked ImmunoSorbent Assay. It is an optical biosensor developed by a multidisciplinary team at Drexel University with the goal of having translational impact and improving patient care. QLISA has seen several modifications and improvements from the initial design and prototype (Babu, Mohapatra, Zubkov, Murthy, & Papazoglou, 2009). It continues to evolve as the team improves sensitivity, detection capabilities, and robustness.

In this section we describe QLISA and highlight the improvements from the first generation to more recent generations of QLISA. Subsequent Chapters will describe the methods and data that have substantiated these improvements. The main goal of this section is to provide readers with sufficient understanding of the QLISA technology.

QLISA is performed in a commercially available PMMA microcapillary (diameter of 250um) and is run as a sandwich-style immunoassay. First, the PMMA surface is activated to favorably increase crosslinking reactions for primary antibody immobilization. We have deployed several primary antibody immobilization strategies and describe these in detail in Chapter 2. Briefly though, for the first generation of QLISA, we used the zero-length crosslinker 1-ethyl-3-(3-dimethylaminopropyl) carbodiimide (EDC) with the stabilizer sulpho-N-hydroxysulfosuccinimide (sNHS) to covalently crosslink the primary antibody to the PMMA microcapillary surface. In the second generation QLISA system we use the homo-bifunctional crosslinkers di-amino polyethylene glycol and glutaraldehyde to immobilize the primary antibodies. Following primary antibody immobilization, irrespective of crosslinking strategy, we introduce our antigen to interact with its antibody. It is important to note that theoretically

QLISA is capable of detecting any protein as long as it has corresponding antibodies, although incubation times could be varied according to antigen-antibody kinetics. We have tested myeloperoxidase and lactoferrin with their corresponding immunoglobulin G antibodies. Subsequent to incubation of antigen we introduce a quantum dot conjugated secondary antibody. This is the final step prior to reading of the assay.

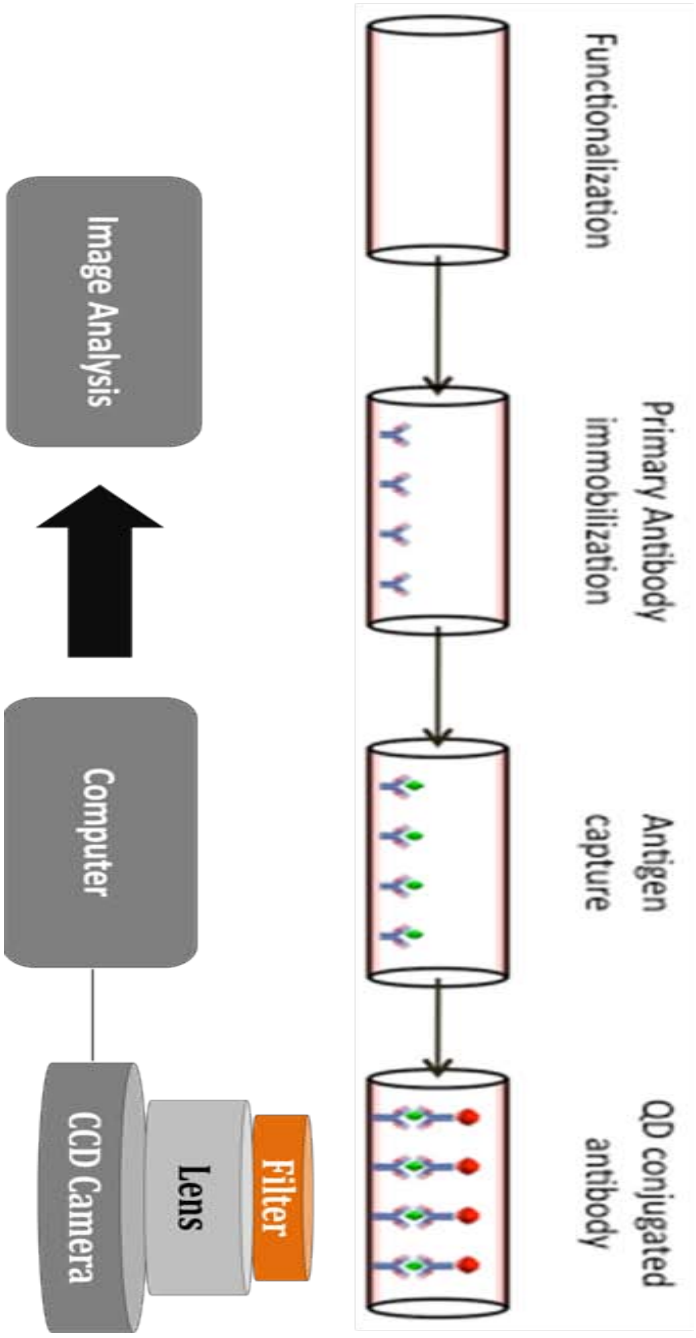

Figure 1: Overview of QLISA. Note the excitation of QD conjugated antibody with a LED is not shown to not over complicate the figure.

To quantify antigen concentration we detect the quantum dot conjugated secondary antibodies bound to antigen. Quantum dots are excited with light under a broad spectrum and have narrow emission spectra based on quantum dot size. QLISA excites the quantum dots with a light emitting diode (LED) with a wavelength of 385nm that has $1mm^2$ area with an intensity of $80mw/cm^2$. The fluorescent emission of the quantum dots is filtered and captured with charge-coupled device (CCD) camera (Stingray, AVT-FS-033B model). Still images captured with the CCD camera can then be processed with ImageJ software, available from the NIH. In Figure 1 we provide a step-by-step schematic of QLISA. Note that the LED is not shown in Figure 1, but is shown in subsequent Figure 2 with orientation to capillary and CCD camera.

The latest generation QLISA technology uses a microcapillary holder fabricated at University of Pennsylvania's Machine Shop. It mounts the excitation source so it is always focused on the same spot of the microcapillary which is loaded into a metal tube slightly larger than the outer diameter of the microcapillary. This ensured the ultraviolet source was focused at the same distance and position independent of user or between different microcapillaries. This is a significant improvement over the original system that relied on manual

focusing for each microcapillary and a microcapillary holder that allowed position variation.

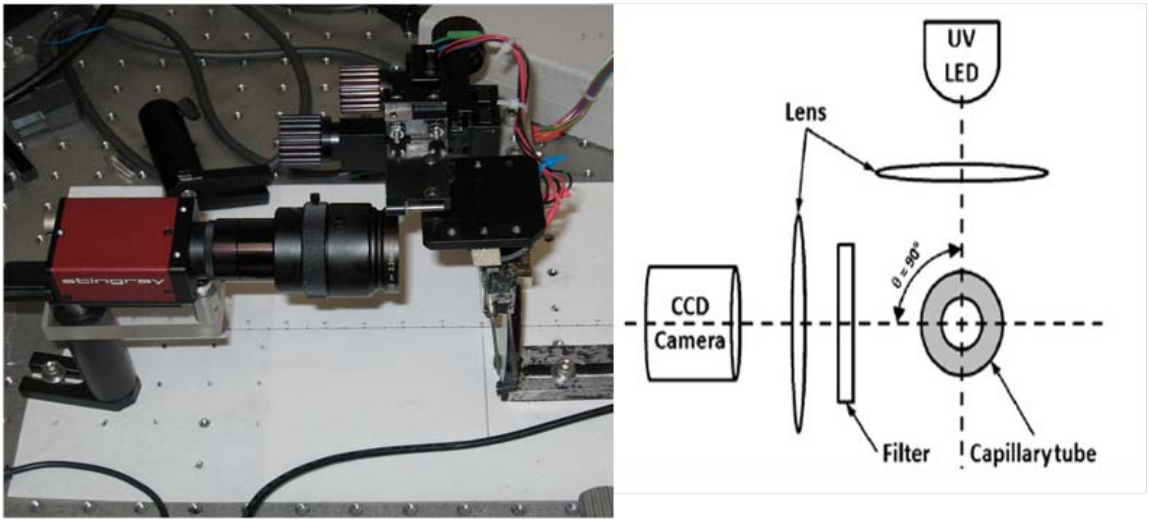

Figure 2: (LEFT) Optical setup with CCD camera, excitation source, and capillary holder. (RIGHT) Schematic of the optical configuration demonstrating the QD excitation in the capillary with the LED and its emission being captured with the CCD camera (image reproduced with permission from Elsevier).

This is a brief overview of QLISA which will be discussed in more detail in the following Chapters. Included in Chapter 3 is a full description of an alternative immunochemical strategy that relies on the strong biotin-streptavidin reaction. To briefly mention here, we bind a secondary antibody conjugated to streptavidin to the antigen. Following this incubation we introduce a biotinylated quantum dot that can be imaged and processed in an identical fashion, as described above.

As the name indicates QLISA is similar to ELISA with distinctive differences that are designed to provide advantages over existing ELISA technology limitations. The most notable differences is QLISA's substrate, which is a PMMA microcapillary that only requires approximately 1uL of sample compared to the 100uL sample needed in a 96-well plate from ELISA. This hundred-fold reduction in sample size is a key advantage over the larger required sample size needed in ELISA. Additionally, QLISA's primary antibody immobilization is improved over ELISA and as mentioned, QLISA uses different detector molecules – quantum dots.

1.3.1 Quantum Dots

As mentioned we use quantum dots as our fluorophore. They are nanoparticles made from semiconductor metals. We purchased our quantum dots from Invitrogen, which are composed of a cadium-selenium (CdSe) core and a zinc-sulfide (ZnS) outer layer, which prevents dissolution of free cadium. The optical properties of quantum dots can be easily manipulated by altering the size, which is done during synthesis. Their favorable optical properties include a broad excitation spectra, narrow emission spectra, large Stokes shift, good

photostability, photobleaching resistance, and strong fluorescence. We use a 5nm diameter quantum dot that emits at a wavelength of 605nm. Larger quantum dots emit light closer towards the near infrared spectra while smaller quantum dots are emitting spectra closer towards ultraviolet light. Figure 3 demonstrates some of the optical properties of various sized quantum dots (Medintz, Uyeda, Goldman, & Mattoussi, 2005).

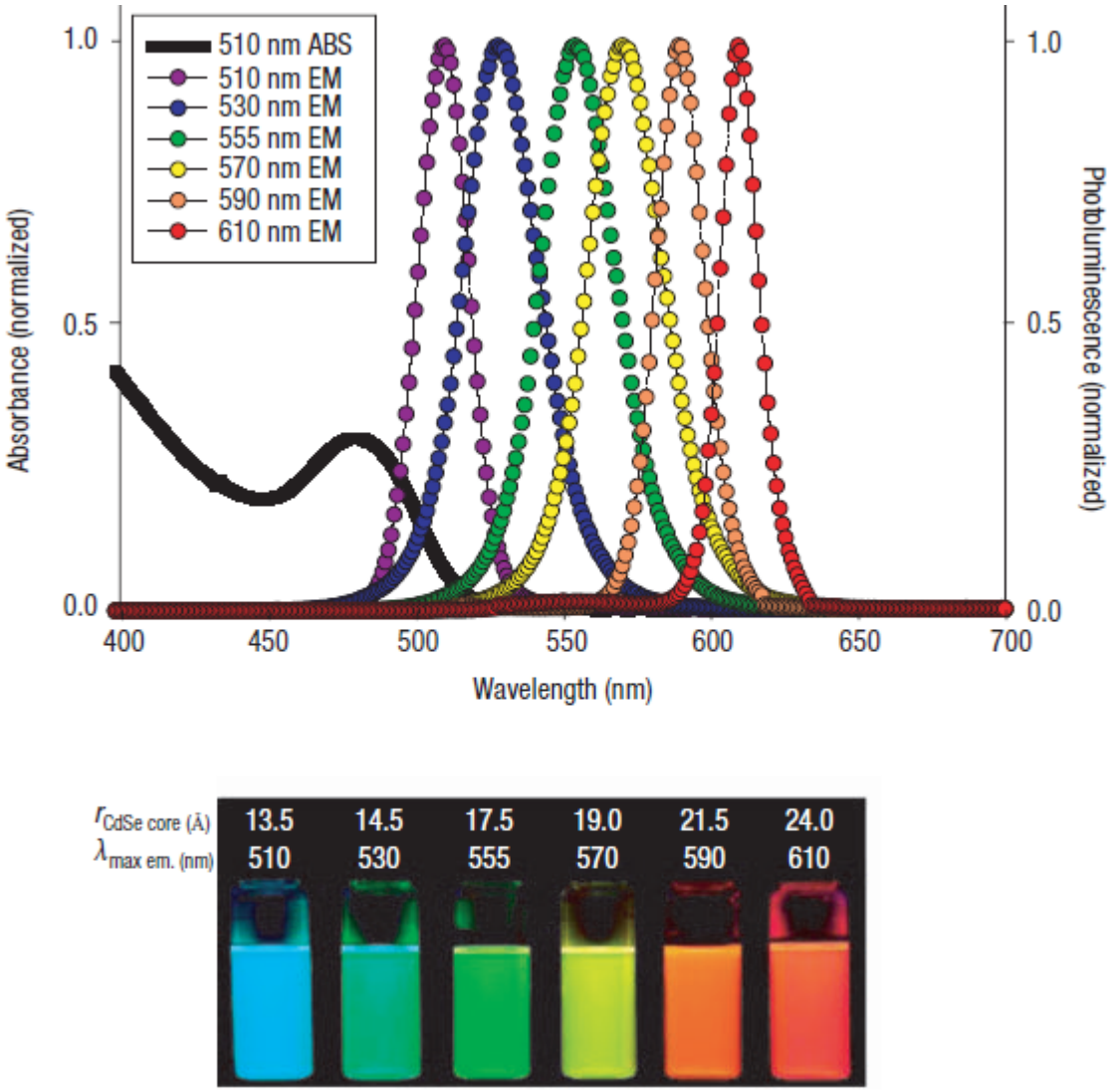

Figure 3: Adapted, with permission, from (Medintz, et al., 2005) demonstrating various emission profiles based on quantum dot size.

Two types of quantum dots are used in this thesis: one that is conjugated to secondary antibody and another that is conjugated to biotin. We describe both here.

The quantum dot conjugated to the secondary antibody is done in house using Invitrogen conjugation kits. Quantum dots come with a PEGalyted coating that allows materials to conjugate to the quantum dot. In our case, the PEG coating binds to thiols of the reduced form of our secondary antibody (immunoglobulin G molecule). The PEGalyted quantum dots are activated with the amine-thiol crosslinker sulfosuccinimidyl 4-[*N*-maleimidomethyl] cyclohexane-1-carboxylate (SMCC) which leaves a reactive maleimide group on the quantum dot surface. This is allowed to react with thiol groups that are present following antibody reduction. The final product is a quantum dot conjugated antibody that is stable for 4-6 weeks at 4^{o}C.

The other quantum dot we use is a streptavidin conjugated quantum dot that is purchased from Invitrogen – double check.

1.4 THESIS OBJECTIVES

This thesis has three main objectives, of which the latter two are presented together.

The first objective, which comprises Chapter 2, involves improving surface modification of PMMA-based immunoassay for improved performance and robustness. My approach involves a systematic characterization of current PMMA activation and functionalization of the first generation of QLISA and subsequent improvement through a unique combination of homo-bifunctional crosslinkers. Our improvement of the surface chemistry for primary antibody immobilization from the first to second generation QLISA is theoretically functional and experimentally beneficial. This improved chemistry involves optimized PMMA surface activation followed by crosslinking diamino polyethylene glycols with glutaraldehyde which subsequently binds a primary antibody in QLISA. Our unique approach has been patented - Hansberry, David, R.; et. al. "Antibody Immobilization Using Poly(ethylene glycol) Crosslinking." U.S. Patent Application No.61/334,056, filed 12, May 2010. Additionally we have submitted a journal manuscript titled, "A Comparative Analysis of Surface Activation Techniques and Antibody Crosslinkers on PMMA Substrates for Biosensor Applications," that highlights our major findings and supports with numerical simulations using COMSOL.

The second and third objectives of this thesis are presented together in Chapter 3. The first of these objectives is the characterization of our novel

immunoassay, QLISA. We describe QLISA in detail and confirm its accuracy through comparative analysis of myeloperoxidase and lactoferrin levels in human stool samples using commercial ELISA kits as standards. The second of these two objectives is correlating myeloperoxidase and lactoferrin levels from the human stool samples to inflammatory bowel diseases (ulcerative colitis and Crohn's disease), other inflammatory bowel diseases (ischemic colitis, infectious diarrhea and clostridium difficile), and healthy patients. We add to the current literature of the sensitivity and specificity of myeloperoxidase and lactoferrin in helping distinguish inflammatory bowel disease patients from healthy patients. Additionally we add valuable insight to the correlation between myeloperoxidase and lactoferrin levels in identifying inflammatory bowel disease. This data is undergoing editing for submission to a journal to be decided.

Not included in this thesis, but worth mentioning is our peripherally related work on identification of myeloperoxidase and its corresponding antibody using signal enhanced Raman spectroscopy that resulted in two journal publications. Again while not immediately relevant enough to be included in this thesis, it is important to note for general reference. The first published in Nano-Micro Letters titled, "Identification of Binding Interactions Between

Myeloperoxidase and its Antibody Using Surface Enhanced Raman Spectroscopy," and a second article published in Spectroscopy: Biomedical Applications titled, "SERS Study on Myeloperoxidase and its Immunocomplex: Identification of Binding Interactions."

1.5 THESIS ORGANIZATION

This thesis is separated into four chapters. Chapter 1 provides the basic scientific and technological background of the project and allows readers to understand basic concepts and thesis objectives that will be discussed further in subsequent chapters. It introduces relative information on biosensors, biomarkers, irritable bowel syndrome and inflammatory bowel disease. It also introduces the QLISA technology and the previous work that laid the foundation for this work. Chapter 2 and Chapter 3 are the bulk of this thesis and systematically discuss, at length, the materials and methods, data results and discussion, both preceded by thorough background sections that allows readers to see the progression of previous authors' work and findings that led to our pursuit of these experiments and findings. In all, Chapter 2 and Chapter 3 are presented as journal manuscripts. Chapter 4 summarizes the principal findings, contributions to the field and possible directions for future work.

CHAPTER 2: SURFACE CHEMISTRY MODIFICATIONS

2.1 SURFACE CHEMISTRY BACKGROUND

Biosensor development continues to rapidly grow as a field because of the wide variety of biosensor platforms and applications. We have focused this research on optical-based biosensors, with a specific interest in immunoassays that run on a PMMA (poly(methyl methacrylate)) substrate. PMMA is frequently used in substrates for immunoassays because of its manufacturability, cost-effectiveness, and desirable optical and mechanical properties (J. Liu, Pan, Woolley, & Lee, 2004; Wen, He, & Lee, 2009; Yuan Yuan, He, & Lee, 2009). Regardless of the immunoassay platform, such as a microfluidic (Y. Bai, W.-C. Huang, & S.-T. Yang, 2007; Y. Bai et al., 2006), microcapillary device (Babu, et al., 2009), beads (Hu, Li, & Liu, 2006; Li, Hu, & Liu, 2004) or other, PMMA can be used as the substrate because of its manufacturability.

Immunoassays, especially those that use an ELISA-type sandwich assay like QLISA, benefit from an activated surface that immobilizes a high density of primary antibody. This is the initial step in an immunoassay and thus has implications for subsequent steps and overall immunoassay performance.

Traditional immunosorbent assays are carried out on the solid-phase of a 96 well polystyrene microtiter plate, with antibodies passively adsorbed onto the polystyrene surface. Passive adsorption of the antibodies is achieved through hydrophobic interactions between the non-polar or aromatic amino acid residues present within the antibody and the hydrophobic polymer chains present on the substrate, resulting in randomly oriented antibody. Some of the adsorbed antibodies are denatured in this process, leaving as few as 5-10% of the total adsorbed antibodies available for an affinity reaction (Butler et al., 1993; Butler et al., 1992). This results in inhomogeneous antibody coverage, waste of reagents, and limited sensitivity potential. To overcome these limitations, biosensor developers have employed various strategies including activating the biosensor surface to facilitate the immobilization of primary antibody through crosslinkers.

Subsequent background sections in this Chapter will discuss PMMA surface activation and some of the crosslinking strategies we explored for our QLISA technology.

2.1.1 Surface Activation

Many biosensors, irrespective of substrate but including PMMA, have their surface activated to help improve performance. The goal is to alter the original substrate from a less reactive surface to a more reactive one which can now be more easily customized with crosslinkers as needed.

The surface of PMMA is covered with ester groups that can be modified to carboxyl groups for favorable crosslinking reactions. Two frequently used PMMA surface activation techniques are ionized gas treatment with oxygen plasma (Ozcan, Zorlutuna, Hasirci, & Hasirci, 2008) and wet chemical treatment with sodium hydroxide (Babu, et al., 2009). Additionally ultraviolet irradiation (Situma, Moehring, Noor, & Soper, 2007) can be used to activate the surface of PMMA. Both methods modify the surface of PMMA, leaving carboxyl groups and increasing PMMAs hydrophilicity. Extended treatment with either method can form oxygen radicals, which are undesirable for crosslinking reactions. The surface chemistry activation of PMMA with different methods is displayed in Figure 4.

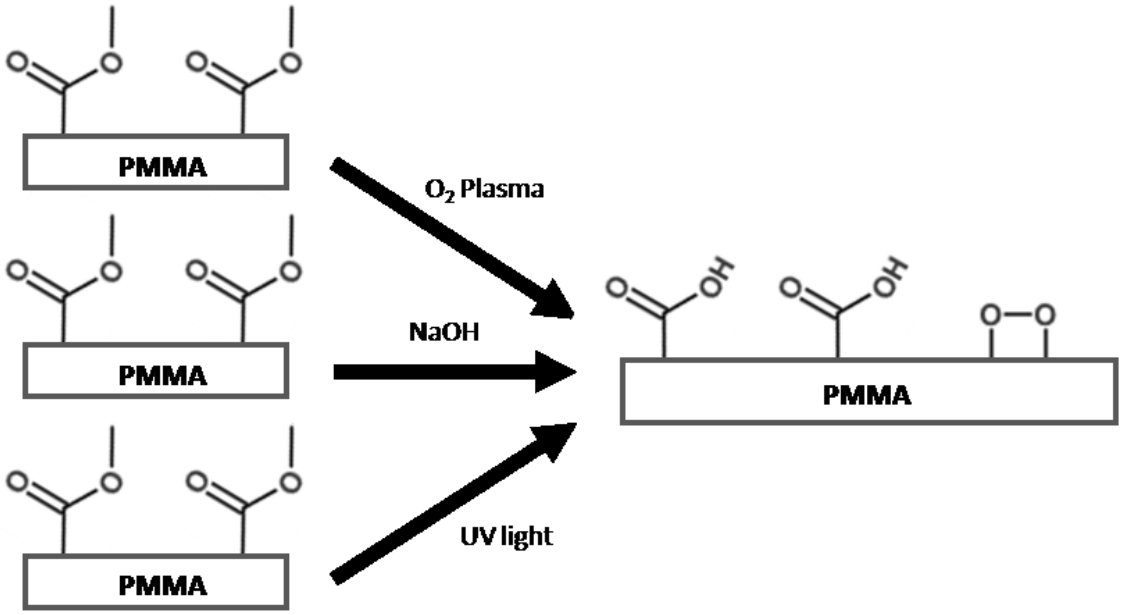

Figure 4: Chemical modifications of PMMA substrate using oxygen plasma, NaOH and UV light treatment. Oxygen radical (o-o) formation is possible on the PMMA surface if the surface is over exposed to the treatment.

One of the most obvious advantages of surface activation is to increase the surface area of the PMMA, allowing more potential binding sites for primary antibodies. This a heavily explored area that includes many crosslinking options for numerous substrates. The wide variety of crosslinkers allows appropriate customization and exploration of crosslinkers in order to meet need.

2.1.2 Crosslinkers

In order to increase antibody surface coverage for biosensor applications, numerous immobilization strategies have been developed using both zero- and non-zero-length crosslinkers. Commonly used chemical crosslinking strategies include the zero-length crosslinker 1-ethyl-3-(3-dimethylaminopropyl) carbodiimide (EDC) with sulpho-N-hydroxysulfosuccinimide (sNHS) (Babu, et al., 2009), non-zero-length polymer crosslinkers (Y. Bai, et al., 2007; Y. Bai, et al., 2006; Mehne et al., 2008), biotin-streptavidin (NeutrAvidin) systems (Chung, Park, Bernhardt, & Pyun, 2006), protein A (Jendeberg et al., 1996; Owaku, Goto, Ikariyama, & Aizawa, 1995; Yuan Yuan, et al., 2009), protein G (Fowler, Stuart, & Wong, 2006), amongst others. Perhaps the most ubiquitous technique used to immobilize antibodies onto a polymeric substrate is through the formation of a covalent amide linkage between the reactive amine groups present within an antibody and a carboxylate moiety on the substrate using the carbodiimide zero-length crosslinker EDC (Staros, Wright, & Swingle, 1986).

2.1.2.1 1-Ethyl-3-(3-Dimethylaminopropyl) Carbodiimide

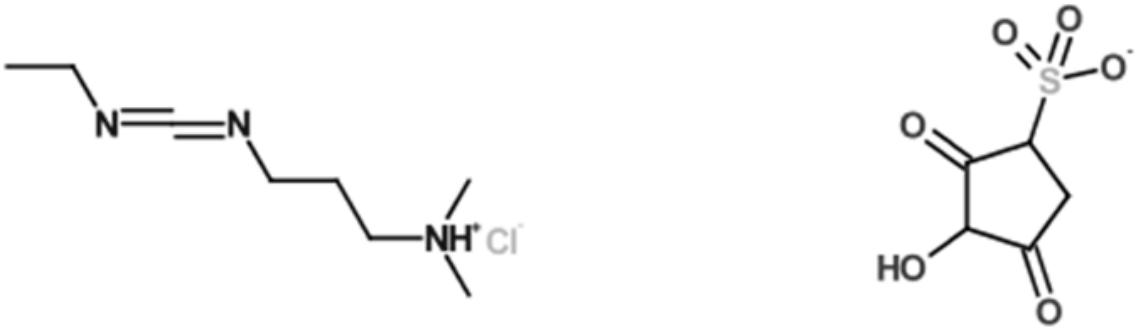

Figure 5: Chemical structures of EDC (left) and sNHS (right).

EDC (structure shown on left in Figure 5) facilitates the formation of a permanent covalent amide bond between the amine group of an antibody and the carboxyl group of the PMMA substrate. EDC first reacts with PMMA's carboxyl group to form an unstable O-acylisourea ester. If then reacted with sNHS (structure shown on right in Figure 5), the O-acylisourea ester will become a semi-stable amine reactive sNHS ester. This molecule can then react with the amine group of an antibody to create a covalent, stable amide bond between the PMMA substrate and antibody. sNHS is needed to further stabilize the O-acylisourea ester, which is susceptible to hydrolysis and can return the carboxyl group to its original form (Hermanson, 2008). This reaction is shown in Figure 6). This immobilization technique is limited because the covalent amide bond can be formed between the PMMAs carboxyl group and *any* reactive amine on the antibody surface. This technique results in the random orientation of

antibodies on the surface and possible denaturing of the active binding site. In addition the number of active carboxyl groups capable of binding antibodies is limited by the surface area of the flat PMMA substrate.

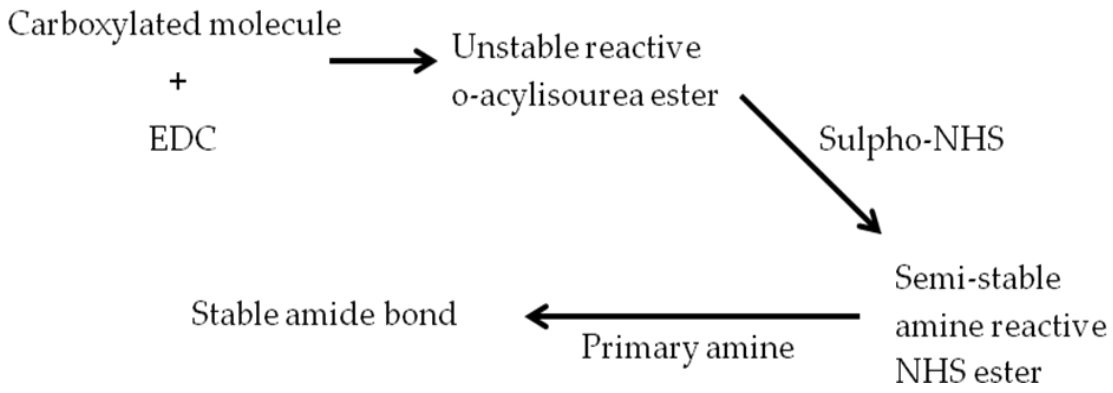

Figure 6: A schematic showing a carboxylated molecule reacting with EDC / sNHS and a primary amine (of a primary antibody) to form a stable amide bond.

As a result of the reduced antigen binding capacity potential of antibodies immobilized using zero-length crosslinkers, long flexible polymeric linkers such as PEI and PEG have been investigated as spacers in an attempt to increase the mobility of the immobilized antibodies while maintaining their active binding sites. Creating a brush border for antibody immobilization has previously shown promise for improving immunoassay performance with different homo- and hetero- bifunctional crosslinkers (Y. Bai, et al., 2007; Y. Bai, et al., 2006). These crosslinkers, like polyethyleneimines and poly(ethylene glycols), provide increased binding sites for primary antibody and can optimally orient primary

antibodies for maximum antigen binding (G. P. Anderson, Jacoby, Ligler, & King, 1997; Y. Bai, et al., 2007; Y. Bai, et al., 2006; Chung, et al., 2006; Fowler, et al., 2006; Ghose, Hubbard, & Cramer, 2007; Guss et al., 1984; Jendeberg, et al., 1996; Johnson, Jensen, Prakasam, Vijayendran, & Leckband, 2003; Owaku, et al., 1995; Yuan Yuan, et al., 2009).

2.1.2.2 Polyethyleneimine

Polyethyleneimine (PEI) is a highly charged cationic synthetic polymer. It is sold commercially in both linear and branched forms at a variety of molecular weights. Linear PEI consists of primary amines (structure on right of Figure 7) while branched PEIs contain primary, secondary, and tertiary amines (structure on left of Figure 7). Additionally PEIs can be produced in a range of molecular weight PEIs high positive charge leads it to strongly react with proteins non-specifically (Hermanson, 2008).

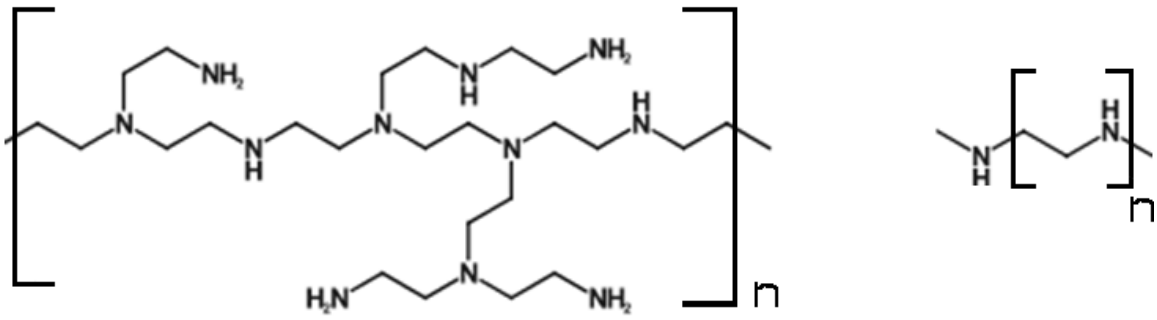

Figure 7: Chemical structures of branched (left) and linear (right) polyethyleneimines.

The use of non-zero-length crosslinkers offers several advantages over passive absorption immobilization methods by allowing a high density of physiologically active antibodies to be immobilized onto a polymeric substrate. Non-zero-length crosslinkers can create brush borders on the immunoassay's substrate, providing an increased surface area and thus more binding sites for primary antibody. This is a clear advantage over zero-length crosslinkers like EDC / sNHS because of the potential increase in antibody surface area. PEI can be immobilized directly on activated PMMA surface and crosslinked further with other polymers, like glutaraldehyde, to bridge the PEI polymer to the antibody. Using the amine bearing polymer PEI as a spacer to immobilize an antibody onto a PMMA substrate effectively has been shown to increase the antigen capture compared to passively adsorbed antibodies (Y. L. Bai et al., 2006). This is done by increasing substrate surface area, limiting steric hindrance of adjacent antibodies, and reducing antibody denaturing following

immobilization. These all lead to enhancing assay sensitivity for the detection of an antigen (Y. L. Bai, W. C. Huang, & S. T. Yang, 2007; Y. L. Bai, et al., 2006). PEI also comes in a variety of molecular weights allowing for further optimization of chain density and flexibility. The effect that PEI spacer length has on antibody density, non-specific adsorption, and the functionality of the immobilized antibodies has not yet been fully elucidated.

2.1.2.3 Polyethylene Glycol

Polyethylene glycol (also known as polyethylene oxide) is an amphiphilic polymer that is widely used because of its customizable synthesis. PEG-modified molecules can enhance the effects of therapeutics through decreasing the molecules immunogenicity, protect it from degradation by proteolytic enzymes, increase its water solubility, and decrease the molecules renal clearance rates. This makes the FDA-approved PEG an attractive molecule to combine with therapeutic drugs to increase its therapeutic effect. In addition, PEG comes in a variety of molecular weights with a number of different terminal groups, including some that have been used in immunoassays (Hermanson, 2008).

PEGs have been used as a crosslinking agent for a variety of applications including immunoassays (Hermanson, 2008). Their range of terminal functional

groups allows biosensors to be performed on different substrates. Further, customized PEGylated molecules can be used for different immunoassays based on need. PEGs have been used to control cell adhesion on PMMA substrates (Patel, Thakar, Wong, McLeod, & Li, 2006). It has been shown that the length of the spacer is a critical determinant of the spacer coil conformation, which in turn alters the antigen binding capacity of the immobilized antibodies (Ting Cao, 2007). We plan to quantitatively determine how molecular weight and chemical structure influence antibody immobilization.

Polyethylene glycols are produced with a variety of terminal functional groups including amine, carboxy, sulfhydryal, methyl, thiol and others, which allows biosensors to be developed on different substrates. PEGs also are available in a range of molecular weights and in linear or branched forms allowing further customization of the immunoassay's crosslinking. PEGs variety and abundant commercial availability is due to its incredibly widespread use in medical and non-medical applications.

We will be investigating di-amino-PEGs, both linear and branched molecules to determine their ability to bind primary antibody as part of an immunoassay. The structures of the PEGs we will be using are shown in Figure

8. The di-amino-PEGs will be immobilized directly on the activated PMMA surface and will use the crosslinker glutaraldehyde to bridge the PEG polymer to the antibody.

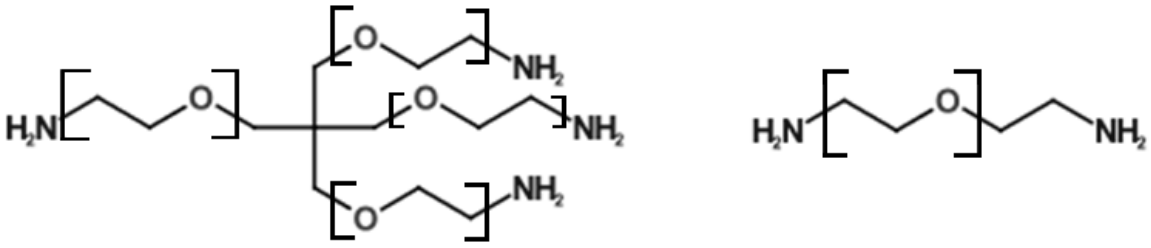

Figure 8: Chemical structure of branched (left) and linear (right) di-amino polyethylene glycols.

The PMMA surface is activated with sodium hydroxide leaving a carboxyl group to interact with the primary amine of the di-amino PEG creating an amide bond. Glutaraldehyde is then introduced and its terminal aldehyde reacts with the primary amines on the other functional ends of the di-amino PEG. The Schiff base formation results in an imine formation. The primary antibody is then introduced and its primary amines interact with the other terminal aldehyde group of the glutaraldehyde. The primary amines of the antibody interact with the aldehyde of glutaraldehyde through another Schiff base reaction resulting in immobilized antibody.

2.1.2.4 Biotin-Streptavidin

It is well known that the biotin-streptavidin complex is one of the strongest, non-covalent bonds known (Ka = 10^{15} M^{-1}). Their strong interaction and stability under severe condition make these molecules well known and frequently used amongst molecular biologist and the like. They have been extensively used in immunoassays (Fan et al., 2008; Lin et al., 2008; R. Liu et al., 2010; Niemeyer, Adler, & Wacker, 2007; Rauf, Glidle, & Cooper, 2010; Rehák, Snejdárková, & Otto, 1994; Wang, Zhang, Gao, Duan, & Wang, 2010; Wilchek, Bayer, & Livnah, 2006; Yu et al., 2010; Yali Yuan et al., 2010), including the most current QLISA configuration discussed in this thesis. These molecules, their complex, and applications in our research are discussed in this section.

Biotin, also known as vitamin B7, is a coenzyme in carboxylation reactions that is required for several metabolic pathways in humans. These reactions add 1-carbon to molecules including reactions that convert pyruvate (3C) → oxaloacetate (4C), acetyl-coenzyme A (3C) → malonyl-coenzyme A (4C), and propionyl-coenzyme A (3C) → methylmalonyl-coenzyme A (4C). Biotin is found in many foods, although no foods in large concentrations, and biotin deficiencies are essentially nonexistent, although possible if excessive raw egg whites are consumed daily for an extended period of time. This is due to high avidin

concentrations in raw egg whites, which binds biotin very tightly (an order of magnitude higher than streptavidin when all molecules are unconjugated).

Biotin's small size (Figure 9) allows it to bind proteins without greatly altering the protein's chemical / physical structure or function (Della-Penna, Christoffersen, & Bennett, 1986). This is extremely important since biotinylated antibodies, like the ones we use for QLISA, have limited alterations from the antibodies native form and increases likelihood of antigen antibody interaction.

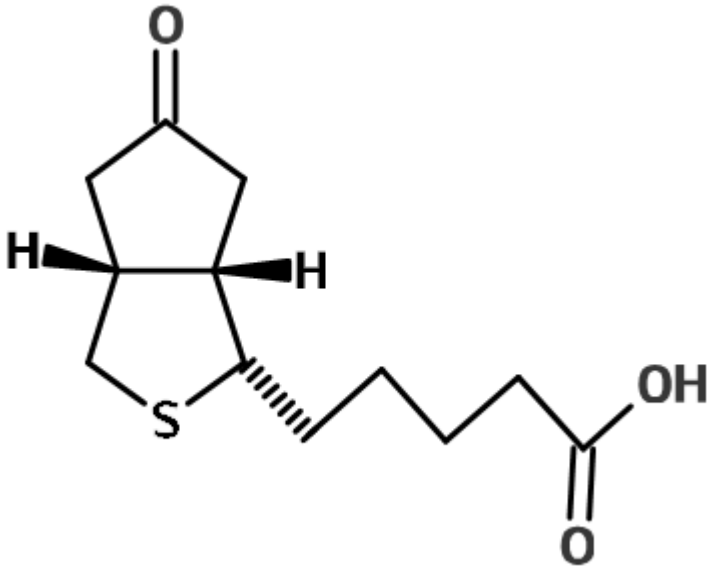

Figure 9: The chemical structure of biotin (vitamin B7).

Streptavidin is a 60kDa biotin-binding protein, similar to avidin, that is composed of four identical subunits each capable of binding one biotin molecule.

Its structure, bound to a biotin molecule, can be seen in Figure 10 It is purified from the bacteria *streptomyces avidinii*. Avidin is a 16.4kDa glycoprotein that is found in raw egg whites, as previously mentioned above. While streptavidin and avidin share similarities like they're high affinity, non-covalent bond to biotin and their incredibly strong resistance to complex denaturing / disassociation from buffer salt, pH, detergents, denaturants, extreme temperatures, or organic solvents. This has clear advantages in bionanotechnology and molecular biology. Streptavidin is distinct from avidin in several ways. For one streptavidin has a lower isoelectric point (around 5, compared to avidin around 10) and is not a glycoprotein. Both traits lead streptavidin to be associated with less non-specific binding, which translates to more sensitive immunoassays. Additionally streptavidin, as well as biotin and avidin, is easily modified to other bioconjugates (Green, 1990; Hermanson, 2008; Jagannath & Sehgal, 1989; Stayton PS et al., 1999; Weber, Ohlendorf, Wendoloski, & Salemme, 1989; Wilchek, et al., 2006).

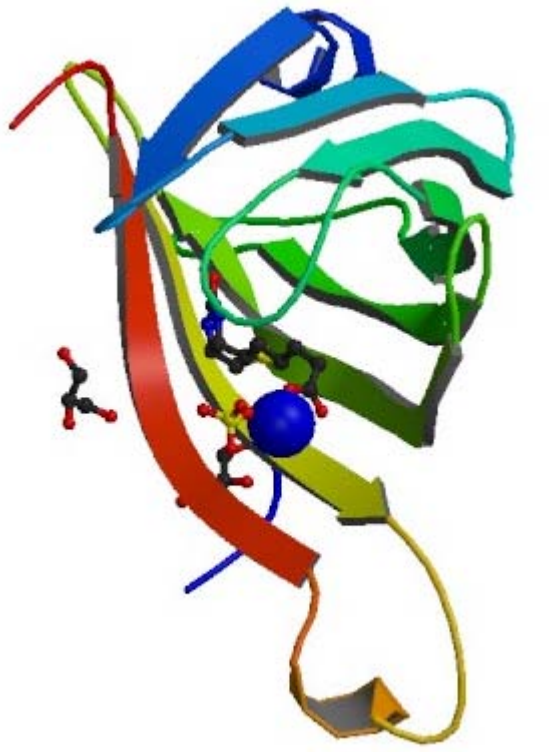

Figure 10: Crystal structure of R 7-2 streptavidin complexed with biotin (Magalhães et al., 2011). Image and caption taken, with permission, from the RCSB Protein Data Bank.

2.1.2.5 Additional Crosslinkers

While we have discussed a few crosslinkers above that we have chosen to focus on for our QLISA research, there are many others, too numerous to list, let alone discuss in any detail. However, what should be known about crosslinkers is that there are homo- and hetero-bifunctional crosslinkers for just about every reactive group in any imaginable combination. Further there are often variations

in the types of each crosslinker with different reactive groups. In other words there are many types of crosslinkers that all have many uses outside of the biosensor realm.

2.2 EXPERIMENTAL SECTION

The Experimental Section is subdivided into two main areas – 2.3.1 Surface Activation and 2.3.2 Surface Functionalization. Each of these sections will discuss the objectives, materials/methods, results and conclusions.

2.2.1 Surface Activation

Many immunoassay surfaces, including those used in microfluidic devices, are often inert and require activation in order to initiate crosslinking reactions and enable primary antibody immobilization. Depending on the immunoassay substrate and desired crosslinker, a number of different surface activation methods can be applied. Two of the most common strategies to activate surfaces include wet chemical treatment (Babu, et al., 2009) and ionized

gas methods (Ozcan, et al., 2008). These immunoassay surface activation methods are a necessary precursor for efficient antibody immobilization, especially when using PMMA as an immunoassay substrate, like QLISA.

2.2.1.1 Overview / Goals

Prior to crosslinking the PMMA to the antibody the PMMA surface needs to be activated. Two frequently used PMMA surface activation techniques are oxygen plasma and sodium hydroxide treatment. While several groups have explored the effect of different crosslinkers on primary antibody immobilization, direct comparisons of surface activation methods to the efficiency of antibody capture are not readily available. There is also significant variation of parameters used and antibodies for each method, rendering comparison of results not possible. Here we quantitatively compare two effective and popular surface activation methods (oxygen plasma and sodium hydroxide treatment) on PMMA surfaces. Each technique is characterized, as a function of time under specific parameters, with contact angle measurements to determine hydrophilicity and a toluidine blue O (TBO) assay to assess carboxyl group surface density (which are produced as a result of these treatments and is used for subsequent crosslinking to antibodies). These surface characterizations

methods will provide immunoassay developers the necessary quantitative information to customize and optimize a biosensor system.

2.2.1.2 Materials / Methods

Polymethylmethacrylate was purchased from McMaster-Carr (Robinsville, New Jersey) in ¼ inch cubes and 12 inch by 12 inch by 1/16 inch sheets. The sheets were cut into 1cm squares. Sodium hydroxide (NaOH), acetic acid, and isopropyl alcohol were purchased from VWR (Radnor, Pennsylvania). Toluidine blue O (TBO) was purchased from Acros Organic (Fair Lawn, New Jersey).

CONTACT ANGLE

The PMMA squares were submerged in 60^{o}C 1N NaOH for 0, 15, 30, 45, or 60 minutes under moderate shaking (100RPM) or treated with oxygen plasma for 0, 0.5, 1, 2, 5, or 10 minutes. Oxygen plasma treatment was performed using a frequency of 40 kHz and a power of 200W (Femto Science). Following treatment, 3uL of DI water was pipetted onto the PMMA squares. The NaOH treated PMMA squares were air-dried prior to the addition of 3uL of DI water. The DI water droplet on the treated PMMA squares was captured using a CCD camera

(Stingray, AVT-FS-033B) and the contact angle was measured with automated Matlab software.

TBO ASSAY

The PMMA squares were submerged in 60°C 1N NaOH for 0, 15, 30, 45, or 60 minutes or treated with oxygen plasma for 0, 0.5, 1, 2, 5, or 10 minutes. Each PMMA square was dried, if needed, and separately placed in 0.5mM TBO solution (DI water, pH 10.0). The PMMA squares were gently shaken while completely submerged in the TBO solution for 4 hours, allowing the TBO to adsorb to the carboxyl groups on the PMMA surface. PMMA squares were then removed from TBO solution and thoroughly rinsed with DI water pH 10.0 to remove the unbound TBO from the PMMA surface. Next the PMMA squares were submerged in 50%w/v acetic acid and vigorously vortexed to desorb the bound TBO from the PMMA surface. This solution was then read in a spectrophotometer (Tecan Infinite 200) and read for absorbance at 633nm. TBO concentration was determined from comparison to a standard curve of TBO in 50%w/v acetic acid solution. TBO concentration was then converted to carboxyl group concentration on the PMMA squares' surface (Uchida, Uyama, & Ikada, 1993).

2.2.1.3 Results / Discussion

The surface of PMMA is covered with ester groups that can be modified to carboxyl groups for favorable crosslinking reactions. Two common methods for doing this are wet chemical treatment of PMMA using NaOH or oxygen plasma treatment of PMMA. Both methods alter the surface of PMMA, leaving carboxyl groups and increasing PMMAs hydrophilicity. Extended treatment with either method can form oxygen radicals, which are undesirable for crosslinking reactions.

Contact angle measurements, Figure 11, were also performed following the two different surface treatments in order to assess the hydrophilicity of the surfaces as a function of time. The contact angle of untreated PMMA with DI water is 69^{o} and after only 1 minute of treatment was reduced to 38^{o}. There is a linear decrease in the contact angle over the first minute of oxygen plasma treatment. Treatment beyond 1 minute, and up to 10 minutes, does not impart any appreciable improvement in the contact angle. This is similar to previous findings on oxygen plasma treated PMMA as a function of time (Choi, Yang, Yoo, & Lee, 2010; Schmalenberg, Buettner, & Uhrich, 2004).

The NaOH treated PMMA also achieves a decrease in contact angle, however, this decrease is seen over a longer time period. The contact angle reaches a minimum, about 35^{o}, after approximately 30-60 minutes of NaOH treatment. These results are also consistent with previously published results, although there tends to be some degree of variation given the different manufacturers of PMMA (Choi, et al., 2010).

These results indicate that after 1 minute of oxygen plasma treatment and after 30-60 minutes of NaOH treatment the PMMA surface has reached a maximum hydrophilic state.

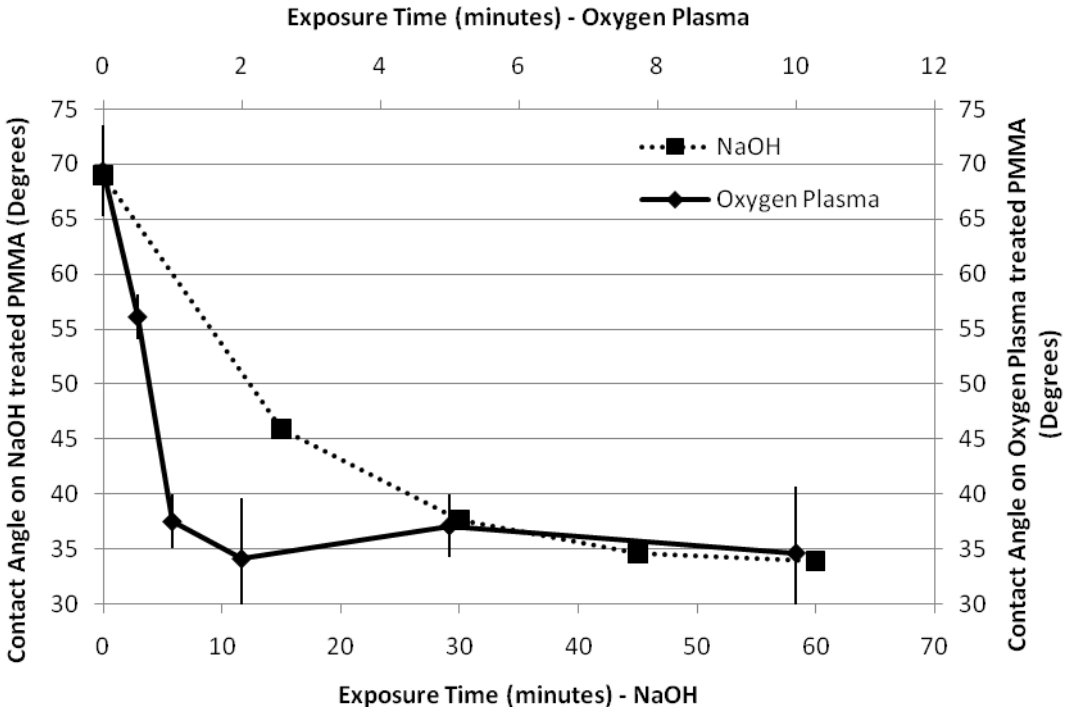

Figure 11: PMMA contact angle following treatment of either NaOH or oxygen plasma. N = 5 for all data points; bars represent standard deviation.

TBO ASSAY

The TBO assay was conducted on the activated surface of PMMA to quantify the number of carboxyl groups. The surface activation treatments, NaOH and oxygen plasma, produce carboxyl groups on the PMMA surface that can then be functionalized with primary antibodies through a crosslinker. Knowing that over exposure to both methods of surface activation treatments can cause oxygen radical formation, we want to minimize the treatment time, in order to minimize potential oxygen radical formation, while maximizing

carboxyl-group formation that can subsequently be used for crosslinking to a primary antibody.

Similar to the contact angle experiments, we analyzed the impact of surface activation time for each treatment. In Figure 5 we see the oxygen plasma treated PMMA surface has an increasing surface density of carboxyl groups up to around 1 minute. Beyond 1 minute there is a gradual decrease in the surface density of carboxyl groups over time. We attribute the decrease in carboxyl groups with extended treatment times to increased oxygen radical formation. This leads to less carboxyl groups available to bind TBO and hence a lower signal. Therefore the maximum carboxyl group surface density on PMMA is formed following 1 minute of oxygen plasma treatment.

The NaOH treated PMMA surfaces behaved similarly when we measured the surface carboxyl groups. Carboxyl group formation increases as a function of time when treated with 1N NaOH up to 30 minutes before decreasing and leveling off (Figure 12). This demonstrates that 30 minutes of treatment of NaOH on PMMA maximizes the surface density of carboxyl groups.

The optimal times of 1 minute of oxygen plasma treatment and 30 minutes of NaOH treatment for maximum carboxyl group formation is not surprising given our previous contact angle data that showed that the PMMA surfaces approached maximal hydrophilicity at 1 minute and 30 minutes for oxygen plasma and NaOH treatment, respectively. We do see an additional 1.3 nanomoles of carboxyl groups generated on the PMMA surface when using NaOH (left y-axis in Figure 12) compared to oxygen plasma (right y-axis in Figure 12) treatment. If all other parameters are equal, then the use of a 30 minute NaOH treatment as a surface activation method for carboxyl groups on PMMA would be preferred. If wet chemical treatment of the PMMA surface is not possible, then 1 minute of oxygen plasma treatment would provide an excellent alternative capable of covering the PMMA surface with about 2.4 nanomoles per square cm. Given the NaOH advantage over oxygen plasma, we used NaOH for the remainder of the experiments, which include evaluating the effectiveness of various crosslinkers in capturing and immobilizing antibodies.

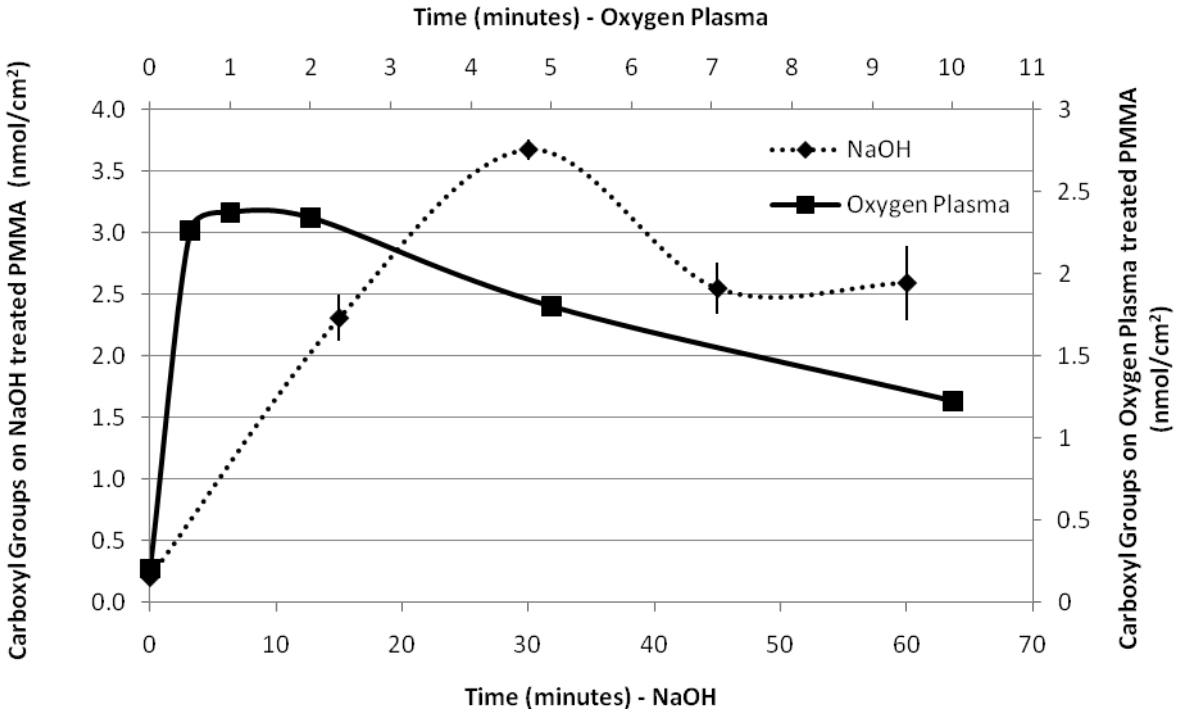

Figure 12: Surface density of carboxyl groups on the PMMA substrate following different surface activation treatments. Data needs to be recollected for NaOH with more time points. N = 5 for all data points; bars represent standard deviation.

2.2.2 Surface Functionalization

Functionalizing the surface of PMMA with primary antibody is critical in producing a high performing biosensor. Functionalization provides an opportunity to influence spacer length between the PMMA surface and primary antibody through use of specific crosslinking agents. This is done, for amongst other reasons, to improve assay performance. Fortunately there are a

tremendous number of crosslinkers that include homobifunctional, heterobifunctinal, and multifunctional crosslinkers all of which can be zero-length or non-zero-length. Crosslinkers can be manufactured or are commercially available with just about every functional chemical group, in different sizes, and with varying chemical structures. This is advantageous to assay developers and others scientist interested in bioconjugate chemistry since applications are wide ranging. While we discuss several crosslinking strategies, we want to highlight that there are many other crosslinking strategies that are utilized in other fields with diverse applications and reagents including liposomes, nucleic acids, oligonucleotides, and gold nanoparticles, to name a few. The widespread availability of different crosslinkers allows considerable customization for assay developers, including the use of multiple consecutive crosslinkers.

2.2.2.1 Overview / Goals

Here we explore how the use of different zero-length and non-zero-length, hetero- and homo-bifunctional crosslinkers influence the ability of an activated PMMA surface to capture antibody that subsequently can be used in QLISA. The first generation of QLSIA relied on the zero-length cross linker 1-ethyl-3-(3-dimethylaminopropyl) carbodiimide (EDC) with sulpho-N-

hydroxysulfosuccinimide (sNHS) to immobilize primary antibody on the PMMA microcapillary surface. Our goal was to characterize this functionalization method and determine, if possible, how to improve the functionalization of primary antibody through the use of non-zero-length crosslinkers. Additionally we wanted to see how molecular weight and chemical structure (linear vs. branched) influence primary antibody functionalization on PMMA. Research groups use a wide variety of functionalization methods but infrequently provide direct comparison or even quantitative characterization that demonstrates their performance.

We look at the widely available and frequently used polyethylene glycol, polyethyleneimine, and glutaraldehyde crosslinkers. We review different molecular weights for the polymers as well as linear and branched forms. The goal is to determine the influence of molecular weight and structure of polyethylene glycol and polyethyleneimine used with glutaraldehyde on ability to capture primary antibody. Again, this is a critical step in an immunoassay and provides an opportunity to increase immunoassay performance over traditional techniques that rely on passive adsorption of primary antibody.

2.2.2.2 Materials / Methods

Polymethylmethacrylate was purchased from McMaster-Carr (Robbinsville, New Jersey) in ¼ inch cubes and 12 inch by 12 inch by 1/16 inch sheets. The sheets were cut into 1cm squares. Sodium hydroxide, acetic acid, and isopropyl alcohol were purchased from VWR (Radnor, Pennsylvania). Polyclonal antibody for human myeloperoxidase was purchased from AbD Serotec (Raleigh, North Carolina). Alexa Fluor488 (AF488) conjugation kits were purchased from Invitrogen (Carlsbad, California). 1-ethyl-3-(3-dimethylaminopropyl) carbodiimide and sulpho-N-hydroxysulfosuccinimide were purchased from Sigma Aldrich (St. Louis, Missouri). Branched polyethyleneimine (molecular weight of 2,000 and 25,000 daltons), linear polyethyleneimine (molecular weight of 25,000 daltons), branched PEG (molecular weight of 1,500 daltons), and linear polyethylene glycol (molecular weight of 2,000 and 20,000 daltons) were purchased from Sigma Aldrich (St. Louis, Missouri). All polyethyleneimines and polyethylene glycols are di-amino. Glutaraldehyde (50%w/v) was also purchased from Sigma Aldrich (St. Louis, Missouri).

Prior to use in all experiments, the PMMA squares (¼ inch by ¼ inch) were sonicated in 50%v/v isopropyl alcohol isopropyl alcohol for 10min, rinsed with deionized (DI) water, and air dried.

AF488-Ab CONJUGATION

Alexa Fluor 488 (AF488) is a fluorescent dye commonly used in bioconjugations with proteins and serves as a reporter molecule. AF488 has absorption and emission spectra at 494nm and 519nm, respectively. AF488 was conjugated to primary polyclonal antibody against MPO using Invitrogen's commercially available kit (Molecular Probes, 2006). AF488 has a tetrafluorophenyl ester that reacts with the primary amines of antibodies.

All PMMA squares (1 cm by 1 cm) were sonicated in 50%v/v isopropyl alcohol isopropyl alcohol for 10min, rinsed with DI water and air dried.

Details of this conjugation protocol are given in Appendix B.

CALIBRATION CURVE

Alexafluor488 conjugated antibodies (AF488-Ab) were diluted to 100, 200, 300, 400, 500ng/mL and 5uL of solution was placed on an inverted PMMA square

resting on a glass cover slip (Figure 13). Alexafluor488 conjugated antibodies were excited and the intensity of their emission spectra was captured using a fluorescent microscope (Leica DMI4000 B). The intensities were correlated to AF488-Ab concentration in the standard curve. Microscope parameters were maintained for the remaining experiments and resulting fluorescent spectra intensities of subsequent experiments were correlated to the standard curve.

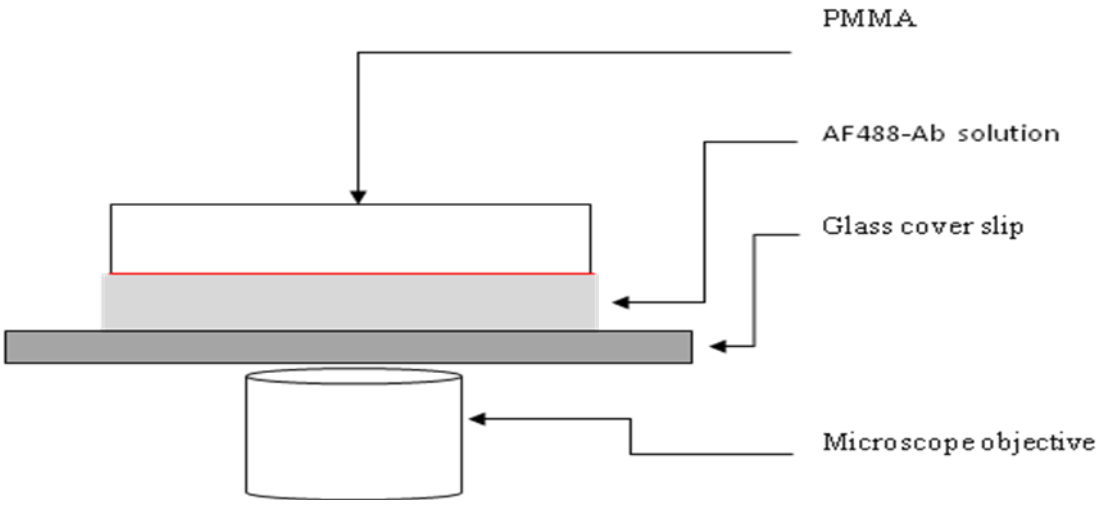

Figure 13: A schematic diagram showing the imaging configuration for Alexafluor488 conjugated antibodies crosslinking experiments.

CROSSLINKERS

Several different crosslinkers were evaluated and their preparation for antibody immobilization will be described individually given their different chemical structure. We evaluate the surface density of immobilized primary antibody using passive adsorption, 1-ethyl-3-(3-dimethylaminopropyl)

carbodiimide with sulpho-N-hydroxysulfosuccinimide, polyethyleneimines, polyethylene glycols, polyethyleneimines with GA, and polyethylene glycols with GA.

1-ethyl-3-(3-dimethylaminopropyl) carbodiimide with sulpho-N-hydroxysulfosuccinimide

Polymethylmethacrylate squares were submerged in 60°C 1N sodium hydroxide for 30 minutes while shaking at 100RPM. The PMMA squares were removed from solution and rinsed with 1X PBS 6.0. They were then submerged in a 43.4mM EDC / 15.4mM sNHS 1X PBS pH 6.0 solution for 1 hour at room temperature while on a shaker at 100RPM. The squares were then washed with 0.05% Tween in 1X PBS pH 7.4. 5uL of 500ng/mL of AF488-Ab was placed on the squares for 1 hour. Squares were then washed with 0.05% Tween in 1X PBS pH 7.4. Polymethylmethacrylate squares were dried and placed on a glass cover slip with 5uL of deionized water in the configuration shown in Figure 13.

Polyethyleneimine

Polymethylmethacrylate squares were submerged in 60°C 1N sodium hydroxide for 30 minutes while shaking at 100RPM. The PMMA squares were removed from solution and rinsed with 1X PBS 7.4 before submersion in 0.2% PEI for 1 hour while on a shaker at 100RPM. The squares were then washed with

0.05% 1X PBS pH 7.4 followed by pipetting 5uL of 500ng/mL of AF488-Ab on the surface. After 1 hour incubation the slides are rinsed with 0.05% Tween in 1X PBS pH 7.4, dried, and placed on a glass cover slip with 5uL of deionized water for imaging.

This procedure was followed for polyethyleneimines with molecular weight of 2,000 and 25,000 daltons.

Polyethyleneimine with glutaraldehyde

Polymethylmethacrylate squares were submerged in 60°C 1N sodium hydroxide for 30 minutes while shaking at 100RPM. The PMMA squares were removed from solution and rinsed with 1X PBS 7.4 before submersion in 0.2% PEI for 1 hour while on a shaker at 100RPM. The squares were then washed with 0.05% 1X PBS pH 7.4 followed by treatment with 1% GA solution for 30minutes while on a shaker at 100RPM. The squares were then washed with 0.05% Tween in 1X PBS pH 7.4. 5uL of 500ng/mL of AF488-Ab was placed on the squares for 1 hour. Squares were washed with 0.05% Tween in 1X PBS pH 7.4, dried, and placed on a glass cover slip with 5uL of deionized water for imaging.

This procedure was followed for polyethyleneimines with molecular weight of 2,000 and 25,000 daltons.

Polyethylene glycol

Polymethylmethacrylate squares were submerged in 60°C 1N sodium hydroxide for 30 minutes while shaking at 100RPM. The PMMA squares were removed from solution and rinsed with 1X PBS 7.4 before submersion in 0.2% PEG for 1 hour while on a shaker at 100RPM. The squares were then washed with 0.05% 1X PBS pH 7.4 followed by pipetting 5uL of 500ng/mL of AF488-Ab on the surface. After 1 hour incubation the slides are rinsed with 0.05% Tween in 1X PBS pH 7.4, dried, and placed on a glass cover slip with 5uL of deionized water for imaging.

This procedure was followed for all polyethylene glycols with molecular weights of 1,500, 2,000, and 25,000 daltons.

Polyethylene glycol with glutaraldehyde

Polymethylmethacrylate squares were submerged in 60°C 1N sodium hydroxide for 30 minutes while shaking at 100RPM. The PMMA squares were removed from solution and rinsed with 1X PBS 7.4 before submersion in 0.2%

PEG for 1 hour while on a shaker at 100RPM. The squares were then washed with 0.05% 1X PBS pH 7.4 followed by treatment with 1% GA solution for 30minutes while on a shaker at 100RPM. The squares were then washed with 0.05% Tween in 1X PBS pH 7.4. 5uL of 500ng/mL of AF488-Ab was placed on the squares for 1 hour. Squares were washed with 0.05% Tween in 1X PBS pH 7.4, dried, and placed on a glass cover slip with 5uL of deionized water for imaging.

This procedure was followed for all polyethylene glycols with molecular weights of 1,500, 2,000, and 25,000 daltons. This chemistry is shown in Figure 14.

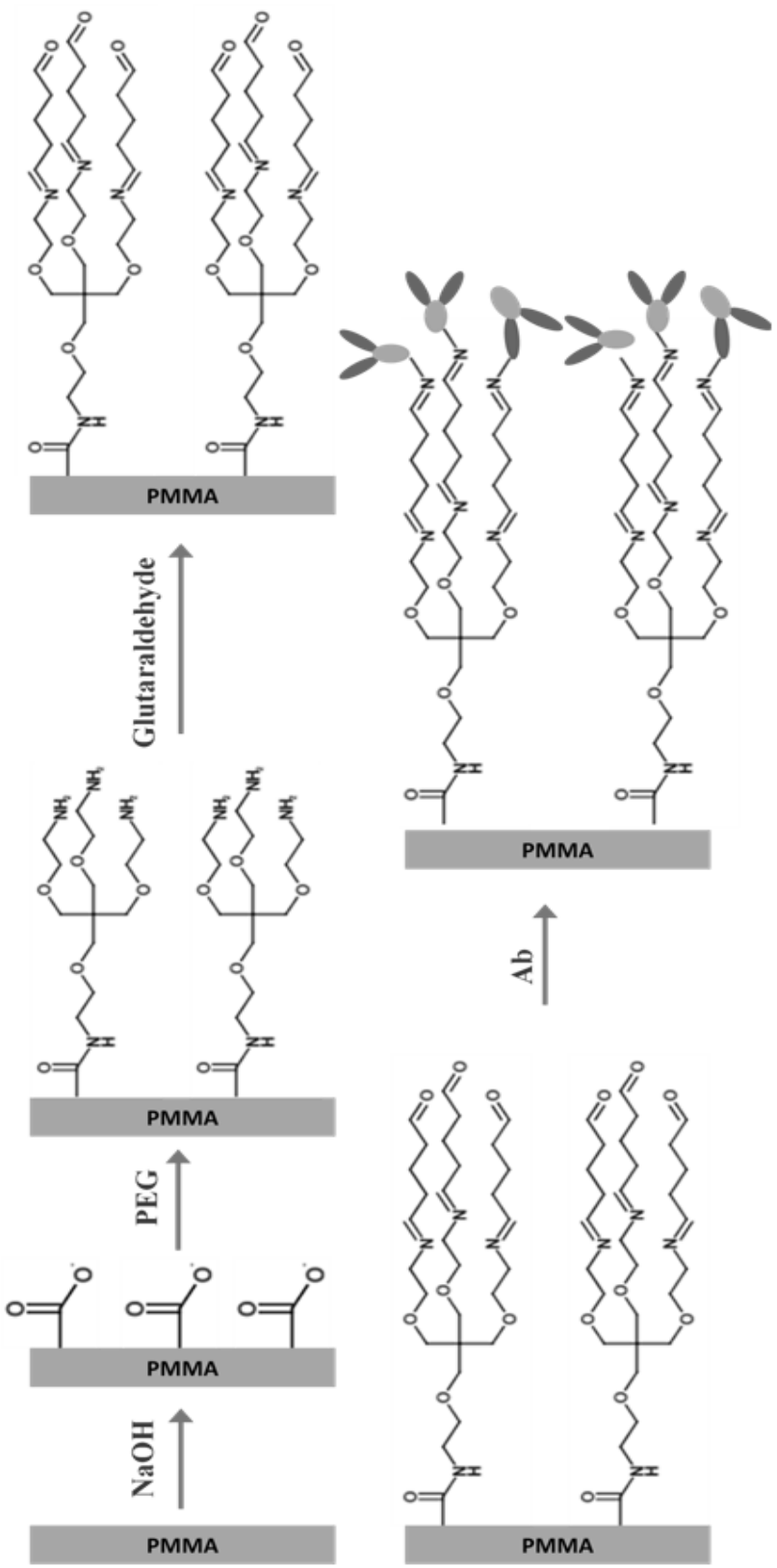

Figure 14: A diagram showing the immobilization of antibody on PMMA using the polyethylene glycol and glutaraldehyde as crosslinkers.

CONTROLS

Passive Adsorption

Polymethylmethacrylate squares were sonicated in isopropyl alcohol for 10min, rinsed with deionized water, and air dried prior to use. 5uL of 500ng/mL of AF488-Ab is placed on the squares for 1 hour. Squares are then washed with 0.05% Tween in 1X PBS pH 7.4. Polymethylmethacrylate squares are then placed antibody side down on a glass slide, with deionized water, and imaged under the calibration curves parameters on the fluorescent microscope.

NaOH only

Polymethylmethacrylate squares were sonicated in isopropyl alcohol for 10min, rinsed with deionized water, and air dried prior to use. Squares were submerged in 60^{o}C 1N sodium hydroxide for 1 hour while shaking at 100RPM. The PMMA squares are then rinsed with 1X PBS 6.0. 5uL of 500ng/mL of AF488-Ab is placed on the squares for 1 hour. Squares are then washed with 0.05% Tween in 1X PBS pH 7.4. Polymethylmethacrylate squares are then placed antibody side down on a glass slide, with deionized water, and imaged under the calibration curves parameters on the fluorescent microscope.

PEI (2k) only

Polymethylmethacrylate squares were sonicated in isopropyl alcohol for 10min, rinsed with deionized water, and air dried prior to use. Polymethylmethacrylate squares are submerged in 0.2% PEI (molecular weight of 2,000 daltons) for 1 hour while on a shaker at 100RPM. The squares are then washed with 0.05% 1X PBS pH 7.4. 5uL of 500ng/mL of AF488-Ab is placed on the squares for 1 hour. Squares are then washed with 0.05% Tween in 1X PBS pH 7.4. Polymethylmethacrylate squares are then placed antibody side down on a glass slide, with deionized water, and imaged under the calibration curves parameters on the fluorescent microscope.

PEI (25k) only

Polymethylmethacrylate squares were sonicated in isopropyl alcohol for 10min, rinsed with deionized water, and air dried prior to use. Polymethylmethacrylate squares are submerged in 0.2% PEI (molecular weight of 25,000 daltons) for 1 hour while on a shaker at 100RPM. The squares are then washed with 0.05% 1X PBS pH 7.4. 5uL of 500ng/mL of AF488-Ab is placed on the squares for 1 hour. Squares are then washed with 0.05% Tween in 1X PBS pH 7.4. Polymethylmethacrylate squares are then placed antibody side down on

a glass slide, with deionized water, and imaged under the calibration curves parameters on the fluorescent microscope.

1% Glutaraldehyde only

Polymethylmethacrylate squares were sonicated in isopropyl alcohol for 10min, rinsed with deionized water, and air dried prior to use. They are then submerged in 1% glutaraldehyde solution for 30minutes while on a shaker at 100RPM. The squares are then washed with 0.05% Tween in 1X PBS pH 7.4. 5uL of 500ng/mL of AF488-Ab is placed on the squares for 1 hour. Squares are then washed with 0.05% Tween in 1X PBS pH 7.4. Polymethylmethacrylate squares are then placed antibody side down on a glass slide, with deionized water, and imaged under the calibration curves parameters on the fluorescent microscope.

NaOH, 1% Glutaraldehyde

Polymethylmethacrylate squares were sonicated in isopropyl alcohol for 10min, rinsed with deionized water, and air dried prior to use. Squares were submerged in 60^{o}C 1N sodium hydroxide for 1 hour while shaking at 100RPM. The Polymethylmethacrylate squares are then rinsed with 1X PBS 6.0. They are then submerged in 1% glutaraldehyde solution for 30minutes while on a shaker at 100RPM. The squares are then washed with 0.05% Tween in 1X PBS pH 7.4.

5uL of 500ng/mL of AF488-Ab is placed on the squares for 1 hour. Squares are then washed with 0.05% Tween in 1X PBS pH 7.4. Polymethylmethacrylate squares are then placed antibody side down on a glass slide, with deionized water, and imaged under the calibration curves parameters on the fluorescent microscope.

PEI (2k), 1% Glutaraldehyde

Polymethylmethacrylate squares were sonicated in isopropyl alcohol for 10min, rinsed with deionized water, and air dried prior to use. Polymethylmethacrylate squares are submerged in 0.2% PEI (molecular weight of 2,000 daltons) for 1 hour while on a shaker at 100RPM. The squares are then washed with 0.05% 1X PBS pH 7.4. They are then submerged in 1% glutaraldehyde solution for 30minutes while on a shaker at 100RPM. The squares are then washed with 0.05% Tween in 1X PBS pH 7.4. 5uL of 500ng/mL of AF488-Ab is placed on the squares for 1 hour. Squares are then washed with 0.05% Tween in 1X PBS pH 7.4. Polymethylmethacrylate squares are then placed antibody side down on a glass slide, with deionized water, and imaged under the calibration curves parameters on the fluorescent microscope.

PEI (25k), 1% Glutaraldehyde

Polymethylmethacrylate squares were sonicated in isopropyl alcohol for 10min, rinsed with deionized water, and air dried prior to use. Polymethylmethacrylate squares are submerged in 0.2% PEI (molecular weight of 25,000 daltons) for 1 hour while on a shaker at 100RPM. The squares are then washed with 0.05% 1X PBS pH 7.4. They are then submerged in 1% glutaraldehyde solution for 30minutes while on a shaker at 100RPM. The squares are then washed with 0.05% Tween in 1X PBS pH 7.4. 5uL of 500ng/mL of AF488-Ab is placed on the squares for 1 hour. Squares are then washed with 0.05% Tween in 1X PBS pH 7.4. Polymethylmethacrylate squares are then placed antibody side down on a glass slide, with deionized water, and imaged under the calibration curves parameters on the fluorescent microscope.

STATSITICAL ANALYSIS

The surface density of various crosslinkers was compared using an ANOVA test to determine their statistical differences. This was followed by a post hoc Tukey HSD (Honestly Significantly Different) test.

2.2.2.3 Results / Discussion

There are a variety of homo- and hetero-bifunctional crosslinkers that can be used for biosensor applications, including immobilization of antibodies for an immunoassay. One of our goals is to determine, what, if any, differences existed between two commonly used crosslinking polymers – PEI and PEG – and how their structure and molecular weight influenced their ability to capture the antibody. Additionally we compared this data to another commonly used crosslinker, EDC with sNHS, as well as the effect of glutaraldehyde as an additional crosslinking component with the different polymers.

AF488-Ab CONJUGATION

The driving force in exploring crosslinking strategies is to improve potential antigen capture detection through increasing primary antibody coverage. This is a critical parameter in producing high-performing biosensors.

The surface density of immobilized primary antibody is quantified with AF488-Ab. Images collected from the Leica microscope were processed using the Leica software. Several unprocessed images are shown in Figure 15. Passive adsorption (no PMMA surface activation or crosslinker) of AF488-Ab is used as a control. In addition to using passive adsorption as a control, we tested all

combinations of crosslinkers with and without surface activation. These include: only sodium hydroxide, only PEI (2,000 daltons, 2,000 daltons), glutaraldehyde only, sodium hydroxide and glutaraldehyde, no sodium hydroxide followed by PEI (2,000 daltons, 25,000 daltons) with glutaraldehyde, only PEG (1,500 daltons, 2,000 daltons, 25,000 daltons), and no sodium hydroxide followed by PEG (1,500 daltons, 2,000 daltons, 25,000 daltons) with glutaraldehyde. All these immobilization methods produced AF488-Ab capture that was significantly less than EDC / sNHS (all less than 4.0ng/mL). They are shown in Figure 16.

Figure 15: Unprocessed fluorescent images, from the Leica microscope, of AF488-Ab on flat PMMA surfaces using various surface chemistries. Control is passive adsorption with no chemical modifications.

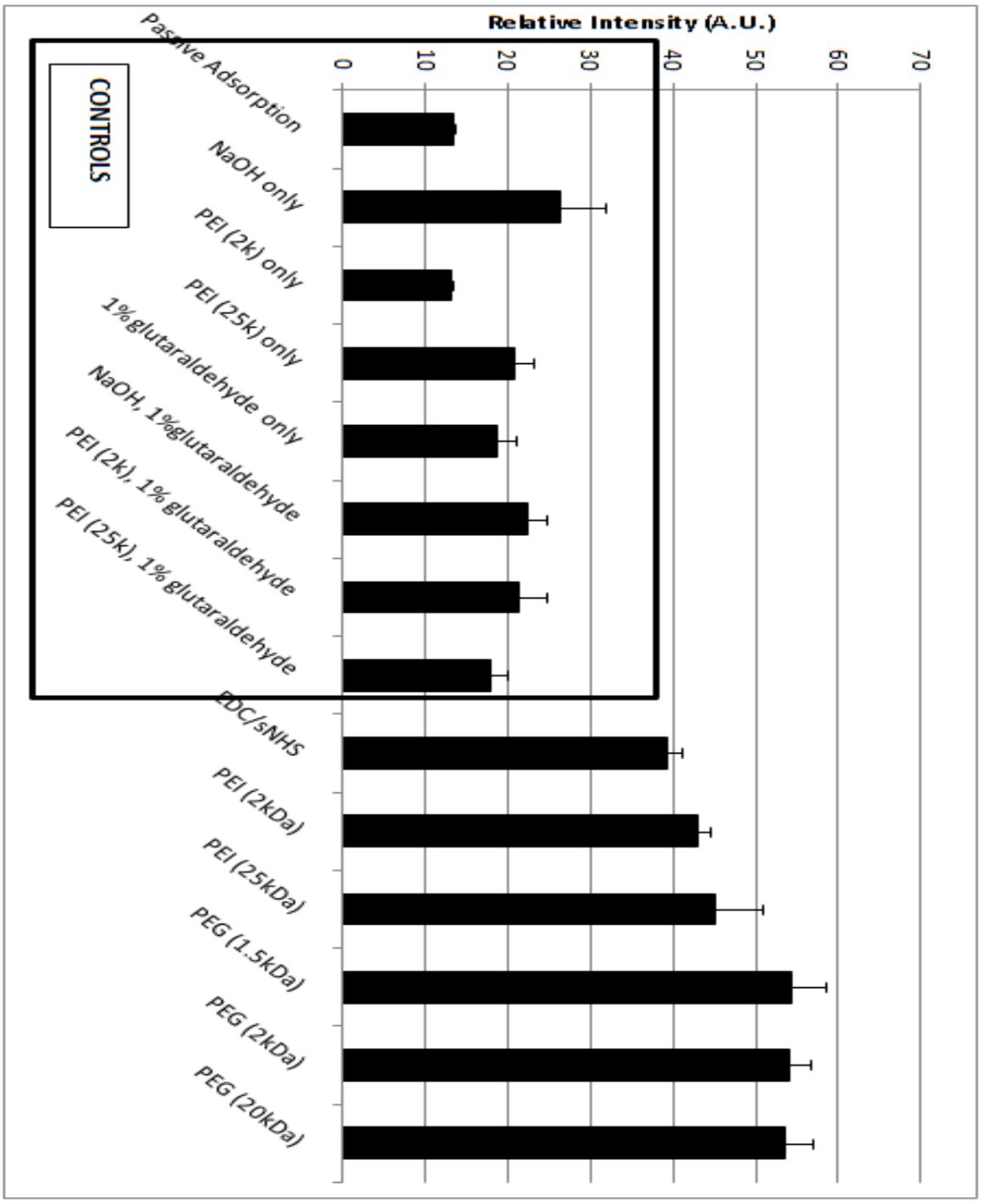

Figure 16: Surface density of immobilized AF488-Ab for all crosslinking combinations. N = 3 for all data points; bars represent standard deviation.

Figure 17 below, highlights the crosslinking combinations of most interest and converts the relative intensity units to surface density (ng/cm^2) of primary antibody using the calibration curve seen in Figure 18. There is more than a 3-fold increase in AF488-Ab immobilization when using the EDC / sNHS crosslinking method, described earlier in the Materials / Methods section, compared to the passive adsorption. We see further immobilization of AF488-Ab using the PEI with glutaraldehyde. The ANOVA test showed there was a significant difference between all crosslinking strategies (passive adsorption, EDC/sNHS, PEIs and PEG) at a $p = 0.001$ level for the conditions [$F(3,18) = 160.48$, $p = 0.0001$. Additionally the post hoc comparison using the Tukey HSD test indicated differences ($p < 0.01$) for all four groups except when comparing EDC/sNHS to the group PEI. Therefore there is no real advantage to using either one of these PEIs over the other. Nonetheless there is increase in AF488-Ab capture ($P < 0.05$, for all PEGs crosslinked with glutaraldehyde) using all PEGs (with glutaraldehyde) over PEIs (with glutaraldehyde). Here we see an immobilization density of just over 8ng of AF488-Ab per square centimeter of PMMA surface for all PEGs with glutaraldehyde. The density is over 4-fold greater than the passive adsorption immobilization and substantially greater than both EDC / sNHS and PEI / glutaraldehyde immobilization methods. As with PEI, we see no difference between AF488-Ab immobilization when using

branched or linear and different molecular weighted PEGs, indicating that all three of these PEGs are equally effective in capturing primary antibody on PMMA. Collectively the ANOVA and Tukey HSD tests suggest there is a real difference between the tested crosslinkers, most notably that the PEG group can immobilize the highest density of antibody.

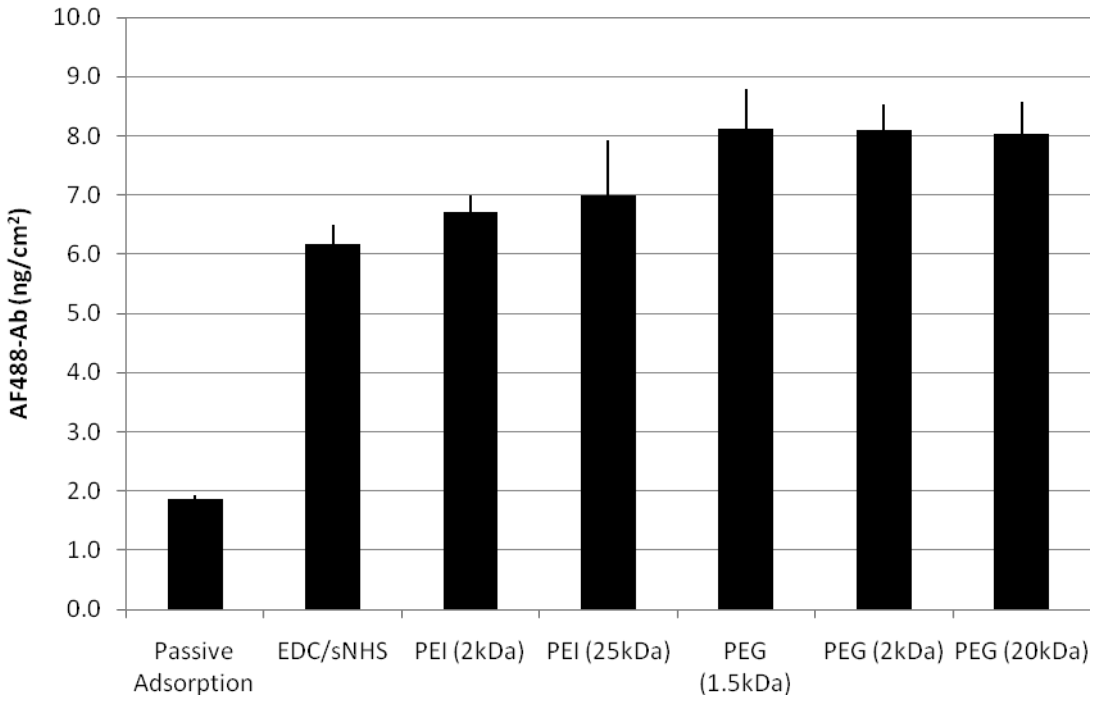

Figure 17: Surface density of immobilized AF488-Ab for various crosslinking combinations. The PEI and PEG displayed were also crosslinked with glutaraldehyde, as described in the Methods section. N = 3 for all data points; bars represent standard deviation. (kDa = kilodaltons)

We have quantitatively determined the surface density of antibody using the calibration curve and the measured intensities. We find the PEG/

glutaraldehyde method binds over 4 times more antibody than passive adsorption, 1.4 times more than EDC/sNHS, and around 1.2-1.3 times more than various PEI /GA. The higher density of primary antibody has potential to capture more antigen in subsequent steps of a sandwich immunoassay. This is of paramount importance in creating a high performing biosensor. Using one of these PEGs crosslinked with glutaraldehyde will give the biosensor a real advantage in sensitivity and lower limit of detection over the other crosslinkers discussed.

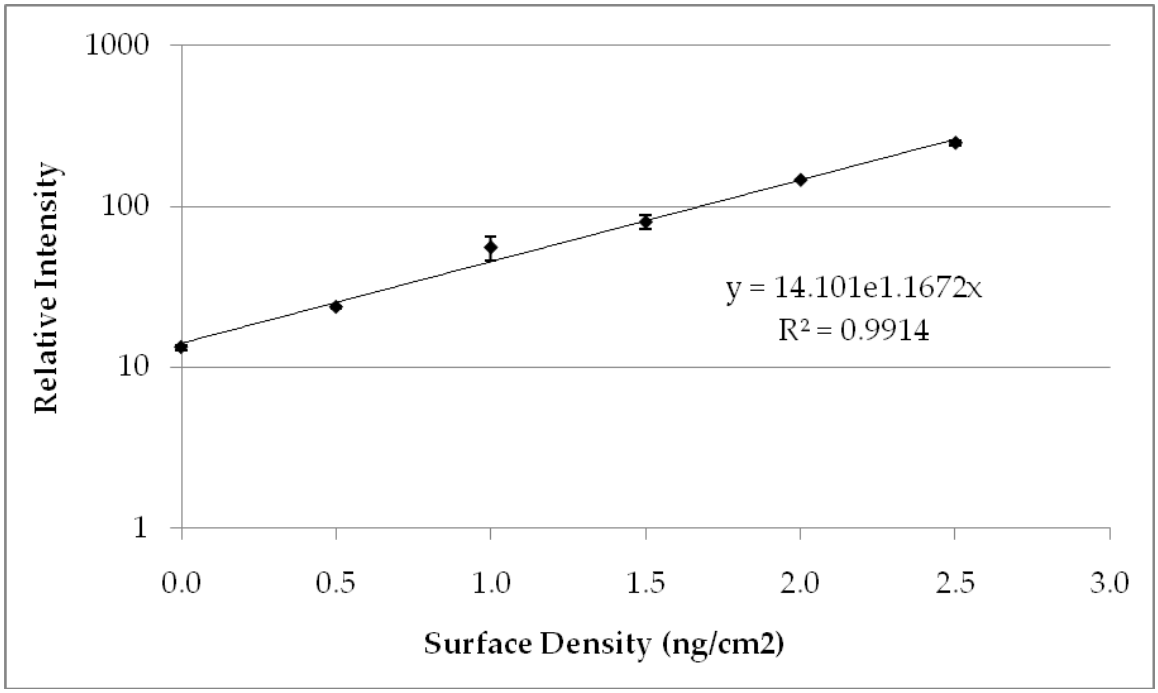

Figure 18: The calibration curve of the AF488-Ab showing the intensity as a function of surface density. Y-axis is plotted on a logarithmic scale. N = 3 for all data points; bars represent standard deviation.

CHAPTER 3: QLISA VALIDATION & BIOMARKERS EVALUATION

3.1 IBD / IBS DIAGNOSTIC BACKGROUND

3.1.1 Myeloperoxidase

Myeloperoxidase (MPO) is a lysosomal protein found in neutrophilic granulocytes, often overexpressed in inflammatory diseases (Kimura & Ikeda-Saito, 1988; Marie-Madeleine CALS, 1991; Merlie, Fagan, Mudd, & Needleman, 1988). Myeloperoxidase is a vital protein found in neutrophilic granulocytes that has an instrumental role in attacking bacteria and foreign pathogens (Klebanoff, 2005). Neutrophilic granulocytes phagocytose pathogens and eliminate them through chemical reactions. It's been reported that myeloperoxidase accounts for 5% of the dry weight of a neutrophilic granulocyte (Scholtz & Kaminker, 1962) . Myeloperoxidase is capable of producing both hypochlorous acid and tyrosyl radicals in independent pathways. Hypochlorous acid and the tyrosyl radical are both cytotoxic and degrade bacteria and foreign pathogens (pathways shown Figure 19). Hypochlorous acid is produced from the oxidation of chloride by hydrogen peroxide, while the tyrosyl radical is produced through the

oxidation of tyrosine by hydrogen peroxide (Hampton, Kettle, & Winterbourn, 1998). It is related to other mammalian peroxidases like eosinophil peroxidase, lactoperoxidase, thyroid peroxidase, and prostaglandin H synthase (Kimura & Ikeda-Saito, 1988; Marie-Madeleine CALS, 1991; Merlie, et al., 1988).

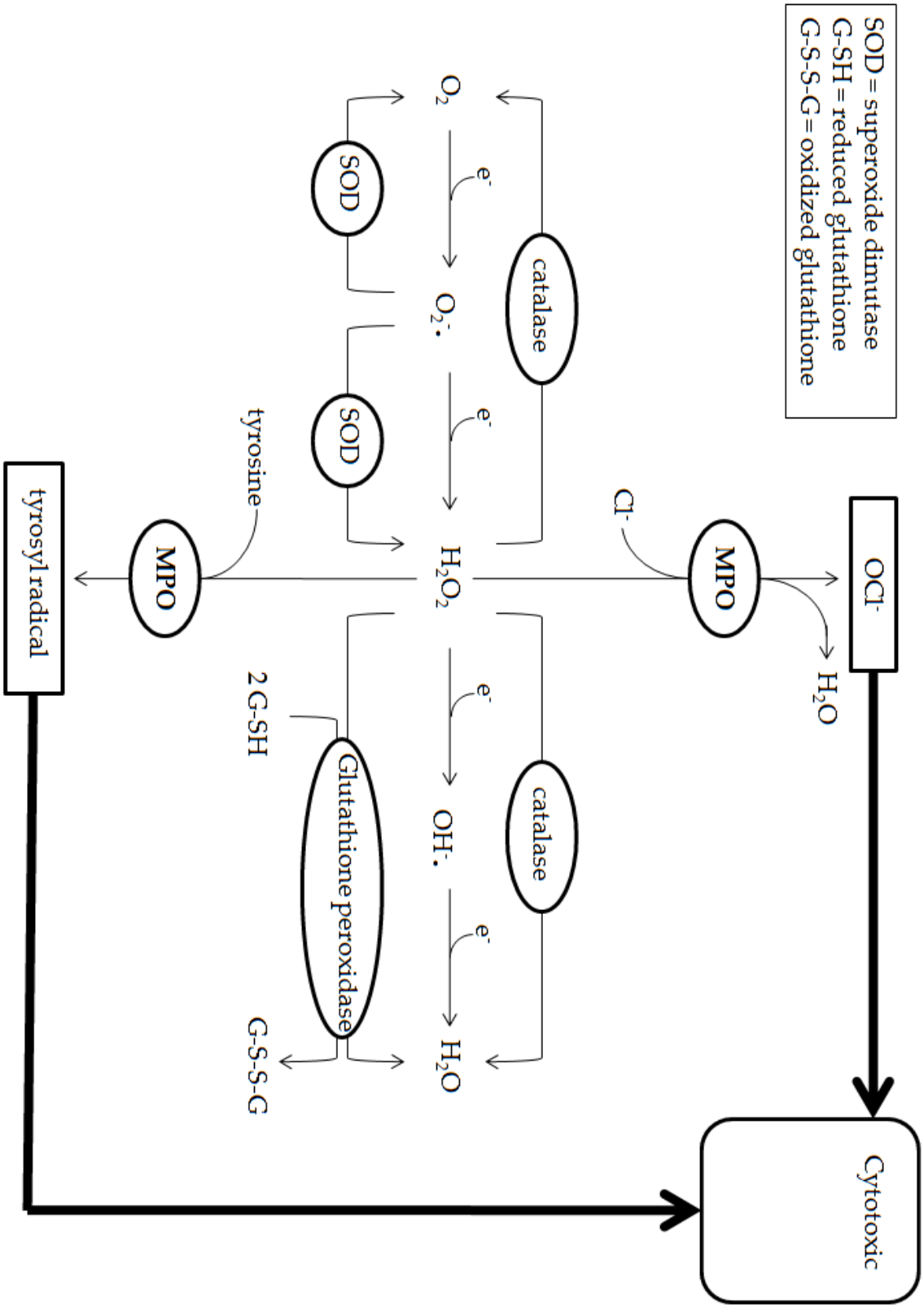

Figure 19: MPO pathways showing the generation of OCl^- and tyrsoyl radical that are responsible for the cytotoxic effects of neutrophils on pathogens.

The crystal structure of human myeloperoxidase was first reported in 1995 (Fenna, Zeng, & Davey, 1995) at a 2.3Å resolution. Later the crystal structure of the native (oxidized) form of myeloperoxidase, as well as myeloperoxidase bound to bromide, chloride (Fiedler, Davey, & Fenna, 2000), and cyanide (–CN) (Blair-Johnson, Fiedler, & Fenna, 2001) have been analyzed at higher resolutions of 1.9Å and 1.8Å. Myeloperoxidase is a 150kDa dimer composed of two identical halves, each with a covalently bound heme. Its crystal structure, taken from RCSB Protein Data Bank, can be seen in Figure 20. The two identical halves of myeloperoxidase are connected by a lone disulfide bond. Myeloperoxidase is composed of two identical sets of polypeptides that are 108 and 466 amino acids long. Their secondary structure is composed predominately of α–helices with very little β–sheets. The heme is bound to myeloperoxidase by two ester linkages of the carboxyl group of Glu^{242} and Asp^{94} to the methyl groups on the pyrrole rings A and C (positions 1 and 5, respectively). The terminal β-carbon on the vinyl group of the pyrrole ring A (position 2) connects the heme to a sulfonium ion linkage at the sulfur atom of Met^{243} (Blair-Johnson, et al., 2001). In addition to the heme group located on each half of the myeloperoxidase molecule there is a bound calcium ion and three Asn-linked glycosylations (at Asn^{189}, Asn^{225}, Asn^{317}) (Zeng & Fenna, 1992).

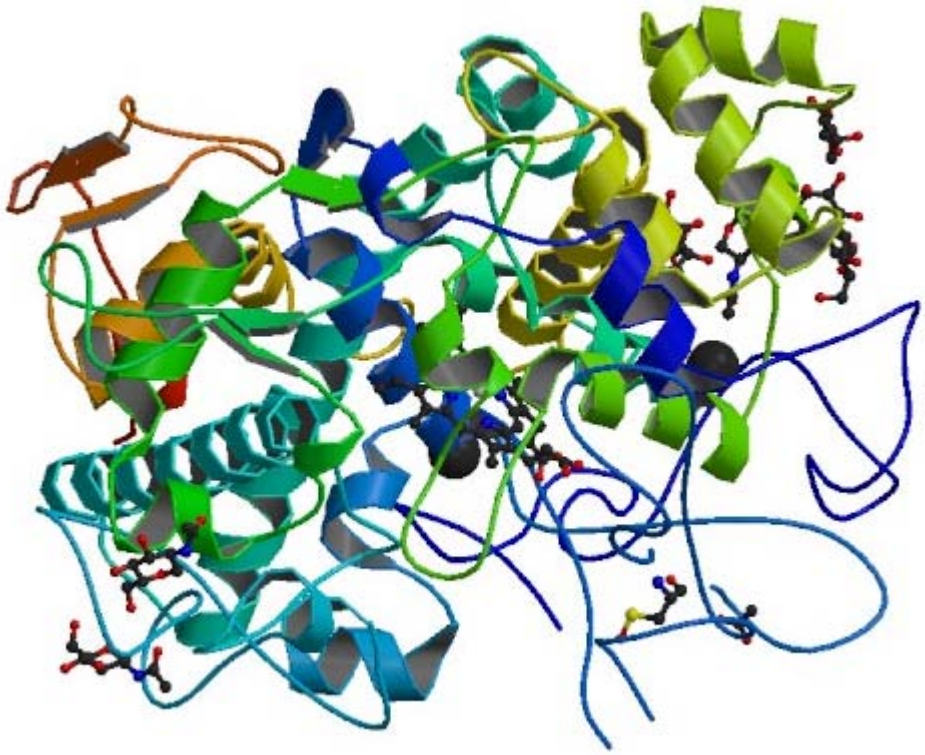

Figure 20: Crystal structure of myeloperoxidase from human leukocytes (Carpena et al., 2009). Image and caption taken, with permission, from the RCSB Protein Data Bank.

Researchers from Cleveland Clinic Foundation discovered myeloperoxidase's correlation to the initiation, progression and further complications of atherosclerotic plaque, and as such, myelpoeroxidase's potential ability to predict prognosis and therapeutic efficacy of atherosclerotic cardiovascular disease (Nicholls & Hazen, 2005).

3.1.2 Lactoferrin

Lactoferrin (LF, also known as lactotransferrin) is an 80kDa, iron-binding glycoprotein from the transferrin family. Transferrin is a beta-1-glycoprotein synthesized in the liver and binds free floating iron via its two non-cooperative binding sites. Although it binds other metals, it binds iron with the highest affinity and only in the Fe^{3+} (ferric) oxidation state, not the Fe^{2+} (ferrous).

Under normal physiological conditions *all* ferric ions are bound to transferrin with plenty of transferrin without any bound ferric ions remaining. This allows the unbound transferrins to bind any new ferric ions that are produced, which keeps the free ferric ion concentration near zero. This is important since many microorganisms are dependent on free iron. So when serum transferrin levels approach saturation with iron there becomes free unbound iron available to microorganisms, which may help them to flourish. For instance, vibrio vulnificus is found on some shellfish, like oysters, and individuals, with extremely high iron, who consume them, may develop a potentially deadly infection. Individuals who consume the same shellfish and have physiological normal levels of iron will be completely fine. Transferrins role in iron absorption through the gut and into the blood for transport can be

seen in Figure 21 (see yellow highlighted regions). The transferrin receptors regulate receptor-mediated endocytosis of ferric bound transferrin which then recycles the transferrin back to the plasma membrane to be recycled.

The lactoferrin protein is secreted in human milk and several other fluids like saliva. It was first discovered in human milk, which is where its name is derived (Groves, 1960). It is found in activated secondary granules of neutrophils and has been shown to increase during acute inflammatory responses (LÃ¶nnerdal & Iyer, 1995) (B. F. Anderson et al., 1987). This is most important to our research, as we believe this inflammatory response is great enough that lactoferrin levels increase at an extremely high rate. Its structure is shown in Figure 22.

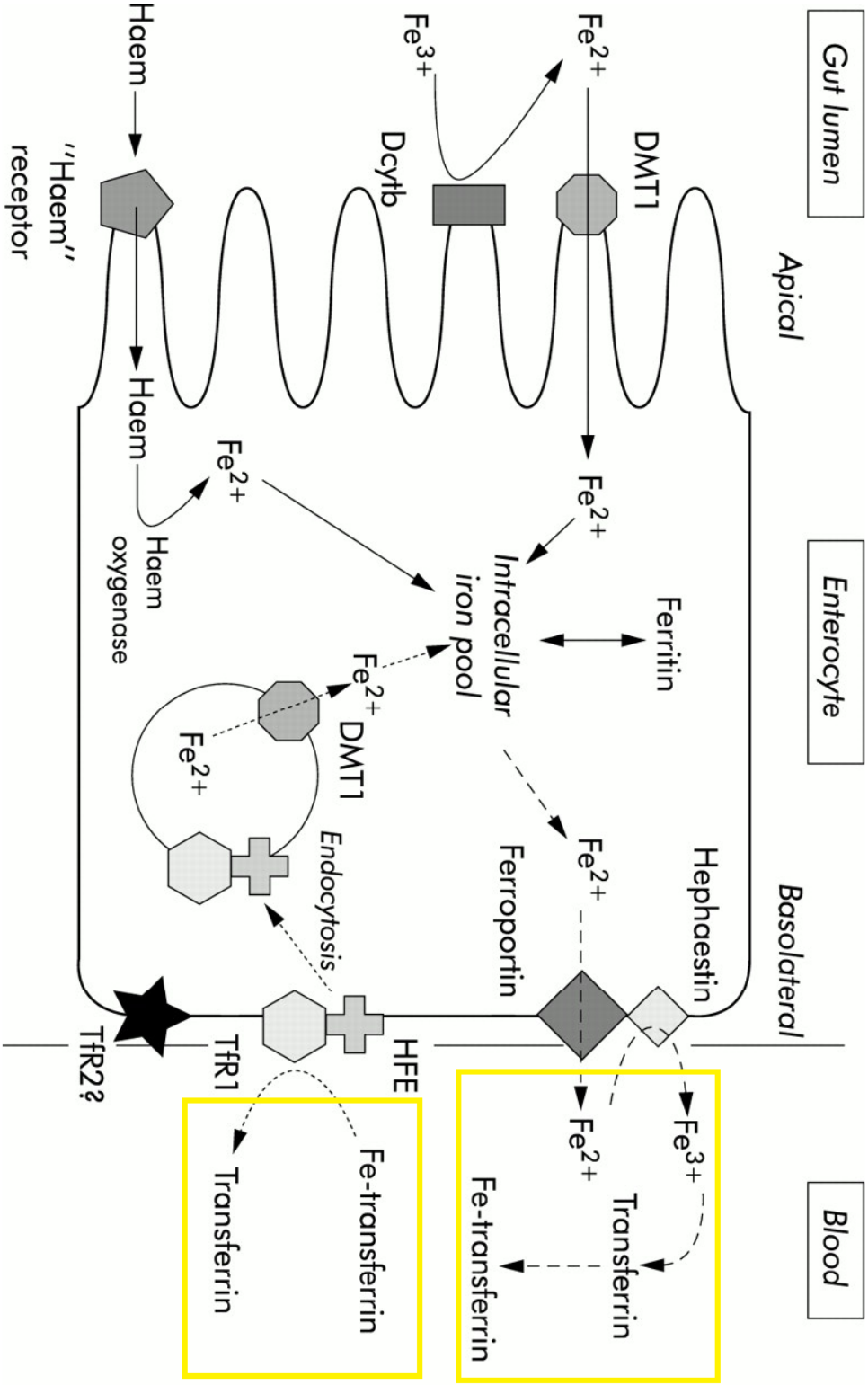

Figure 21: Pathway of iron absorption from the intestines to the blood where iron binds the glycoprotein transporter transferrin. This schematic is adapted, with permission, from Trinder, D., et. al. (Trinder, Fox, Vautier, & Olynyk, 2002)

Figure 22: Crystal Structure of C-lobe of Bovine lactoferrin complexed with lipopolysaccharide at 2.0 A Resolution (Shukla, 2011). Image and caption taken, with permission, from the RCSB Protein Data Bank.

3.1.3 Clinical Significance

Both myeloperoxidase and lactoferrin have been associated with general inflammation given neutrophils rapid response in acute inflammation (Peterson,

Eklund, Taha, Raab, & Carlson, 2002). Raab et. al. (Raab, Gerdin, Ahlstedt, & HÃ¤llgren, 1993) showed a seven-fold increase in MPO in perfusion fluid of 16 ulcerative colitis patients compared to healthy controls. Lettesjo et. al. (LettesjÃ¶ et al., 2006) demonstrated an increase in myeloperoxidase from stool samples in patients with collagenous colitis (18 patients) over both irritable bowel syndrome and healthy control patients. Another study of 18 inflammatory bowel disease patients showed an elevation of neutrophil proteins in stool samples, including myeloperoxidase, over healthy controls (Peterson, et al., 2002). The most interesting findings came from Saiki, T., where he found increased stool concentrations of myeloperoxidase in active ulcerative colitis and Crohn's Disease patients compared to inactive ulcerative colitis and Crohn's Disease patients, as well as the healthy controls, but not other non-IBD, inflammatory controls (Saiki, 1998). This study included 65 inflammatory bowel disease patients and showed potential for myeloperoxidase as a biomarker for monitoring progression of treatment of inflammatory bowel disease. These studies all used a commercial radioimmunoassay (Pharmacia Diagnostics AB, Uppsala, Sweden) to measure myeloperoxidase levels. While radioimmunoassays have advantages their most obvious disadvantage is the use of radioactive material and the associated safety and regulation oversight. Regardless, these earlier studies have demonstrated the feasibility of

myeloperoxidase as a biomarker for inflammatory bowel disease. Additional studies have elevated levels of myeloperoxidase might indicate an incomplete response to treatment (of ulcerative colitis and Crohn's disease patients) while decreased levels indicate a full response to treatment (Wagner, Peterson, Ridefelt, Sangfelt, & Carlson, 2008). What remains unknown is how myeloperoxidase correlates to different types of inflammatory bowel disease, is myeloperoxidase effective as a diagnostic and/or prognostic biomarker, can it monitor treatment efficacy and what are cutoff values to distinguish between healthy and diseased patiented.

Lactoferrin has also demonstrated an association between increased levels in stool samples and inflammatory bowel disease (Turkay & Kasapoglu, 2010). Compared to myeloperoxidase, lactoferrin has been investigated more extensively and thus would be considered a more established biomarker for inflammatory bowel disease. Some notable studies include Dai et. al. who looked at fecal lactoferrin levels in active / inactive ulcerative colitis and Crohn's disease patients, irritable bowel syndrome patients and healthy volunteers (Dai, Liu, Zhao, Hu, & Ge, 2007). They found that active inflammatory bowel disease patients had higher fecal levels of lactoferrin. Further they found high sensitivity and specificity for ulcerative colitis and Crohn's disease – 92% and 88%, and 92%

and 80%, respectively. Another group (Kane et al., 2003), who examined a ulcerative colitis, Crohn's disease, irritable bowel syndrome along with healthy controls for fecal concentrations of lactoferrin concluded that elevated levels were 100% accurate at ruling out irritable bowel syndrome while they were also 90% accurate in identifying inflammatory bowel disease. This study supports the use of lactoferrin as a diagnostic biomarker to help differentiate inflammatory bowel disease and irritable bowel syndrome. Another group (A. M. Schoepfer, M. Trummler, P. Seeholzer, D. H. Criblez, & F. Seibold, 2007) expanded their inflammatory bowel disease patients to also examine ischemic colitis, collagenous colitis and medically-induced colitis, in addition to ulcerative colitis, Crohn's disease, irritable bowel syndrome and healthy patients. They looked at several fecal biomarkers including lactoferrin, which had 91% accuracy in discriminating inflammatory bowel disease from irritable bowel syndrome. These studies demonstrate that lactoferrin has great potential in helping diagnose inflammatory bowel disease, possibly even the type of inflammatory bowel disease, as well as helping rule out irritable bowel syndrome as a diagnosis. These questions lead to the ultimate question of how and where lactoferrin evaluation is best suited to help physicians treat patients.

However several areas still need to be better defined, including threshold cutoffs between diseased and healthy patients and lactoferrin's true sensitivity and specificity to inflammatory bowel disease since research groups have reported a range of values that are typically limited to a specific populations and don't necessarily consider the broader population (Otten et al., 2008) (Sipponen et al., 2008) (Langhorst et al., 2008) (A. Schoepfer, M. Trummler, P. Seeholzer, D. Criblez, & F. Seibold, 2007; Schoepfer, Trummler, Seeholzer, Seibold-Schmid, & Seibold, 2008).

Myeloperoxidase and lactoferrin have also been identified as potential biomarkers for medical conditions like urinary tract infections (Pan et al., 2010; Steinhoff et al., 1997), rhemutoid arthritis (Lefkowitz & Lefkowitz, 2001), and other inflammatory diseases.

3.2 EXPERIMENTAL SECTION

The Experimental Section is laid out over four subsections: Objectives / Goals, Materials / Methods, Results and Discussion. Here we discuss some of the most critical findings from this research, including the validation of QLISA

through comparison with ELISA and conclusions regarding myeloperoxidase and lactoferrin fecal concentrations in patients with different inflammatory bowel disease.

3.2.1 Overview / Goals

The goal of the following experiments is two-fold. First we want to establish that the QLISA system we have developed is a functional system that can determine concentrations of both myeloperoxidase and lactoferrin. This goal requires complete system optimization of all steps from biofunctionalization of the inert PMMA surface through image acquisition and processing. The QLISA system is validated through different experiments including quantitative comparison using ELISA kits. The second goal of this chapter is to correlate our myeloperoxidase and lactoferrin concentrations found in human fecal samples to their clinical condition (i.e. a type of inflammatory bowel disease or healthy control). These findings correlating myeloperoxidase and lactoferrin to inflammatory bowel disease patients is probably the most exciting finding since these correlations have very little presence in literature

3.2.2 Materials / Methods

3.2.2.1 Protein Extraction – Human Stool Sample

Human stool samples are collected, aliquoted, and stored at -80°C by our clinical collaborators at Drexel University's College of Medicine. Samples are then brought to Main Campus for QLISA analysis. Procedures are followed as outlined in the approved IRB.

Stool samples are weighed and diluted 5 times (v/w) with an extraction buffer. The extraction buffer is 8.359mg of ethylenediaminetetraacetic acid (EDTA), 250uL of fetal bovine serum (FBS), 5mL of glycerol, 12.5uL of tween, 250uL protease inhibitor cocktail and 25mL of 1X PBS pH 7.4. Once the samples are diluted, they are allowed to incubate at 4°C for 15 minutes. The solution is then homogenized and then incubated again at 4°C for 15 minutes. This solution is then centrifuged at 4°C at 14,000RPM for 30 minutes. All samples were diluted 1:10, 1:100, 1:1000, and 1:10,000 in 1X PBS pH 7.4. Each of these dilutions was tested for both QLISA and ELISA.

Polymethylmethacrylate was purchased from Paradigm Optics Inc. (Vancouver, Washington) in a microcapillary shape with an inner diameter of

250um and an outer diameter of 500um. Sodium hydroxide, and isopropyl alcohol were purchased from VWR (Radnor, Pennsylvania). Branched, di-amino polyethylene glycol (molecular weight of 1,500 daltons), and linear di-amino polyethylene glycol (molecular weight of 2,000 and 20,000 daltons) were purchased from Sigma Aldrich (St. Louis, Missouri). Glutaraldehyde (50%w/v) was also purchased from Sigma Aldrich (St. Louis, Missouri). A rabbit anti-human polyclonal myeloperoxidase antibody was purchased from AbD Serotec (Raleigh, North Carolina). Additionally a sheep anti-human polyclonal lactoferrin antibody was purchased from AbD Serotec (Raleigh, North Carolina). The myeloperoxidase antigen was purchased from Lee Biosolutions and the lactoferrin antigen was purchased from AbD Serotec (Raleigh, North Carolina). A quantum dot antibody conjugation kit was purchased from Invitrogen (Carlsbad, California). A biotinylated monoclonal myeloperoxidase antibody was purchased from US Biological (Swampscott, Massachusetts). The biotinylated polyclonal lactoferrin antibody was purchased from Abcam (Cambridge, MA). Streptavidin conjugated quantum dot was purchased from Invitrogen (Carlsbad, California). Fetal Bovine Serum (FBS) was purchased from Sigma Aldrich (St. Louis, Missouri). 10X phosphate buffer saline (PBS) was purchased from AbD Serotec (Raleigh, North Carolina) and diluted to 1X.

3.2.2.2 1st Generation QLISA

This is the original protocol for the QLISA system. This protocol is very similar to the 2nd generation QLISA protocol except for differences in secondary antibody and quantum dot capture. That protocol is presented immediately following this protocol.

Preparing Microcapillary Surface

1.1 The PMMA microcapillary with an inner diameter of 250um and outer diameter of 500um is cut into a 50cm piece. 70% isopropanol is circulated through the 50cm piece of microcapillary for 10 minutes at room temperature using the peristaltic pump set to 1.8%. A labeled photograph is shown in Figure 23 of the peristaltic pump, which is used in this step and subsequent steps.

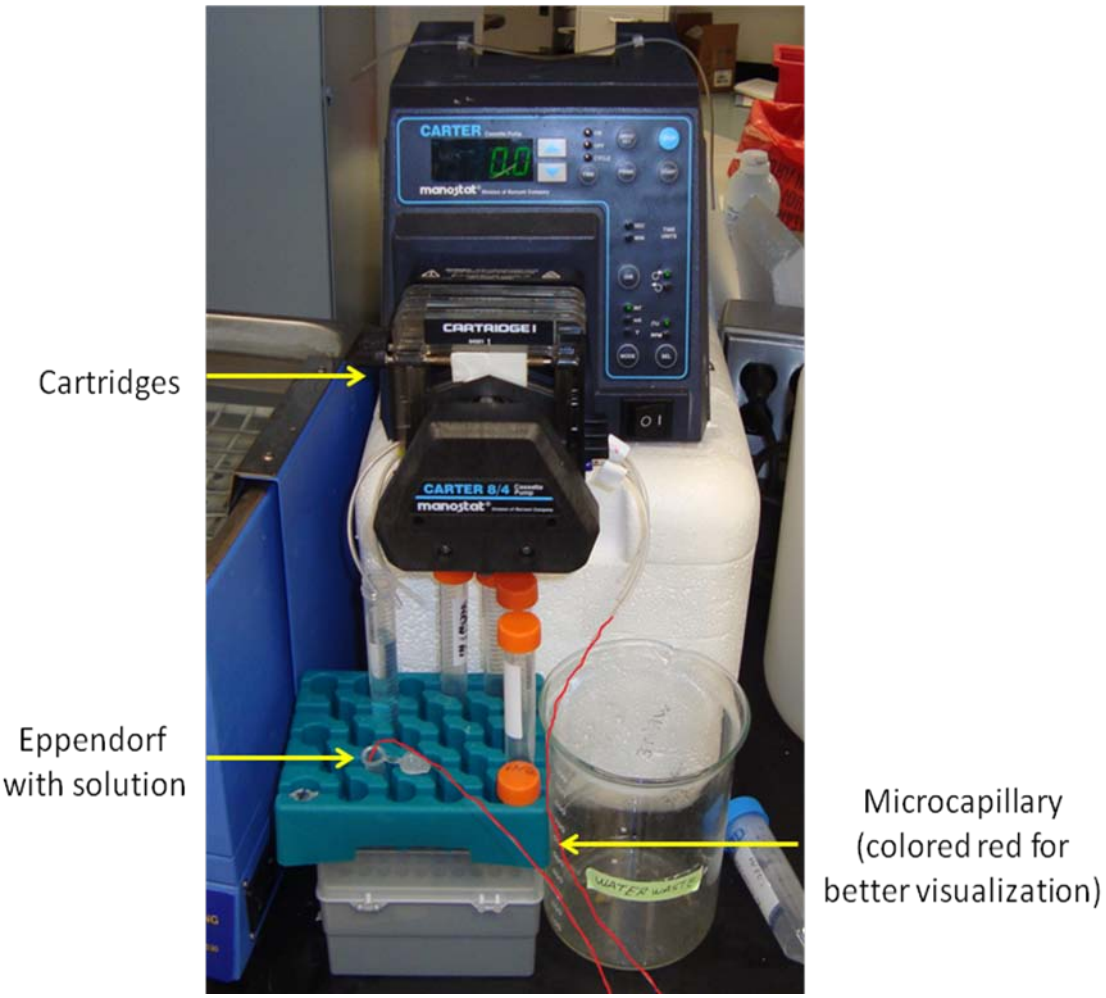

Figure 23: Photograph of the peristaltic pump to demonstrate how it works. Multiple cartridges can be loaded allowing parallel QLISA assays to be run simultaneously. The red line is the microcapillary and colored to help better visualize it.

1.2 Rinse with deionized water for 4 minutes at room temperature using the peristaltic pump set to 1.8%.

Microcapillary Surface Activation

2.1 Incubate 1N sodium hydroxide for 30minutes at 60°C.

2.2 Rinse with deionized water for 4 minutes at room temperature using the peristaltic pump set to 1.8%.

Microcapillary Surface Functionalization

3.1 Circulate 1.5mL of 104.7mM 1-ethyl-3-(3-dimethylaminopropyl) carbodiimide with 21.7mM sulpho-N-hydroxysulfosuccinimide of sNHS in 1X PBS pH 6.0 for 1 hour at room temperature using the peristaltic pump set to 1.8%.

3.2 Rinse with deionized water for 4 minutes at room temperature using the peristaltic pump set to 1.8%.

Primary Antibody Immobilization

4.1 Circulate 1.5mL of 200nM polyclonal myeloperoxidase antibody for 1 hour at room temperature using the peristaltic pump set to 1.8%.

4.2 Rinse with 0.05% Tween in 1X PBS pH 7.4 for 4 minutes at room temperature using the peristaltic pump set to 1.8%.

4.3 Circulate 1.5mL of 2% FBS in 1X PBS pH 7.4 for 1 hour at room temperature.

4.4 Rinse with 0.05% Tween in 1X PBS pH 7.4 for 4 minutes at room temperature using the peristaltic pump set to 1.8%.

Antigen Capture

5.1 Cut the PMMA microcapillary into 5cm pieces.

5.2 Using a syringe with a Hamilton septum adapter introduce the sample. Allow the sample to incubate in the microcapillary for 1 hour at room temperature.

Note: Here, *sample* can refer to human fecal samples following protein extraction, positive controls with various concentrations of either myeloperoxidase or lactoferrin, or a negative control that's 1X PBS pH 7.4.

5.3 Rinse with 0.05% Tween in 1X PBS pH 7.4 for 10 minutes at room temperature using the syringe pump set to 20uL/minute (200uL total washing volume). This process is demonstrated in Figures 24 and 25, which is the syringe pump that can simultaneously hold and pump 10 syringes.

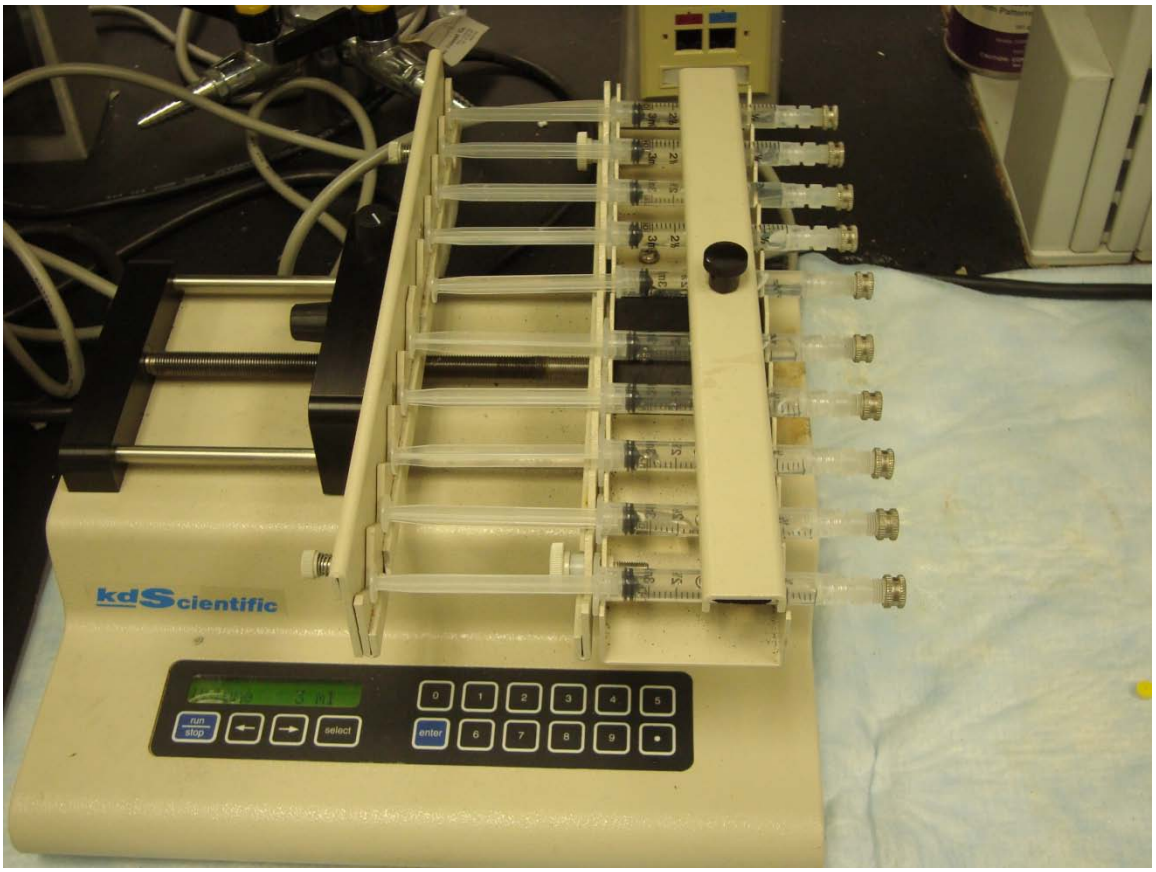

Figure 24: A photograph of the syringe pump loaded with 10 3mL syringes with Hamilton septum adapters and connecters that allow connection to the microcapillary.

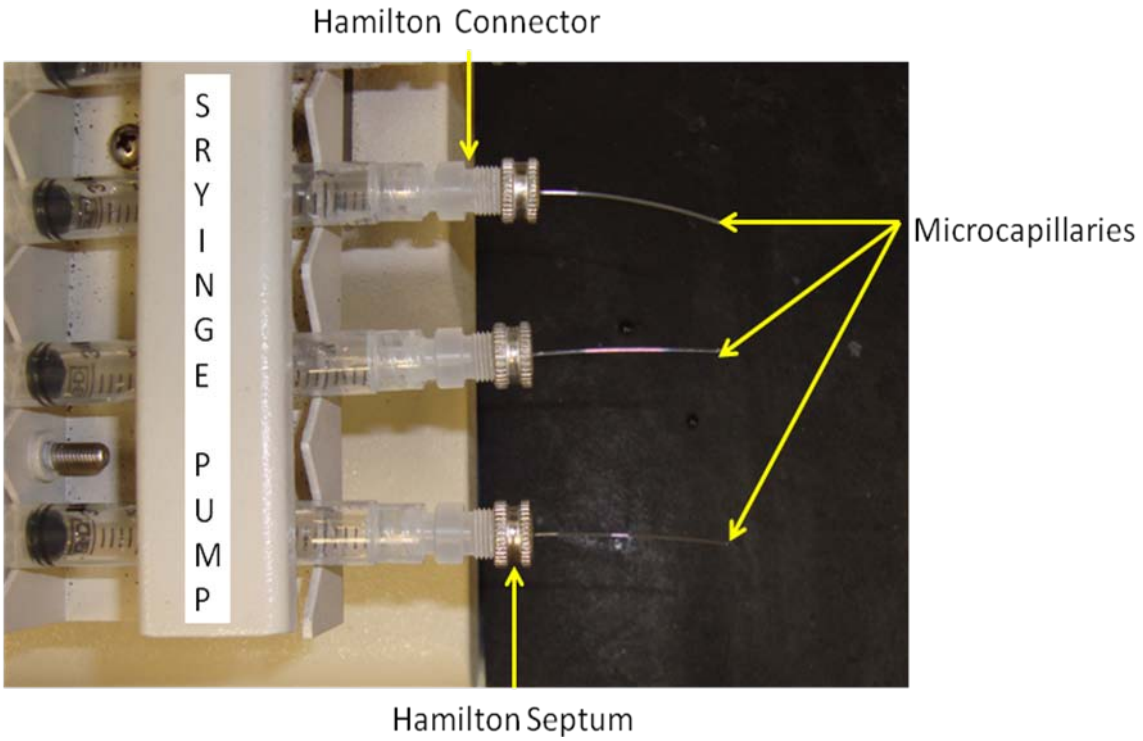

Figure 25: Zoomed up view of microcapillaries loaded via Hamilton connectors with septum into the syringe pump.

Secondary Antibody Capture

6.1 Incubate 100nm of quantum dot – antibody conjugate (previously conjugated using Invitrogen's conjugation kit) for 1 hour at room temperature.

Note: The protocol for conjugation of quantum dot to secondary antibody is given in Appendix C since this is a critical procedure for this QLISA protocol.

6.2 Rinse with 0.05% Tween in 1X PBS pH 7.4 for 10 minutes at room temperature using the syringe pump set to 20uL/minute (200uL total washing volume).

Image Acquisition

7.1 The 5cm piece microcapillaries are individually loaded into the microcapillary holder. The quantum dots are excited with an ultraviolet light (385nm wavelength) emitting diode with an 80mW optical power rating (Nichia Corporation). The LED has a $1mm^2$ spot size. This configuration is shown in Figure 26 and 27.

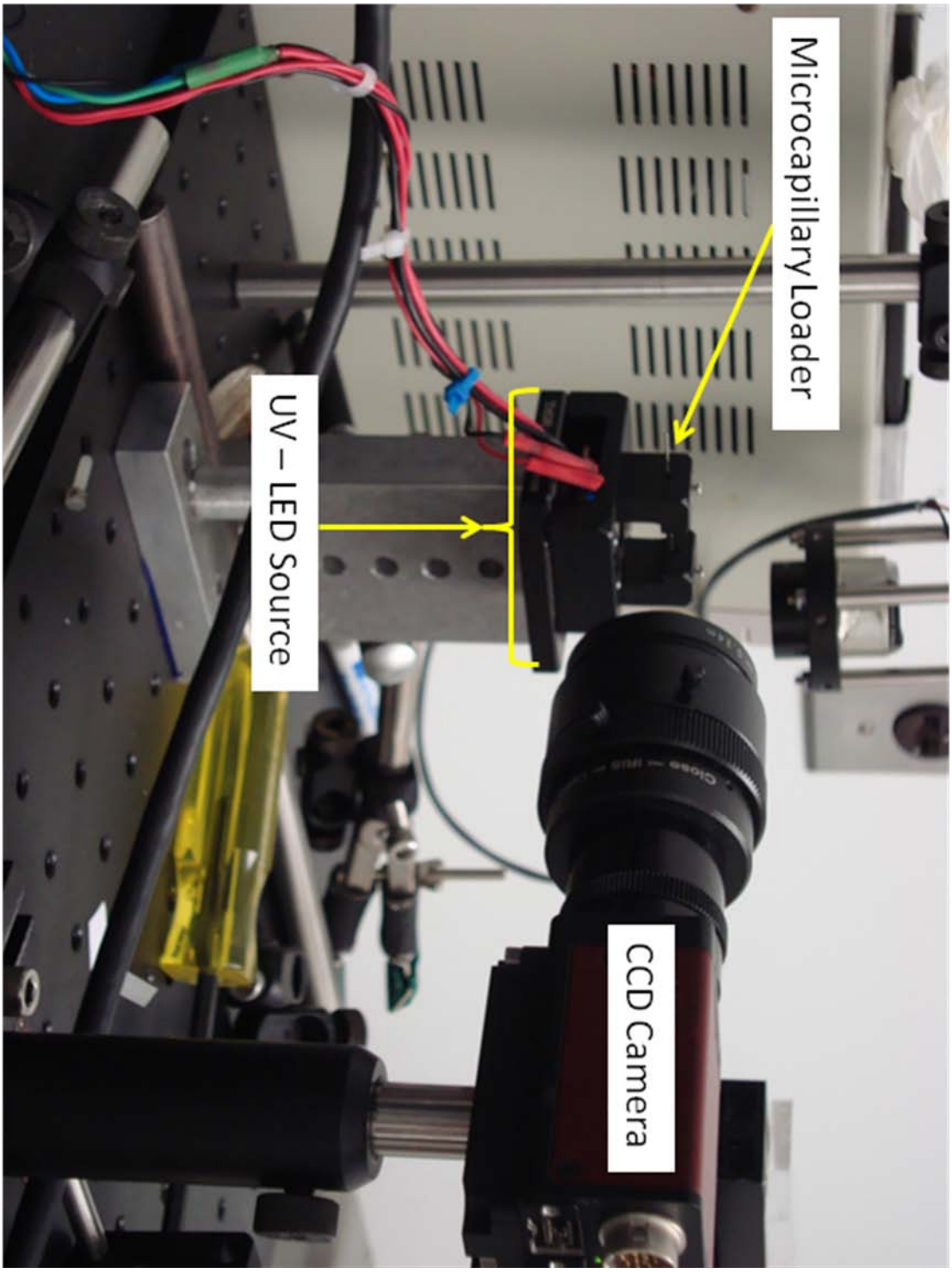

Figure 26: Setup of optical detection system with the UV - LED source focused directly below the microcapillary that is loaded into the loader. The CCD camera is focuseddirectly on the microcapillary and is orthoganol to the UV - LED source.

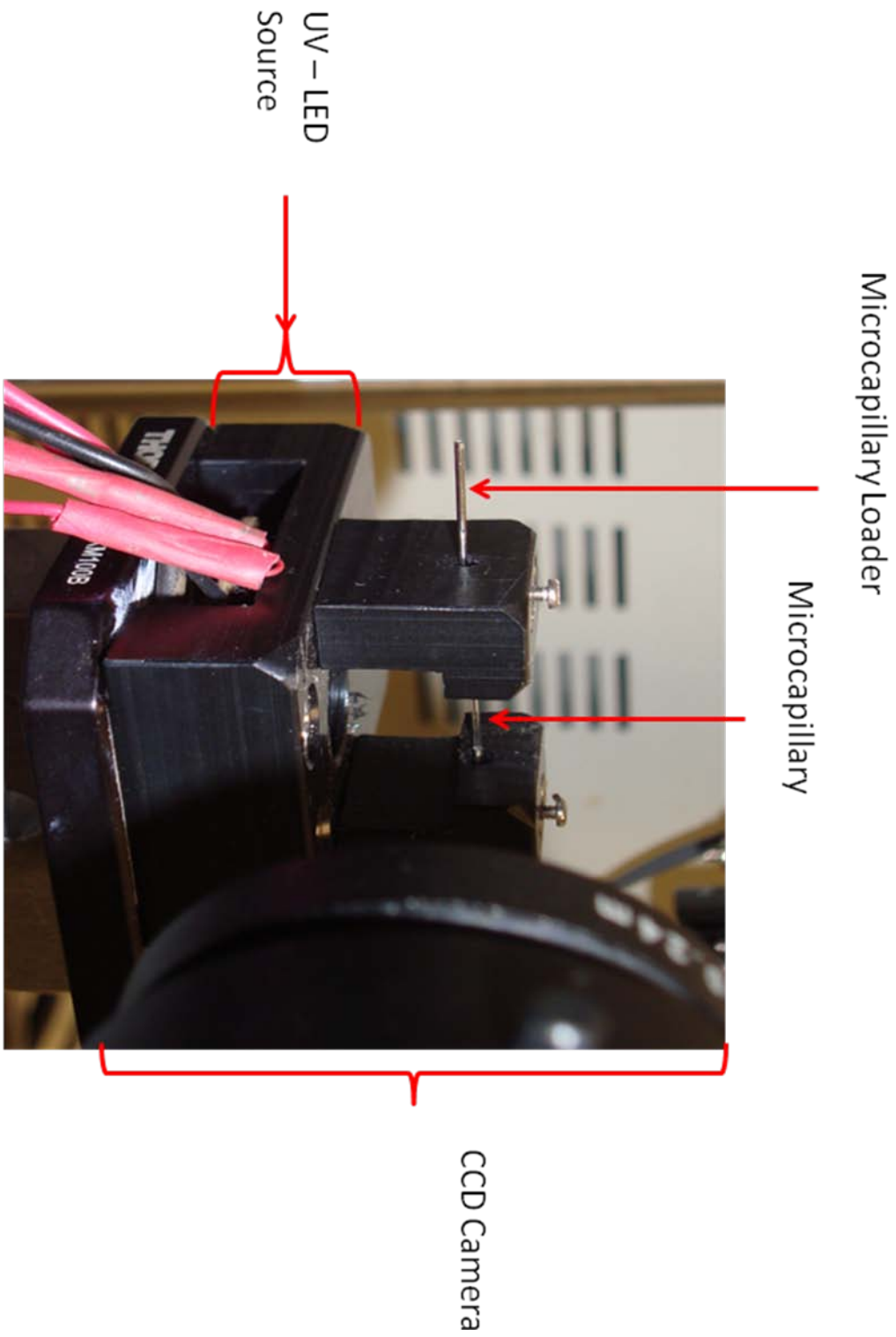

Figure 27: Here is a zoomed in view of the microcapillary loader showing the microcapillary in position with the UV -- LED source and CCD camera.

7.2 When the quantum dots fluoresces the computer software program AVT SmartView can capture an image.

Image Processing

8.1 Images are downloaded from the computer and processed with NIH's ImageJ software package to determine the fluorescent level inside the capillaries. Raw images are zoomed in on the region of interest (ROI). The ROI is selected between the capillary walls. That region is measured for average pixel intensity. This number can then be compared to a standard calibration curve to determine the myeloperoxidase or lactoferrin concentration. An overview is depicted in Figure 28.

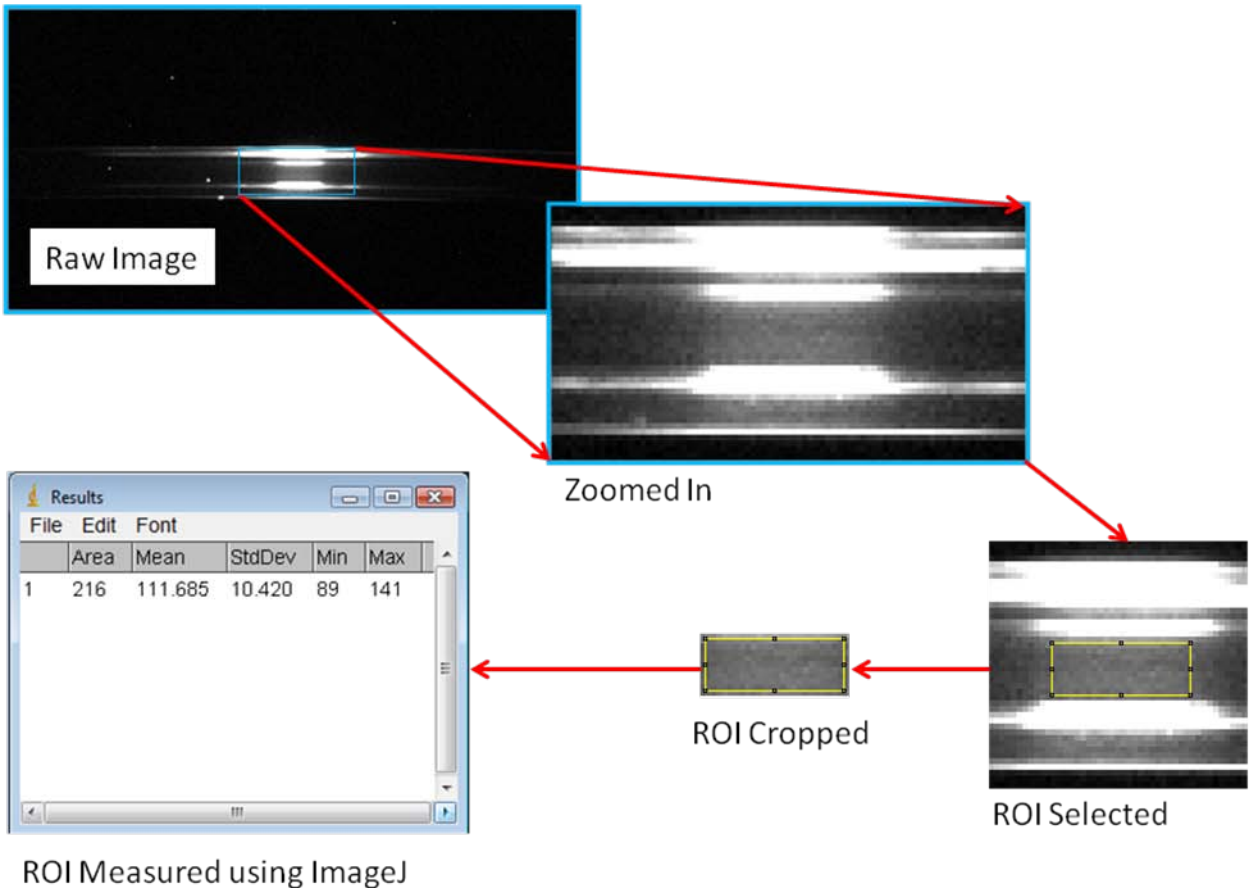

Figure 28: Overview of the image processing. The raw image is zoomed in on the ROI, which is then selected and processed with ImageJ to determine the intensity of quantum dot fluorescence.

3.2.2.3 2nd Generation QLISA

The major difference between this QLISA system and the one described above is the use of a biotinylated secondary antibody that subsequently binds a streptavidin conjugated quantum dot.

Preparing Microcapillary Surface

1.2 The PMMA microcapillary with an inner diameter of 250um and outer diameter of 500um is cut into a 50cm piece. 70% isopropanol is circulated through the 50cm piece of microcapillary for 10 minutes at room temperature using the peristaltic pump set to 1.8%.

1.2 Rinse with deionized water for 4 minutes at room temperature using the peristaltic pump set to 1.8%.

Microcapillary Surface Activation

2.1 Incubate 1N sodium hydroxide for 30minutes at 60^{o}C.

2.2 Rinse with deionized water for 4 minutes at room temperature using the peristaltic pump set to 1.8%.

Microcapillary Surface Functionalization

3.1 Circulate 1.5mL of 0.2% di-amino polyethylene glycol (molecular weight 1,500 Daltons) for 1 hour at room temperature using the peristaltic pump set to 1.8%.

3.2 Rinse with deionized water for 4 minutes at room temperature using the peristaltic pump set to 1.8%.

3.3 Circulate 1.5mL of 1% glutaraldehyde for 30 minutes at room temperature using the peristaltic pump set to 1.8%.

3.4 Rinse with deionized water for 4 minutes at room temperature using the peristaltic pump set to 1.8%.

Primary Antibody Immobilization

4.1 Circulate 1.5mL of 200nM polyclonal myeloperoxidase antibody for 1 hour at room temperature using the peristaltic pump set to 1.8%.

4.2 Rinse with 0.05% Tween in 1X PBS pH 7.4 for 4 minutes at room temperature using the peristaltic pump set to 1.8%.

4.3 Circulate 1.5mL of 2% FBS in 1X PBS pH 7.4 for 1 hour at room temperature.

4.4 Rinse with 0.05% Tween in 1X PBS pH 7.4 for 4 minutes at room temperature using the peristaltic pump set to 1.8%.

Antigen Capture

5.1 Cut the PMMA microcapillary into 5cm pieces.

5.2 Using a syringe with a Hamilton septum adapter introduce the sample. Allow the sample to incubate in the microcapillary for 1 hour at room temperature.

Note: Here, *sample* can refer to human fecal samples following protein extraction, positive controls with various concentrations of either myeloperoxidase or lactoferrin, or a negative control that's 1X PBS pH 7.4.

5.3 Rinse with 0.05% Tween in 1X PBS pH 7.4 for 10 minutes at room temperature using the syringe pump set to 20uL/minute (200uL total washing volume).

Secondary Antibody Capture

6.1 Incubate 100nM of biotinylated secondary antibody (purchased already conjugated) for 1 hour at room temperature.

6.2 Rinse with 0.05% Tween in 1X PBS pH 7.4 for 10 minutes at room temperature using the syringe pump set to 20uL/minute (200uL total washing volume).

6.3 Incubate 100nM of streptavidin conjugated quantum dots for 1 hour at room temperature.

6.4 Rinse with 0.05% Tween in 1X PBS pH 7.4 for 10 minutes at room temperature using the syringe pump set to 20uL/minute (200uL total washing volume).

Image Acquisition

7.1 The 5cm piece microcapillaries are individually loaded into the microcapillary holder. The quantum dots are excited with an ultraviolet light (385nm wavelength) emitting diode with an 80mW optical power rating (Nichia Corporation).

7.2 When the quantum dots fluoresces the computer software program AVT SmartView can capture an image.

Image Processing

8.1 Images are downloaded from the computer and processed with NIH's ImageJ software package to determine the fluorescent level inside the capillaries. Raw images are zoomed in on the region of interest (ROI). The ROI is selected between the capillary walls. That region is measured for average pixel intensity. This number can then be compared to a standard calibration curve to determine the myeloperoxidase or lactoferrin concentration.

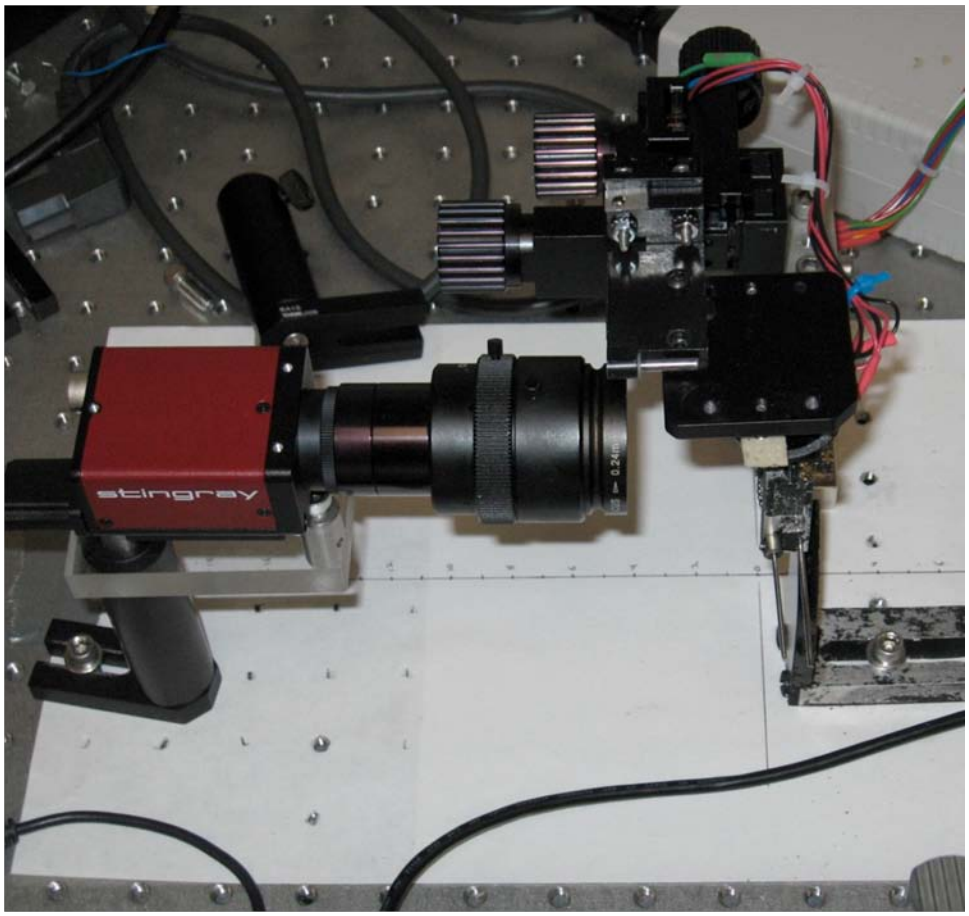

Figure 29: Optical setup with CCD camera, excitation source, and capillary holder.

3.2.2.4 Myeloperoxidase / Lactoferrin ELISA

Commercially available ELISA kits for myeloperoxidase and lactoferrin were purchased from Hycult Biotech (Plymouth Meeting, Pennsylvania). The protocol is identical for both ELISA kits and listed below. It is taken directly from the manufacturer's protocol. A schematic of the protocol is shown in Figure 30, also taken directly from the manufacturer's protocol.

REAGENT PREPARATION

Allow all the reagents to equilibrate to room temperature (20 – 25°C) prior to use. Return to proper storage conditions immediately after use.

Wash buffer

Prepare wash buffer by mixing 40 ml of 20 x wash buffer with 760 ml of distilled or de-ionized water, which is sufficient for 2 x 96 tests. Where less volume is required, prepare the desired volume of wash buffer by diluting 1 part of the 20 x wash buffer with 19 parts of distilled or de-ionized water.

Dilution buffer

Prepare dilution buffer by mixing 20 ml of the 5x dilution buffer A with 30 ml of distilled or deionized water and 10 ml of 10x dilution buffer B with 40 ml distilled or de-ionized water.

Combine both solutions equally and mix well. This 100 ml is sufficient for 2 x 96 tests. Where less volume is required, prepare the desired volume of dilution buffer by diluting 2 parts of the 5x dilution buffer A with 3 parts of distilled or de-ionized water and 1 part of 10x dilution buffer B with 4 parts distilled or de-ionized water. Combine both solutions equally and mix well.

Concentrated dilution buffer may contain crystals. In case the crystals do not disappear at room temperature within 1 hour, concentrated dilution buffer can be warmed up to 37°C. Do not shake the solution.

Standard solution

The standard is reconstituted by injection of 0.5 ml of distilled or de-ionized water. Prepare each human MPO standard in polypropylene tubes by serial dilution of the reconstituted standard with dilution buffer. Final concentrations should include 100ng/mL, 40 ng/mL, 16 ng/mL, 6.4 ng/mL, 2.6 ng/mL, 1.0 ng/mL, 0.4 ng/mL and 0 ng/mL.

Tracer solution

The tracer is reconstituted by injection of 1 ml distilled or de-ionized water. Dilute the reconstituted 1 ml tracer with 11 ml dilution buffer, which is sufficient for 1 x 96 tests. Where less volume is required, prepare the desired volume of tracer by diluting 1 part of the reconstituted tracer with 11 parts of dilution buffer.

Streptavidin-peroxidase solution

The streptavidin-peroxidase is reconstituted by injection of 1 ml distilled or de-ionized water.

Dilute the reconstituted 1 ml streptavidin-peroxidase with 23 ml dilution buffer, which is sufficient for 2 x 96 tests. Where less volume is desired, prepare the required volume of streptavidin-peroxidase solution by diluting 1 part of the reconstituted streptavidin-peroxidase with 23 parts of dilution buffer.

1. Determine the number of test wells required, put the necessary microwell strips into the supplied frame, and fill out the data collection sheet. Return the unused strips to the storage bag with desiccant, seal and store at 2 - 8°C.

2. Transfer 100 µl in duplicate of standard, samples, or controls into appropriate wells. Do not touch the side or bottom of the wells.

3. Apply an adhesive cover to the tray. Tap the tray to eliminate any air bubbles. Be careful not to splash liquid onto the cover.

4. Incubate the strips or plate for 1 hour at room temperature.

5. Wash the plates 4 times with wash buffer using a plate washer or as follows:

a. Carefully remove the plate sealer, avoid splashing.

b. Empty the plate by inverting plate and shaking contents out over the sink, keep inverted and tap dry on a thick layer of tissues.

c. Add 200 µl of wash buffer to each well, wait 20 seconds, empty the plate as described in 5b.

d. Repeat the washing procedure 5b/5c three times.

e. Empty the plate and gently tap on thick layer of tissues.

6. Add 100 µl of diluted tracer to each well using the same pipetting order as applied in step 2. Do not touch the side or bottom of the wells.

7. Cover the tray with an adhesive cover. Incubate the tray for 1 hour at room temperature.

8. Repeat the wash procedure described in step 5.

9. Add 100 µl of diluted streptavidin-peroxidase to each well, using the same pipetting order as applied in step 2. Do not touch the side or bottom of the wells.

10. Cover the tray with an adhesive cover, incubate the tray for 1 hour at room temperature.

11. Repeat the wash procedure described in step 5.

12. Add 100 µl of TMB substrate to each well, using the same pipetting order as applied in step 2. Do not touch the side or bottom of the wells.

13. Cover the tray with a new adhesive cover, incubate the tray for 20 – 30 minutes at room temperature. Avoid exposing the microwell strips to direct sunlight. Covering the plate with aluminum foil is recommended.

14. Stop the reaction by adding 100 µl of stop solution with the same sequence and timing as used in step 12. Mix solutions in the wells thoroughly by gently swirling the plate. Gently tap the tray to eliminate any air bubbles trapped in the wells.

15. Read the plate within 30 minutes after addition of stop solution at 450 nm using a plate reader, following the instructions provided by the instrument's manufacturer.

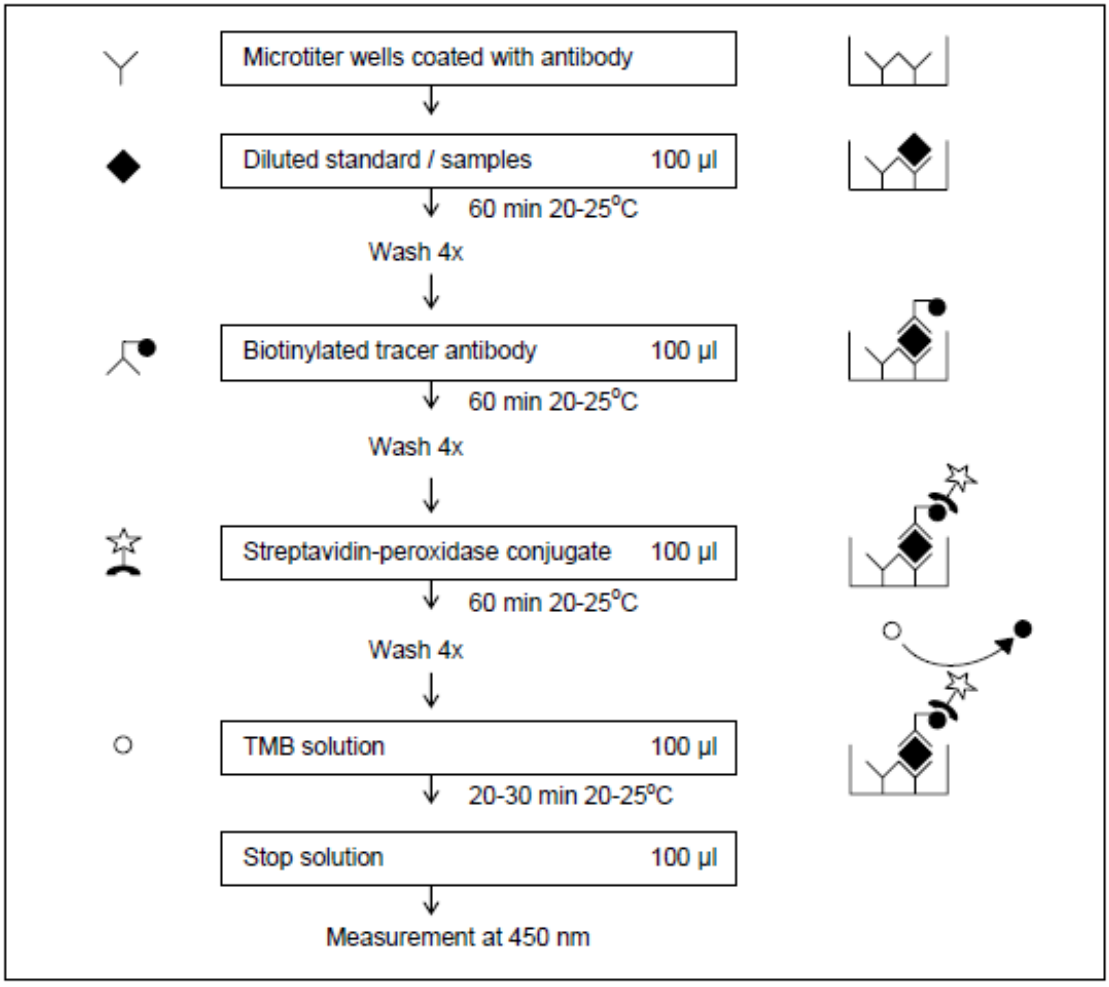

Figure 30: Schematic showing the protocol, taken, with permission, from the Hycult Biotech protocol for the MPO ELISA kit.

Interpretation of Results

1. Calculate the mean absorbance for each set of duplicate standards, control and samples.

2. If individual absorbance values differ by more than 15% from the corresponding mean value, the result is considered suspect and the sample should be retested.

3. The mean absorbance of the zero standard should be less than 0.3.

4. Create a standard curve using computer software capable of generating a good curve fit. The mean absorbance for each standard concentration is plotted on the vertical (Y) axis versus the corresponding concentration on the horizontal (X) axis (logarithmic scale).

An example of the standard curve generated from Hycult Biotech for the MPO ELISA kit is shown in Figure 31. After speaking with Hycult Biotech, they determined that their standard curves for their ELISA kits were best modeled using a 5-parameter logistics curve. It was also

determined that modeling just the dynamic range with a logistics model was simpler and sufficiently accurate in determining unknown values.

If the standard is out of range, the results of the test samples are not reliable. The test should be repeated.

Human MPO (ng/ml)	Absorption
0.0	0.039
0.4	0.256
1.0	0.386
2.6	0.729
6.4	1.283
16.0	2.085
40.0	2.976
100.0	3.325

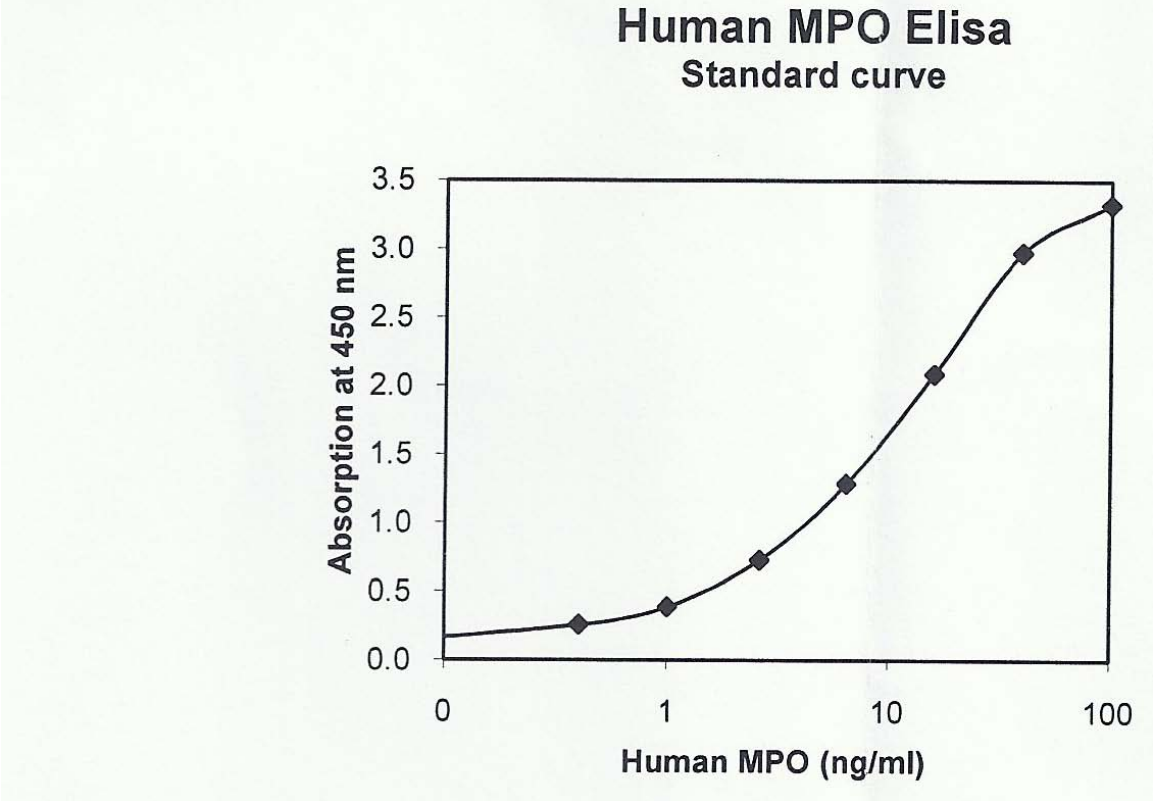

Figure 31: A sample standard curve given with Hycult Biotech's MPO ELISA kit showing a dynamic range from around 3ng/mL to 30ng/mL. Reproduced with permission from Hycult Biotech.

5. If samples have been diluted, the concentration read from the standard curve must be multiplied by the dilution factor.

6. Samples that give a mean absorbance above the absorbance for the highest standard concentration are out of range of the assay. These samples should be retested at a higher dilution.

Additionally there are extracted human stool samples analyzed with Invitrogen's Zen Myleoperoxidase ELISA kit. This is only where indicated in this text and a detailed protocol is given in Appendix D.

3.2.2.5 Statistical Analysis

QLISA and ELISA results for both myeloperoxidase and lactoferrin were plotted together to develop the simple linear regression equation, from which R-squared values were determined. Additionally we compared QLISA and ELISA results for both myeloperoxidase and lactoferrin using Spearman's rank correlation and Pearson product-moment correlation coefficient. Results are reported below and shown graphically as well. Additionally we compared QLISA and ELISA values for both myeloperoxidase and lactoferrin for each

patient. While the results reported in the next section are encouraging for this analysis it has limited significance given our sample size of three.

3.2.3 Results

The results of the previously described protocols are given in subsequent sections below. They are divided into two subsections: one reporting on the results for myeloperoxidase detection using both QLISA and ELISA and the other reporting results for lactoferrin detection using both QLISA and ELISA. The conclusions of the results are discussed separately in 3.2.4 Discussion.

3.2.3.1 QLISA / ELISA – Myeloperoxidase

Experiments for myeloperoxidase detection were carried out using QLISA first, then ELISA to compare how our novel immunoassay compared to a commercially available myeloperoxidase detection system. The data reported below is using the second generation QLISA system.

Prior to testing the human samples with QLISA we tested the efficacy of our system using known concentrations of myeloperoxidase ranging from

25ng/mL to 800ng/mL. We found this system fairly reproducible. Once this was accomplished we tested a healthy stool sample (not one of the patients from the IRB protocol) with spiked concentrations of myeloperoxidase. This was done to test the specificity of the QLISA system to detecting myeloperoxidase and not erroneously detect other proteins in the stool sample non-specifically believing they were myeloperoxidase. We found identical signal between spiked samples and our standard curve for myeloperoxidase detection, as seen in Figure 32.

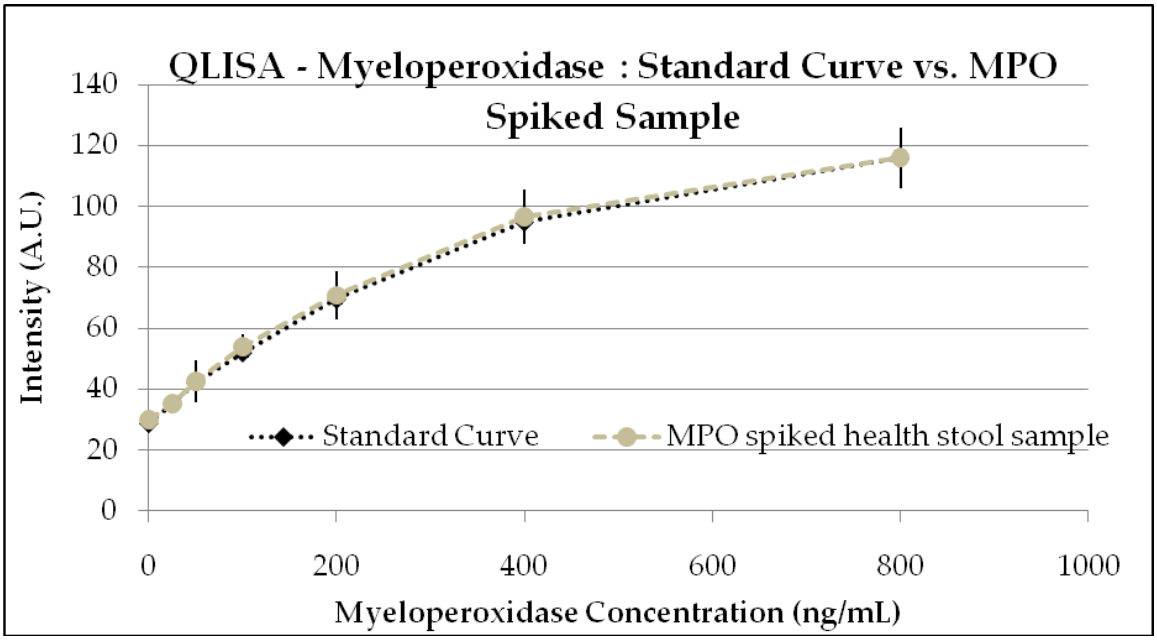

Figure 32: Comparison of a myeloperoxidase standard curve with QLISA using known concentrations of myeloperoxidase and a standard curve with QLISA using known spiked concentrations of myeloperoxidase in healthy stool sample. N = 3 for all data points; bars represent standard deviation.

Next human stool samples underwent the protein extraction procedure described in the above section 3.2.2.1 Protein Extraction – Human Stool. We then ran the QLISA for myeloperoxidase detection in all 16 patients in triplicates. Standard curves were generated for each run, and if the standard curve fell out of the range of our known values we discarded all human sample analysis. The standard curve is shown in Figure 33 and includes standard error bars demonstrating the reliability of our detection of myeloperoxidase standards. Myeloperoxidase values for unknown samples were taken from the linear region shown as an all black line. Additionally we took the myeloperoxidase concentration that corresponded to the most diluted sample that was still in this linear region. Our dynamic range for QLISA – myeloperoxidase is from 25ng/mL to 200ng/mL.

Before reporting myeloperoxidase values from QLISA we briefly introduce ELISA results, so we can then directly compare myeloperoxidase concentrations from each assay.

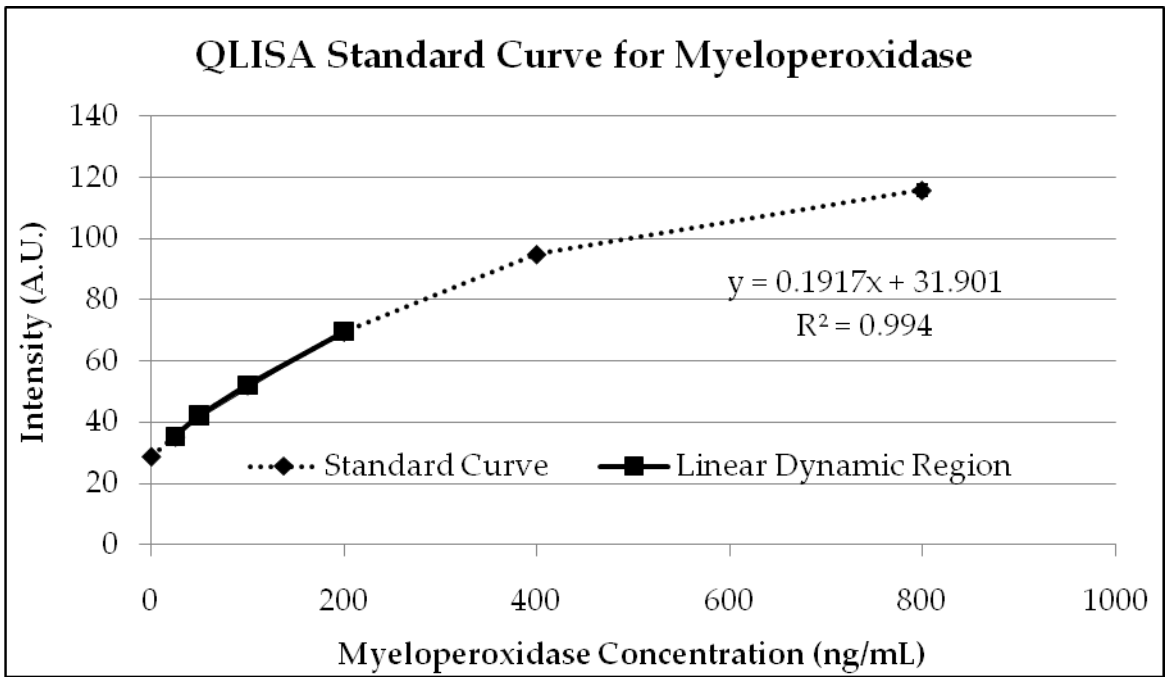

Figure 33: The standard curve for myeloperoxidase detection using QLISA (2nd generation) showing intensity from immobilized quantum dots as a function of myeloperoxidase concentration. N = 3 for all data points; bars represent standard deviation.

In Figure 34 below there is a standard curve of myeloperoxidase levels from the Hycult Biotech ELISA kit, which includes standard error bars. Like the QLISA standard curve, and as mentioned by Hycult Biotech, the standard curve behaves like a 5-parameter logistics curve but has a linear region. Again, like QLISA this linear region is of most interest for determining unknown concentrations of myeloperoxidase. We determined myeloperoxidase values based on the most dilute unknown human stool sample that still fell in this region.

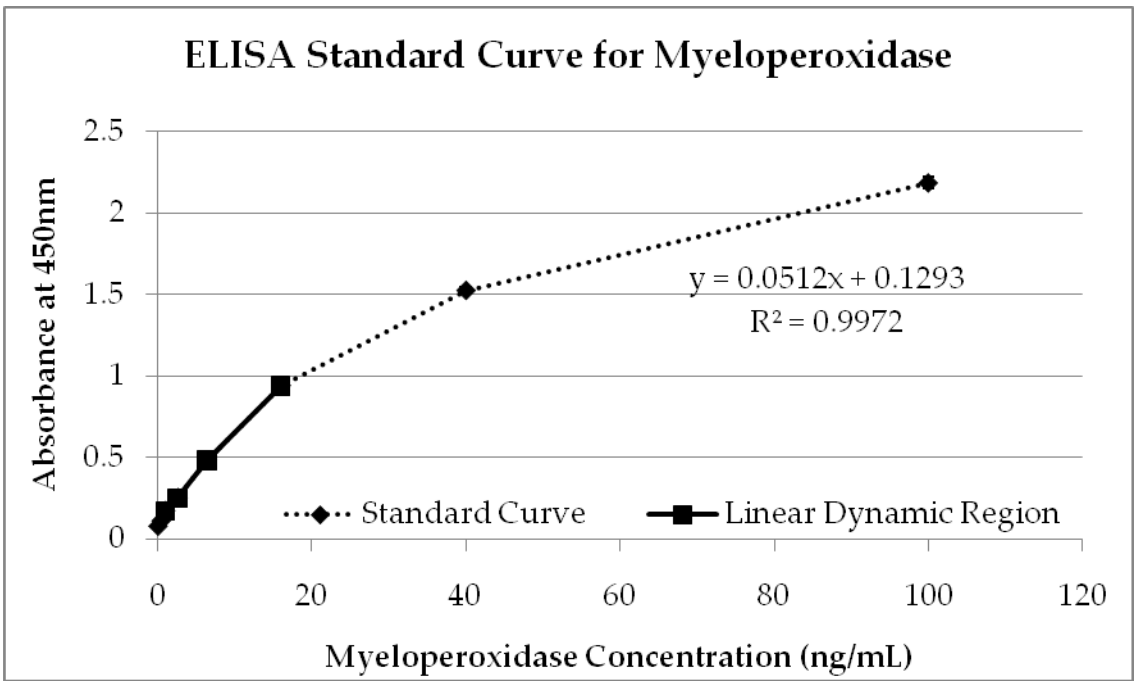

Figure 34: The standard curve for myeloperoxidase detection using ELISA (Hycult Biotech) showing intensity from immobilized quantum dots as a function of myeloperoxidase concentration. N = 3 for all data points; bars represent standard deviation.

Below are a series of Figures that individually compares myeloperoxidase values from QLISA and ELISA. Concentrations are reported in ug/g of sample. There are at least 3 samples analyzed for each immunoassay and standard deviations are shown for each immunoassay with standard error bars. Statistical differences between QLISA and ELISA values for myeloperoxidase samples are given as a P-value which is calculated from a T-test. The majority of P-values indicate there is no statistical difference between QLISA and ELISA myeloperoxidase detection. This is shown through only a few P-values < 0.05

and only two samples with P-values < 0.001. There are 16 human stool samples analyzed and shown in below Figures. The three letter / number identification under the bars refers to the patients identity. We, the testers who evaluated the samples were blinded to the condition of the patients.

The Spearman's rank correlation and Pearson product-moment correlation coefficient for myeloperoxidase was 0.996 and 0.993, respectively. The Spearman's rank correlation and Pearson product-moment correlation coefficient for lactoferrin was 0.985 and 0.989, respectively.

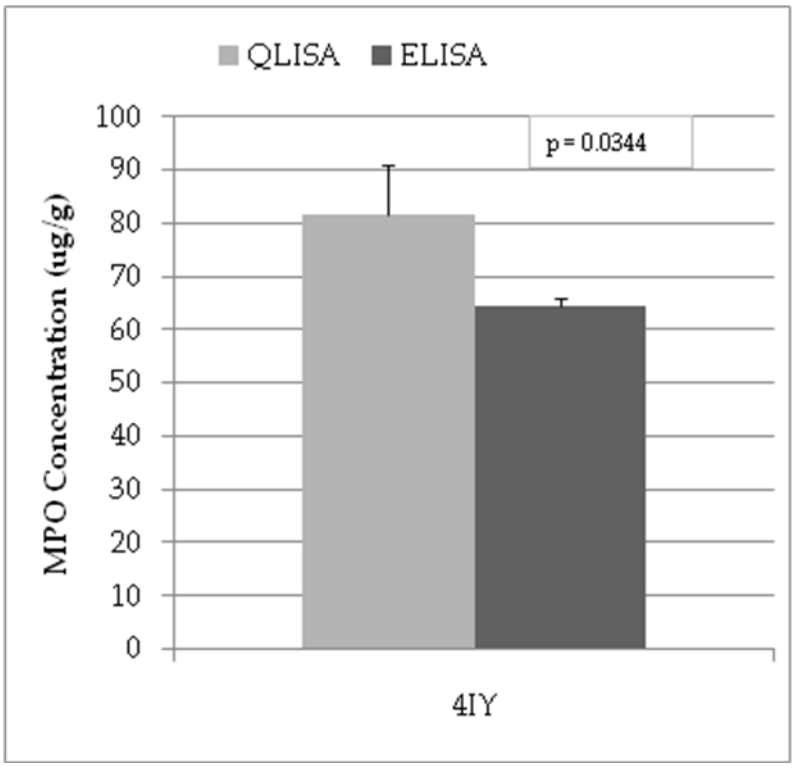

Figure 35: A comparison between myeloperoxidase levels detected in the stool sample from patient 4IY using QLISA and ELISA systems. P-values from a T-test are towards the upper right corner.

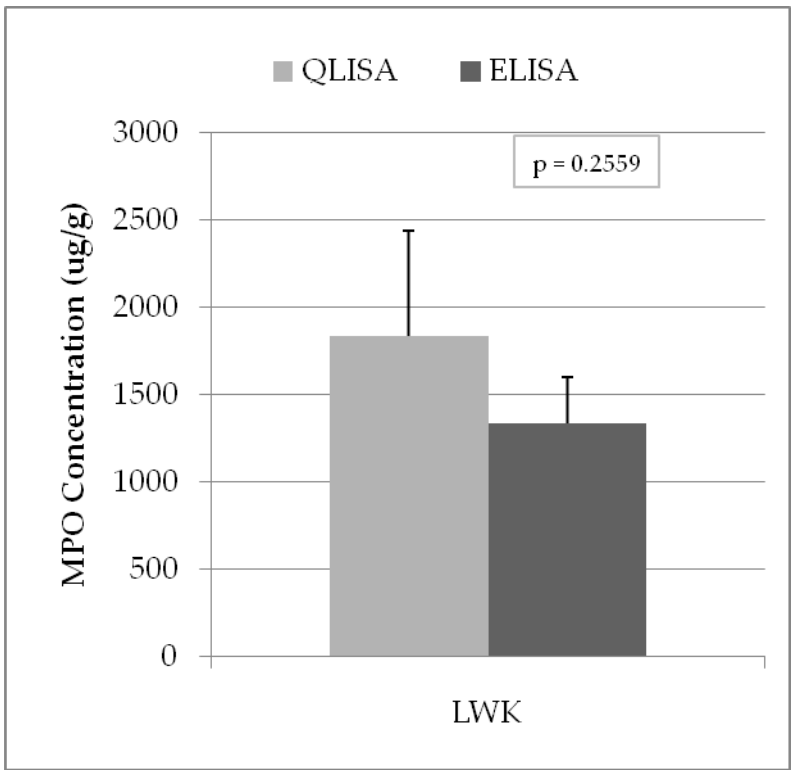

Figure 36: A comparison between myeloperoxidase levels detected in the stool sample from patient LWK using QLISA and ELISA systems. P-values from a T-test are towards the upper right corner.

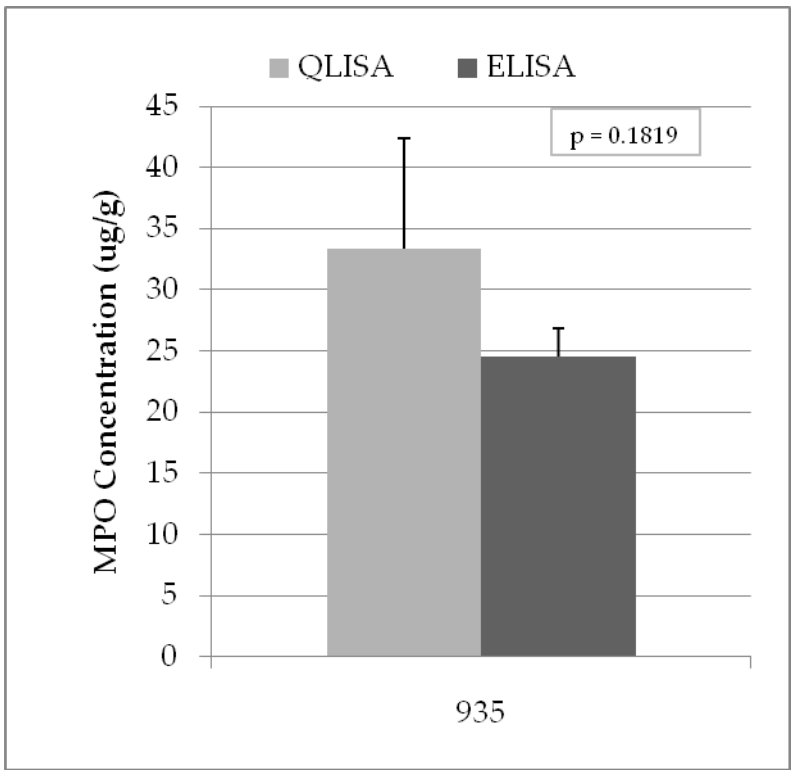

Figure 37: A comparison between myeloperoxidase levels detected in the stool sample from patient 935 using QLISA and ELISA systems. P-values from a T-test are towards the upper right corner.

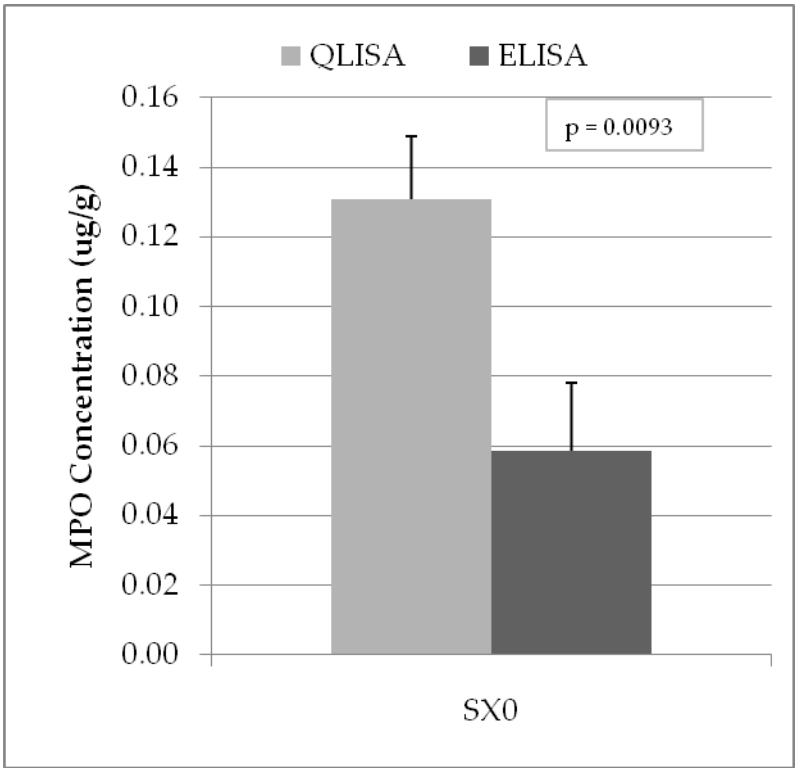

Figure 38: A comparison between myeloperoxidase levels detected in the stool sample from patient SX0 using QLISA and ELISA systems. P-values from a T-test are towards the upper right corner.

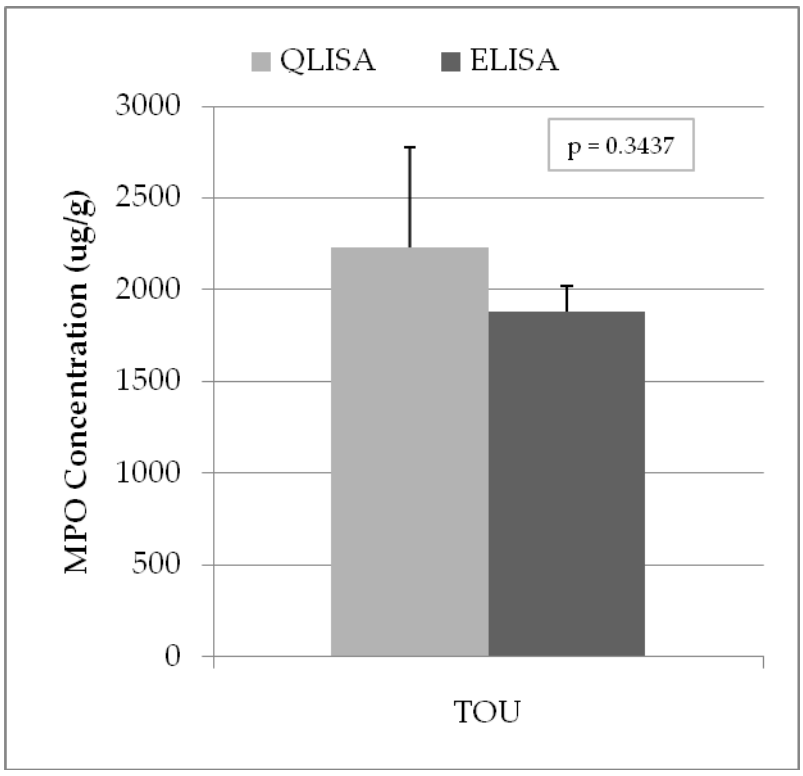

Figure 39: A comparison between myeloperoxidase levels detected in the stool sample from patient TOU using QLISA and ELISA systems. P-values from a T-test are towards the upper right corner.

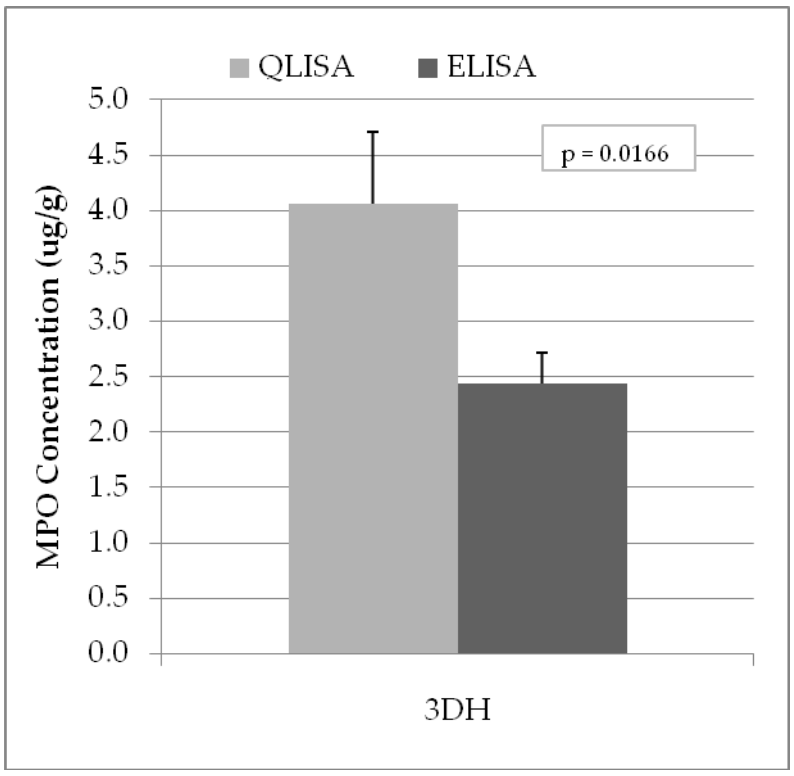

Figure 40: A comparison between myeloperoxidase levels detected in the stool sample from patient 3DH using QLISA and ELISA systems. P-values from a T-test are towards the upper right corner.

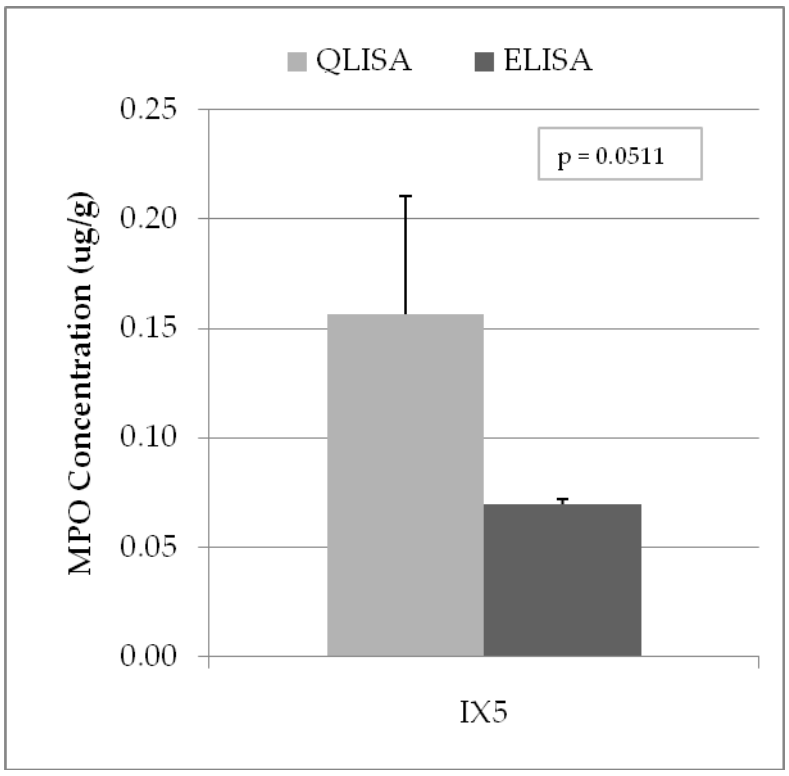

Figure 41: A comparison between myeloperoxidase levels detected in the stool sample from patient IX5 using QLISA and ELISA systems. P-values from a T-test are towards the upper right corner.

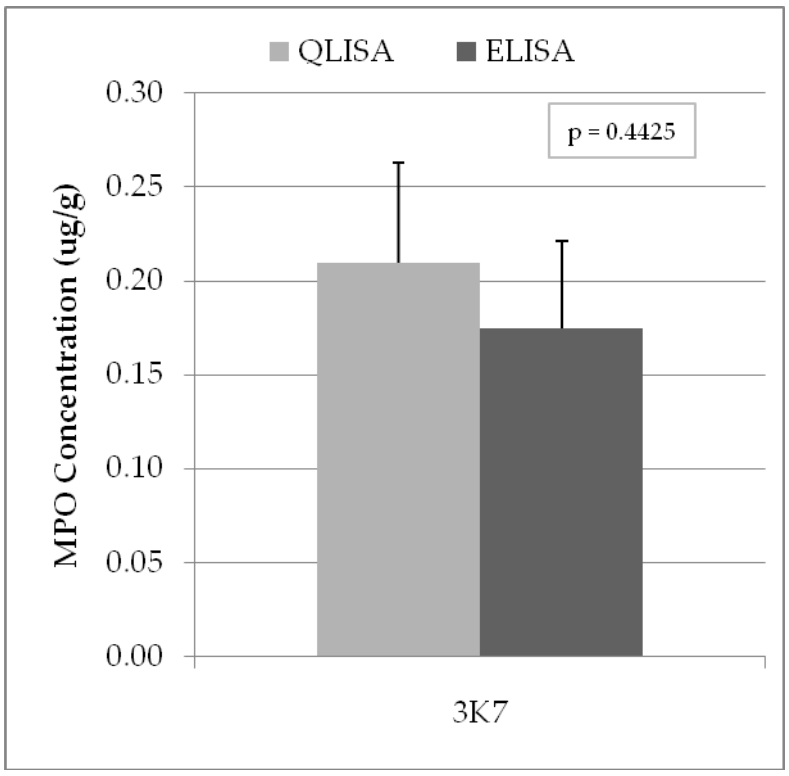

Figure 42: A comparison between myeloperoxidase levels detected in the stool sample from patient 3K7 using QLISA and ELISA systems. P-values from a T-test are towards the upper right corner.

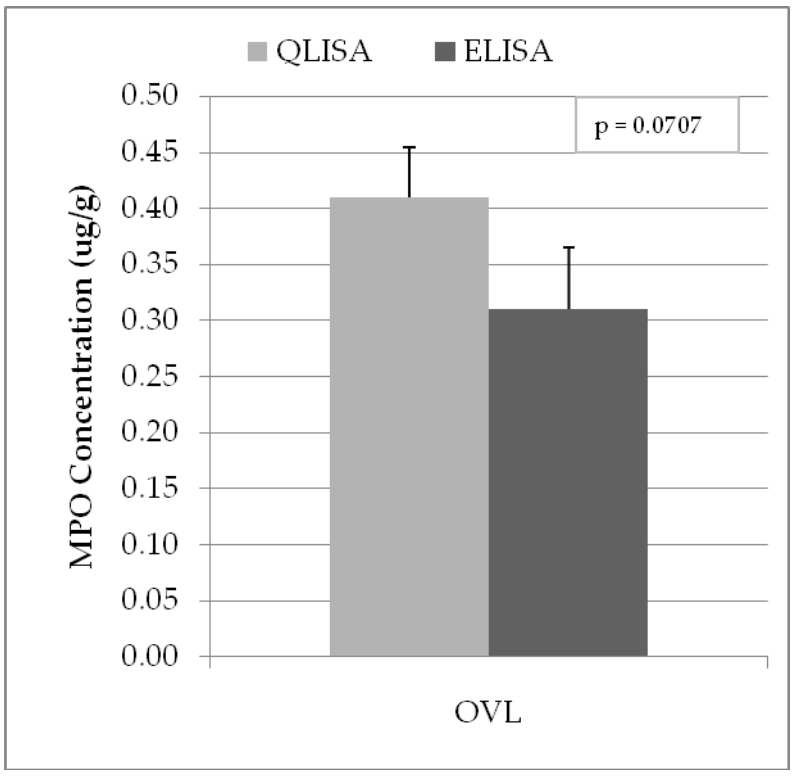

Figure 43: A comparison between myeloperoxidase levels detected in the stool sample from patient OVL using QLISA and ELISA systems. P-values from a T-test are towards the upper right corner.

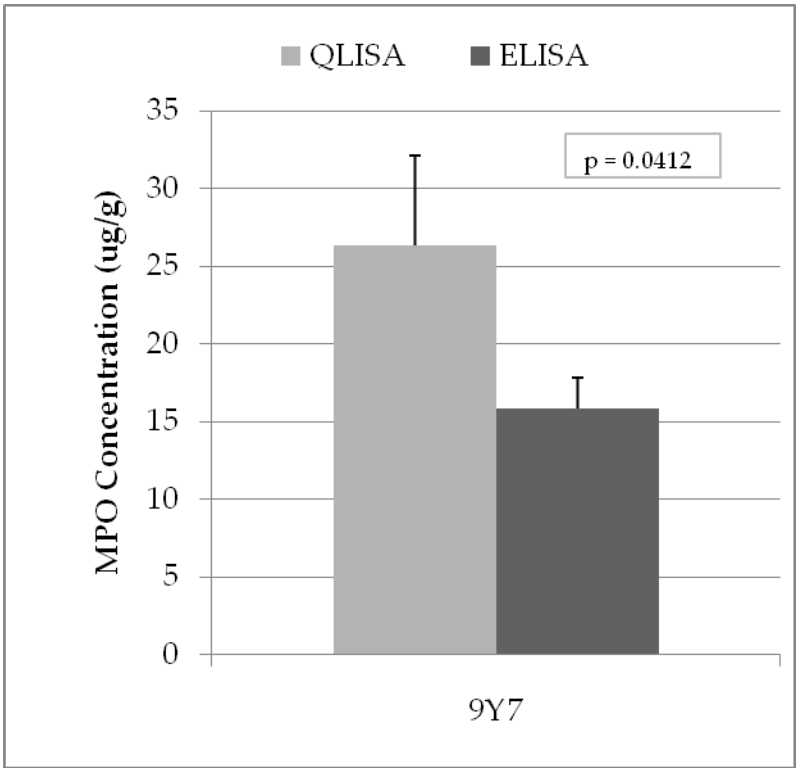

Figure 44: A comparison between myeloperoxidase levels detected in the stool sample from patient 9Y7 using QLISA and ELISA systems. P-values from a T-test are towards the upper right corner.

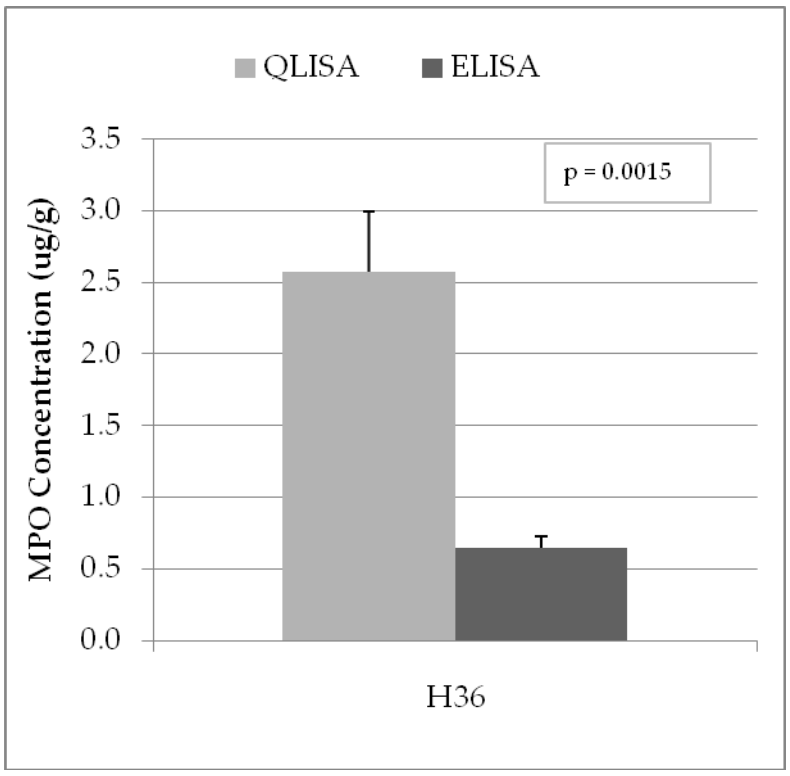

Figure 45: A comparison between myeloperoxidase levels detected in the stool sample from patient H36 using QLISA and ELISA systems. P-values from a T-test are towards the upper right corner.

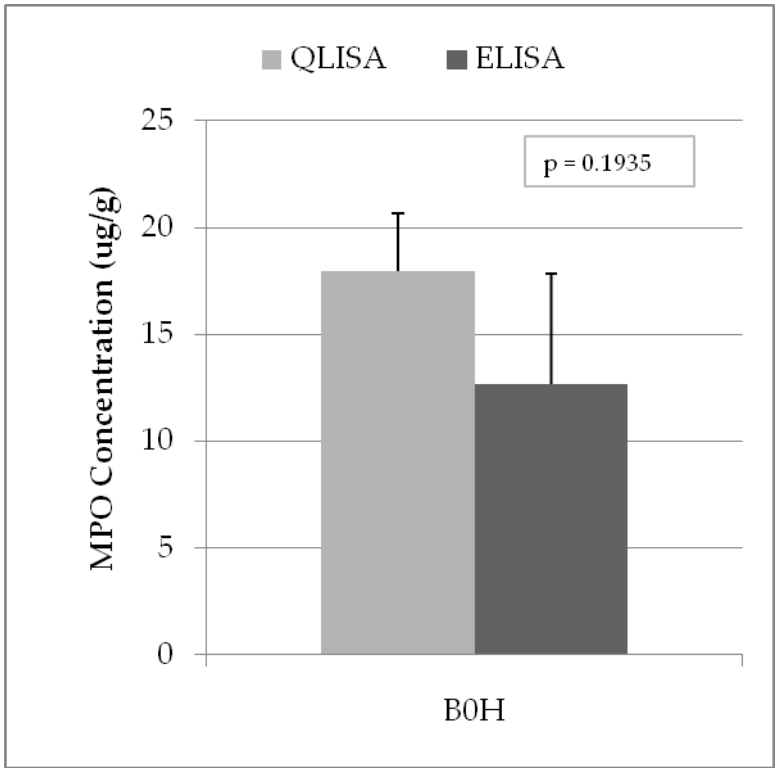

Figure 46: A comparison between myeloperoxidase levels detected in the stool sample from patient B0H using QLISA and ELISA systems. P-values from a T-test are towards the upper right corner.

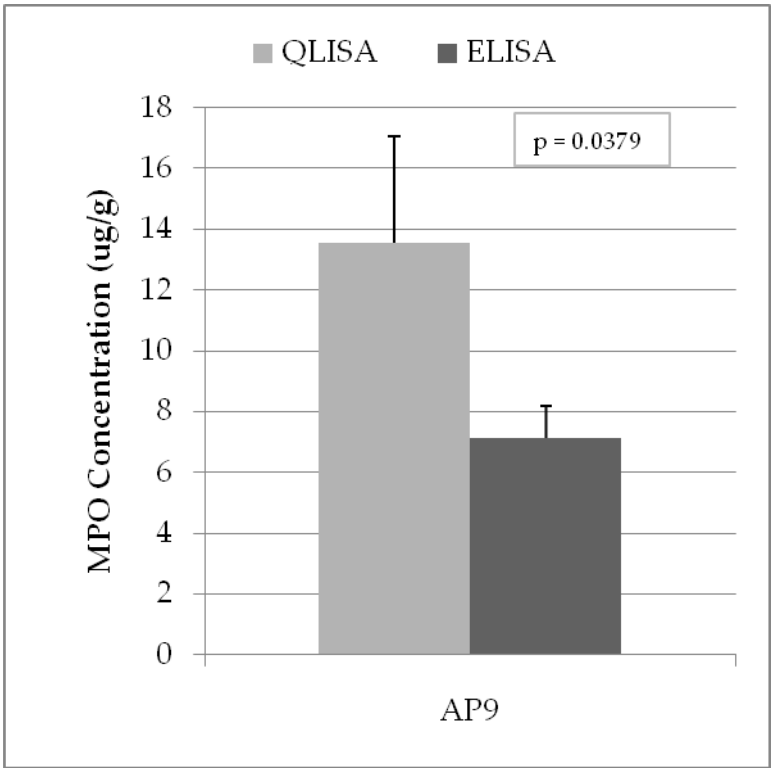

Figure 47: A comparison between myeloperoxidase levels detected in the stool sample from patient AP9 using QLISA and ELISA systems. P-values from a T-test are towards the upper right corner.

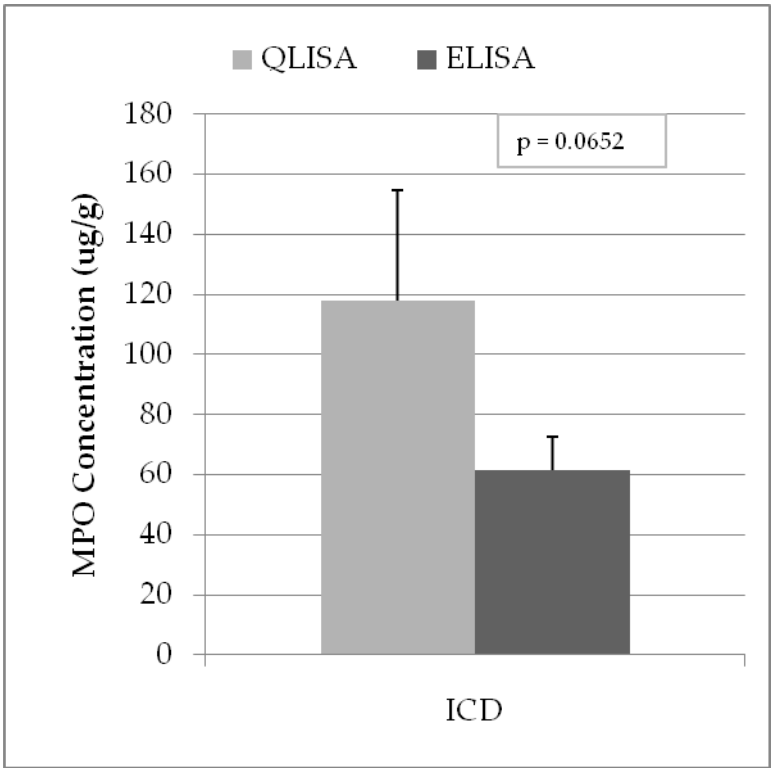

Figure 48: A comparison between myeloperoxidase levels detected in the stool sample from patient ICD using QLISA and ELISA systems. P-values from a T-test are towards the upper right corner.

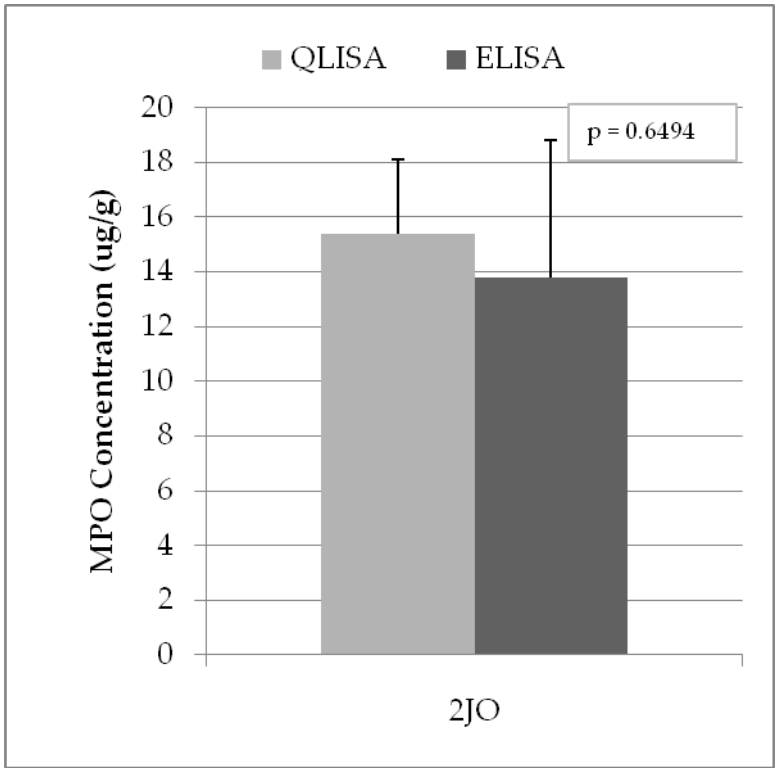

Figure 49: A comparison between myeloperoxidase levels detected in the stool sample from patient 2JO using QLISA and ELISA systems. P-values from a T-test are towards the upper right corner.

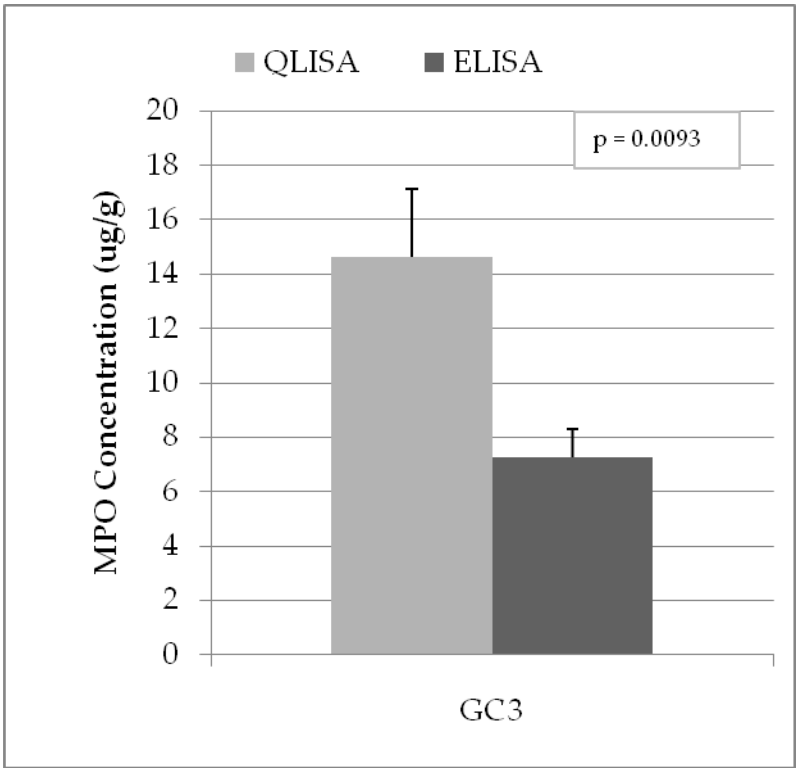

Figure 50: A comparison between myeloperoxidase levels detected in the stool sample from patient GC3 using QLISA and ELISA systems. P-values from a T-test are towards the upper right corner.

3.2.3.2 QLISA / ELISA – Lactoferrin

The evaluation of lactoferrin levels using both QLISA and ELISA methods followed steps equivalent to those discussed in 3.2.3.1 QLISA / ELISA – Myeloperoxidase.

Here in Figure 51 is a standard curve for lactoferrin levels ranging from 25ng/mL to 800ng/mL. We see behavior similar to that seen with myeloperoxidase levels and fluorescent intensity. The linear region of this

lactoferrin standard curve also ranges from 25ng/mL to about 200ng/mL. Unknown samples were diluted until their fluorescence was detected in this linear region and if multiple dilutions were detected in that linear region the sample diluted the most was measured.

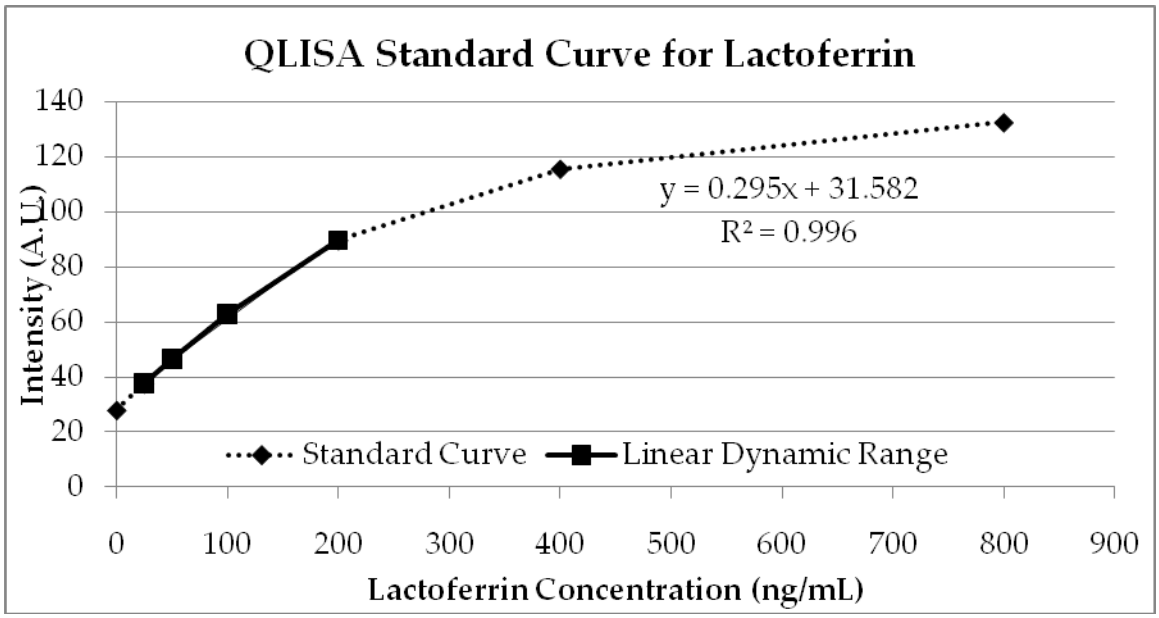

Figure 51: The standard curve for lactoferrin detection using QLISA (2nd generation) showing intensity from immobilized quantum dots as a function of lactoferrin concentration. N = 3 for all data points; bars represent standard deviation.

The standard curve for lactoferrin using Hycult Biotech's ELISA kit is shown in Figure 52. It is best modeled with a 5-parameter logistics curve and can accurately be modeled using a logarithmic function in the dynamic range from about 1ng/mL to 20ng/mL.

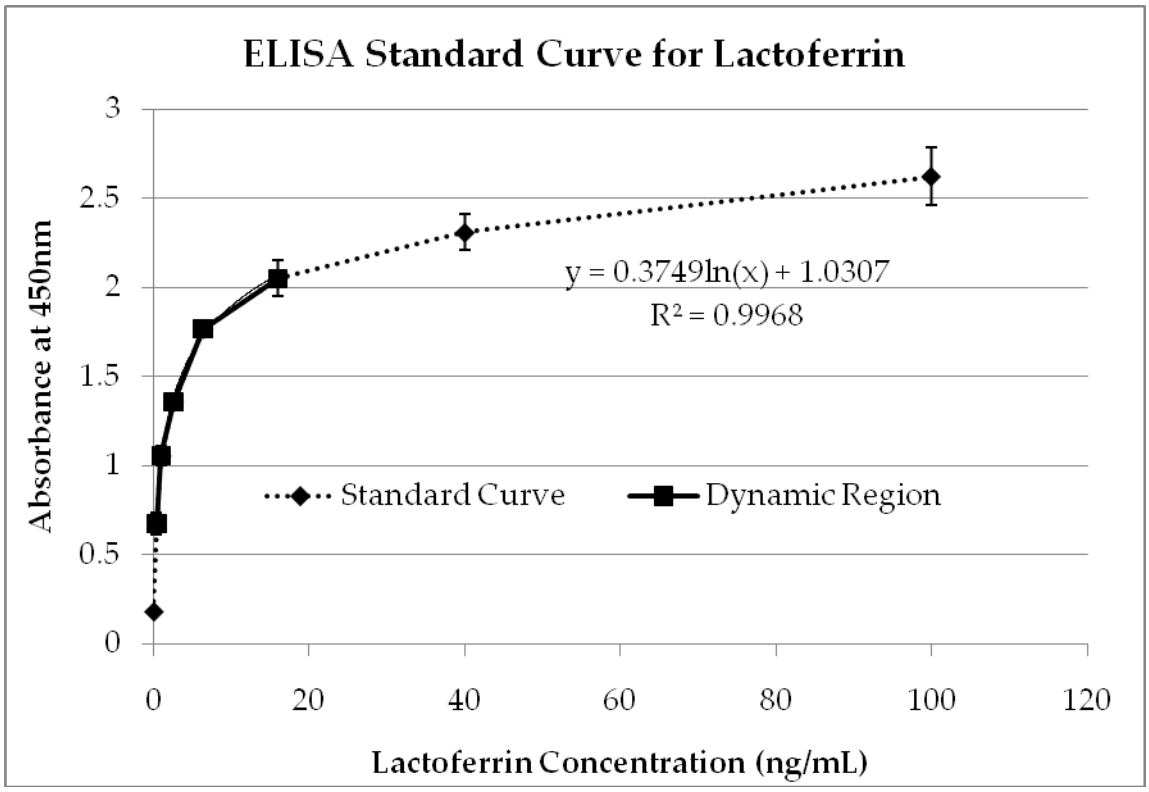

Figure 52: The standard curve for lactoferrin detection using ELISA (Hycult Biotech) showing intensity from immobilized quantum dots as a function of lactoferrin concentration. N = 3 for all data points; bars represent standard deviation.

Below are a series of Figures that individually compares lactoferrin values from QLISA and ELISA for each human sample. Concentrations are reported in ug/g of sample. There are at least 3 samples analyzed for each immunoassay and standard deviations are shown for each immunoassay with standard error bars. Statistical differences between QLISA and ELISA values for lactoferrin samples are given as a P-value which is calculated from a T-test. The majority of P-values

indicate there is no statistical difference between QLISA and ELISA lactoferrin detection. This is shown through only three P-values < 0.05 and no samples with P-values < 0.001. There are 16 human stool samples analyzed and shown in below Figures. The three letter / number identification under the bars refers to the patients identity. As testers we were blinded to the conditions of the patients.

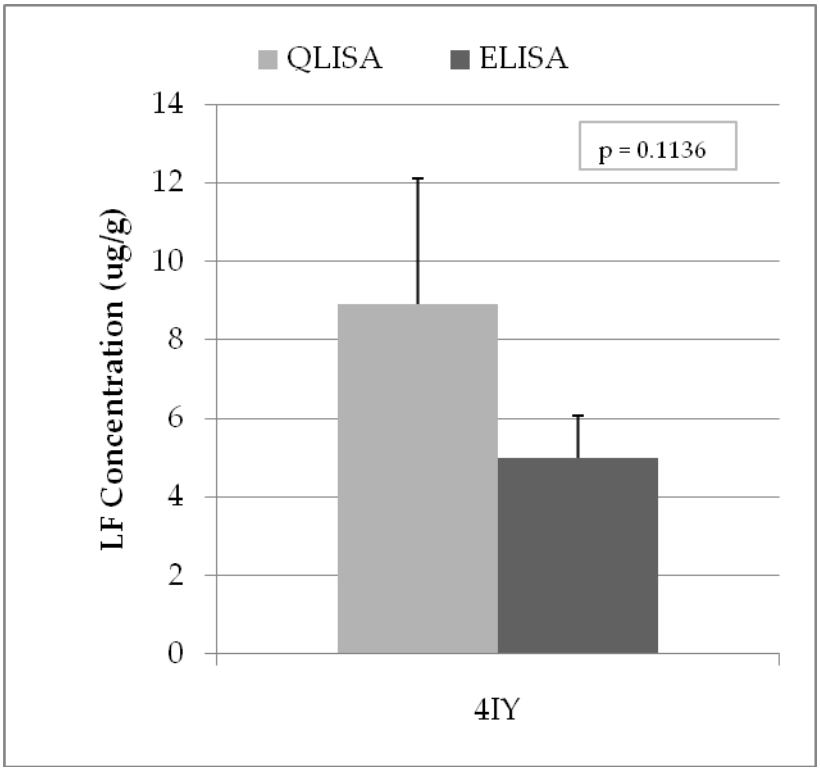

Figure 53: A comparison between myeloperoxidase levels detected in the stool sample from patient 4IY using QLISA and ELISA systems. P-values from a T-test are towards the upper right corner.

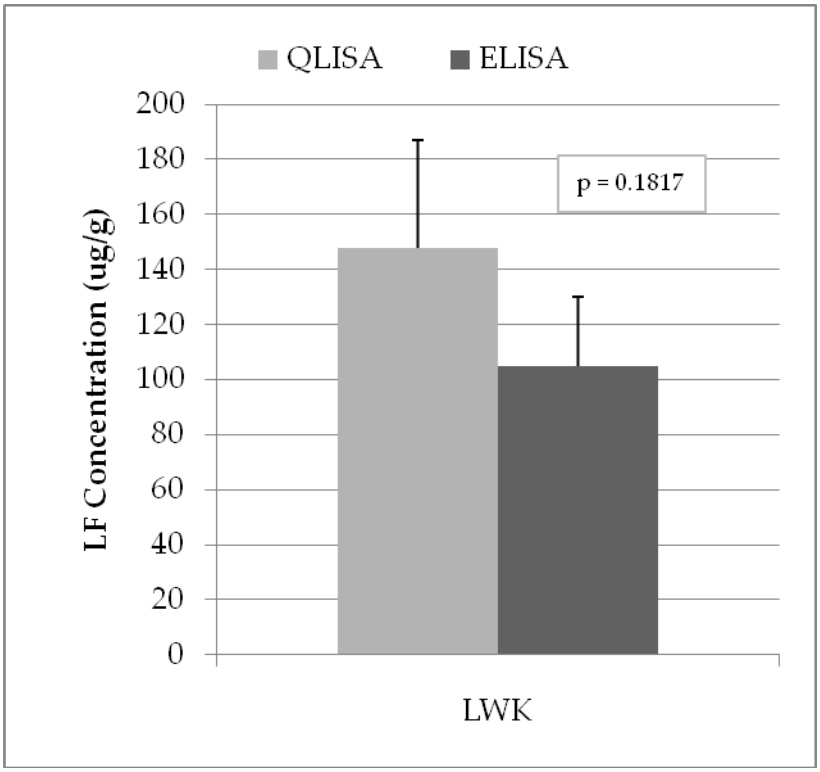

Figure 54: A comparison between myeloperoxidase levels detected in the stool sample from patient LWK using QLISA and ELISA systems. P-values from a T-test are towards the upper right corner.

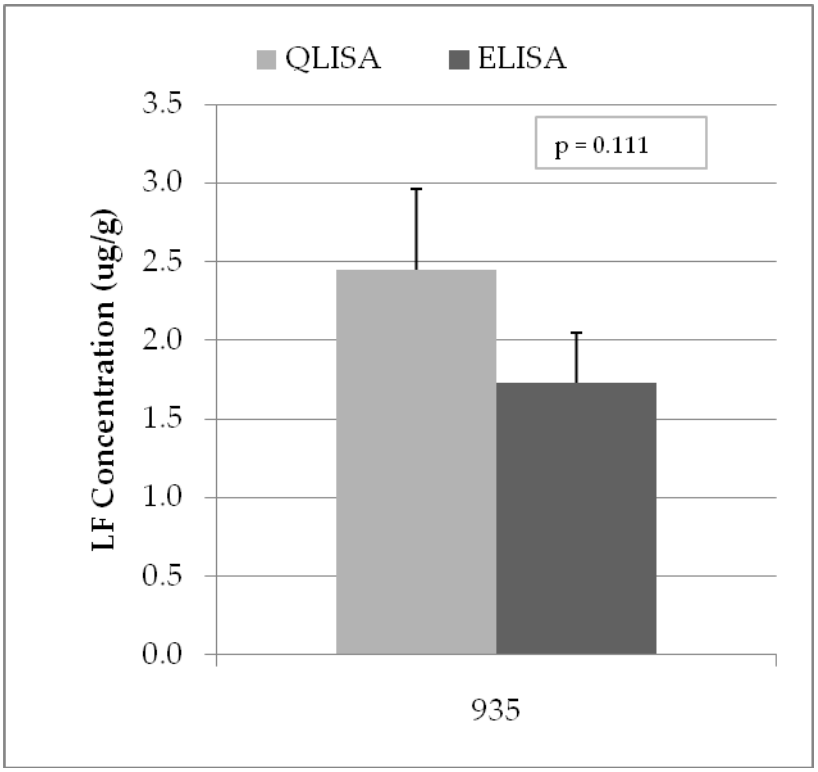

Figure 55: A comparison between myeloperoxidase levels detected in the stool sample from patient 935 using QLISA and ELISA systems. P-values from a T-test are towards the upper right corner.

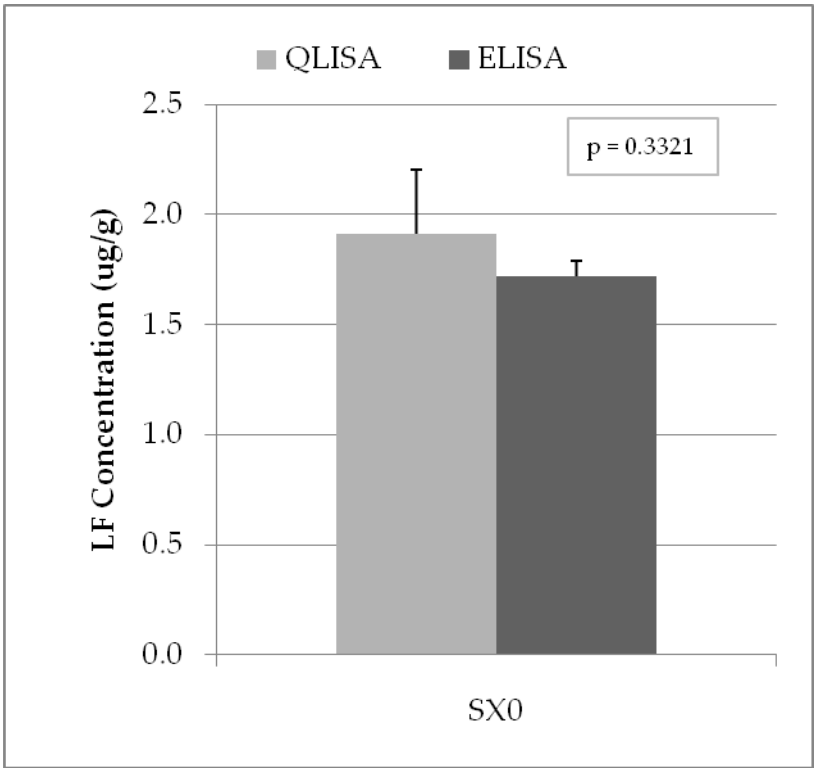

Figure 56: A comparison between myeloperoxidase levels detected in the stool sample from patient SX0 using QLISA and ELISA systems. P-values from a T-test are towards the upper right corner.

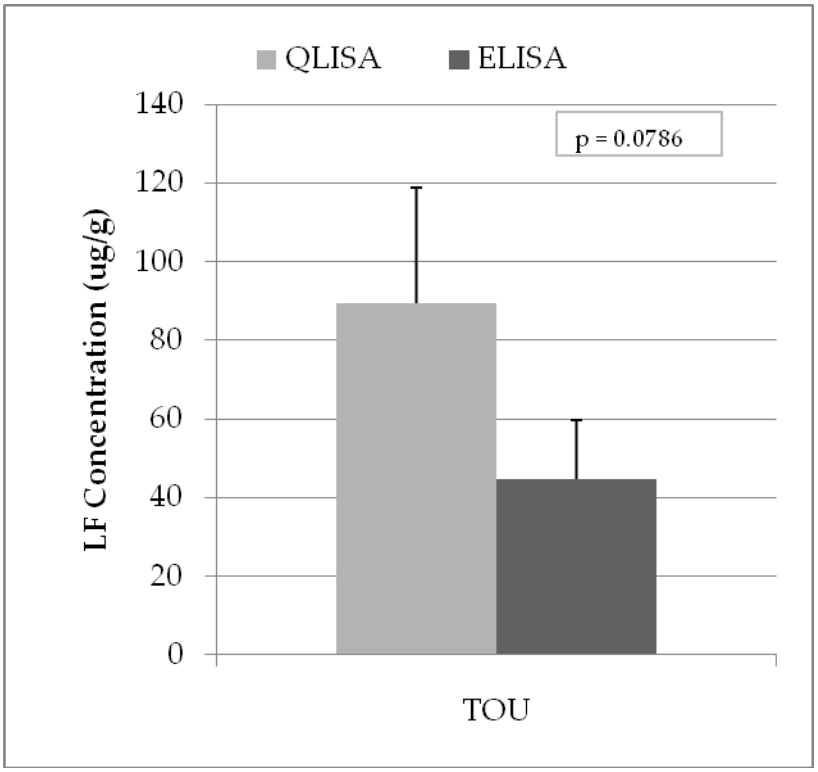

Figure 57: A comparison between myeloperoxidase levels detected in the stool sample from patient TOU using QLISA and ELISA systems. P-values from a T-test are towards the upper right corner.

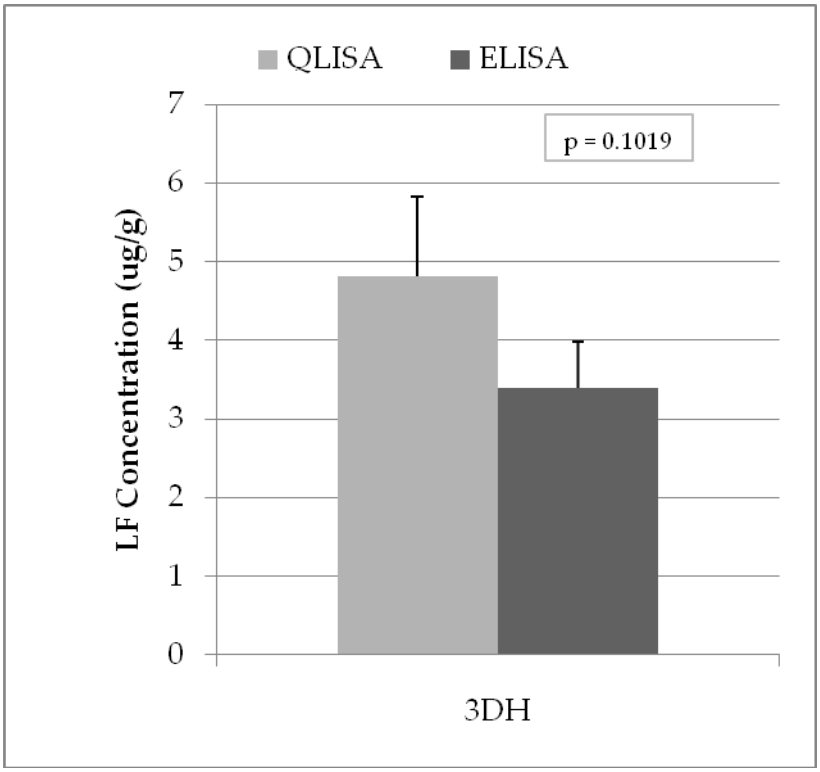

Figure 58: A comparison between myeloperoxidase levels detected in the stool sample from patient 3DH using QLISA and ELISA systems. P-values from a T-test are towards the upper right corner.

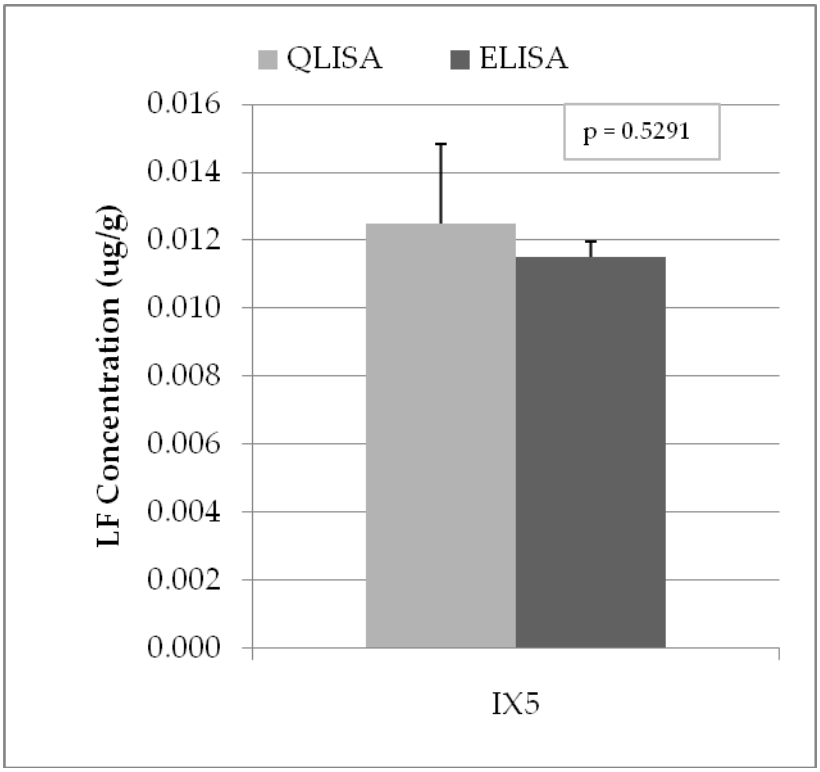

Figure 59: A comparison between myeloperoxidase levels detected in the stool sample from patient IX5 using QLISA and ELISA systems. P-values from a T-test are towards the upper right corner.

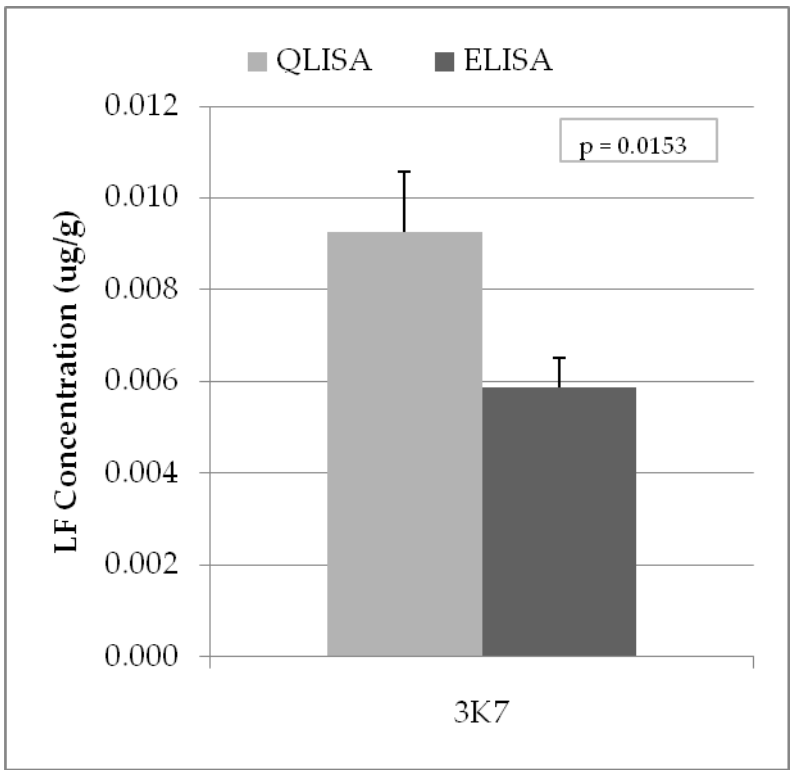

Figure 60: A comparison between myeloperoxidase levels detected in the stool sample from patient 3K7 using QLISA and ELISA systems. P-values from a T-test are towards the upper right corner.

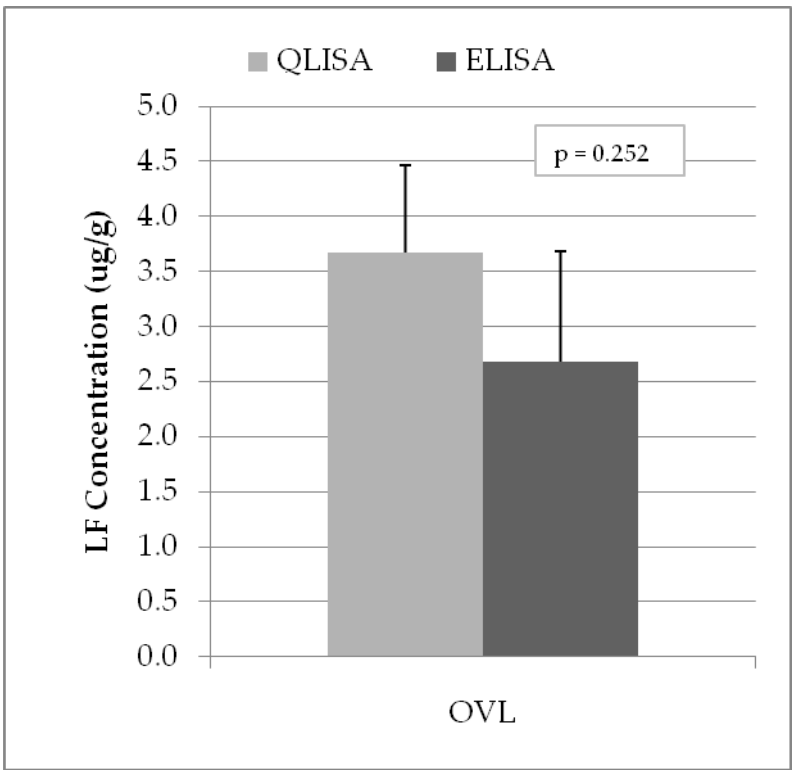

Figure 61: A comparison between myeloperoxidase levels detected in the stool sample from patient OVL using QLISA and ELISA systems. P-values from a T-test are towards the upper right corner.

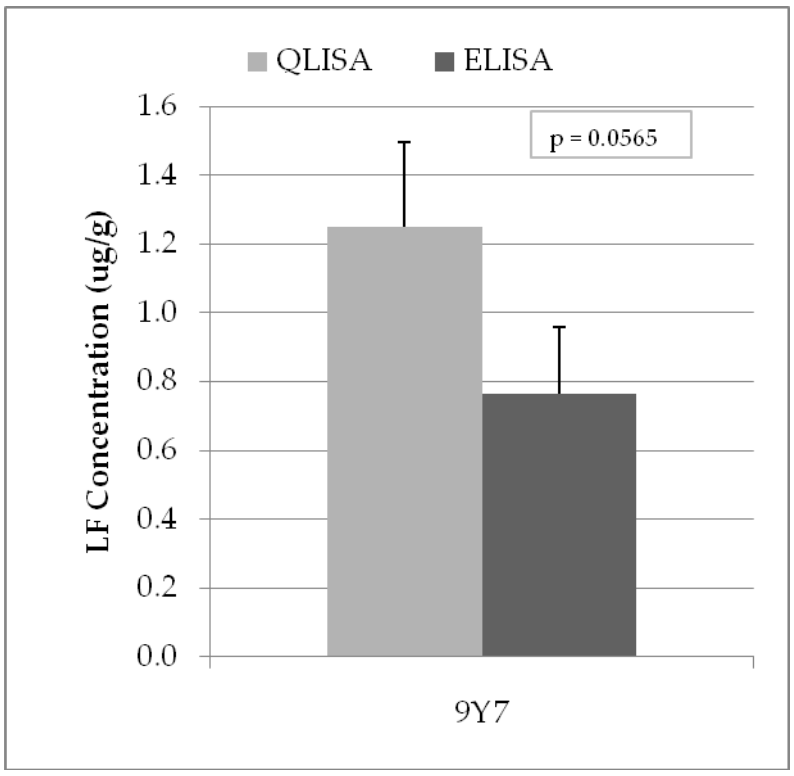

Figure 62: A comparison between myeloperoxidase levels detected in the stool sample from patient 9Y7 using QLISA and ELISA systems. P-values from a T-test are towards the upper right corner.

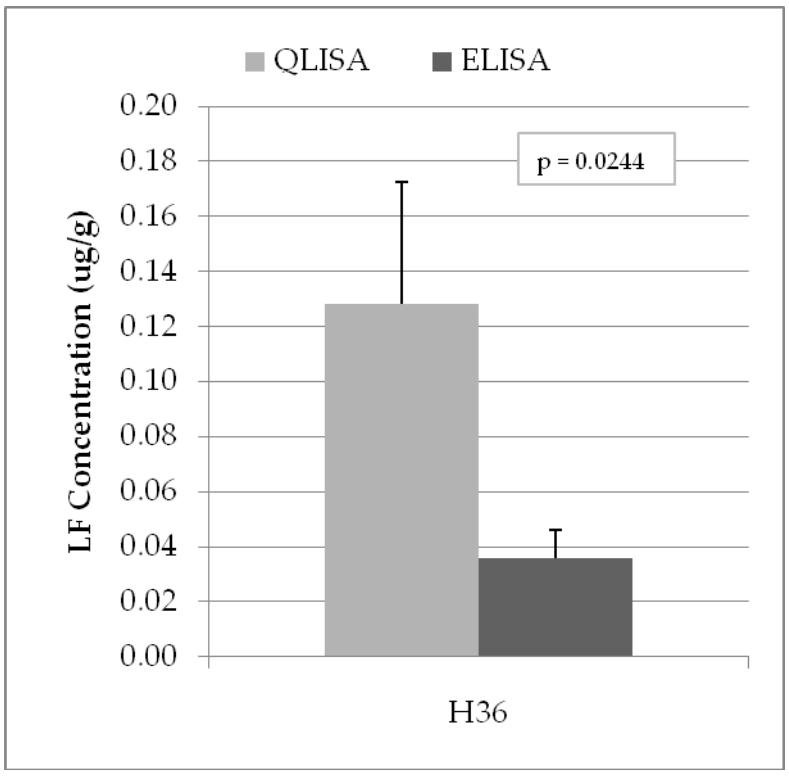

Figure 63: A comparison between myeloperoxidase levels detected in the stool sample from patient H36 using QLISA and ELISA systems. P-values from a T-test are towards the upper right corner.

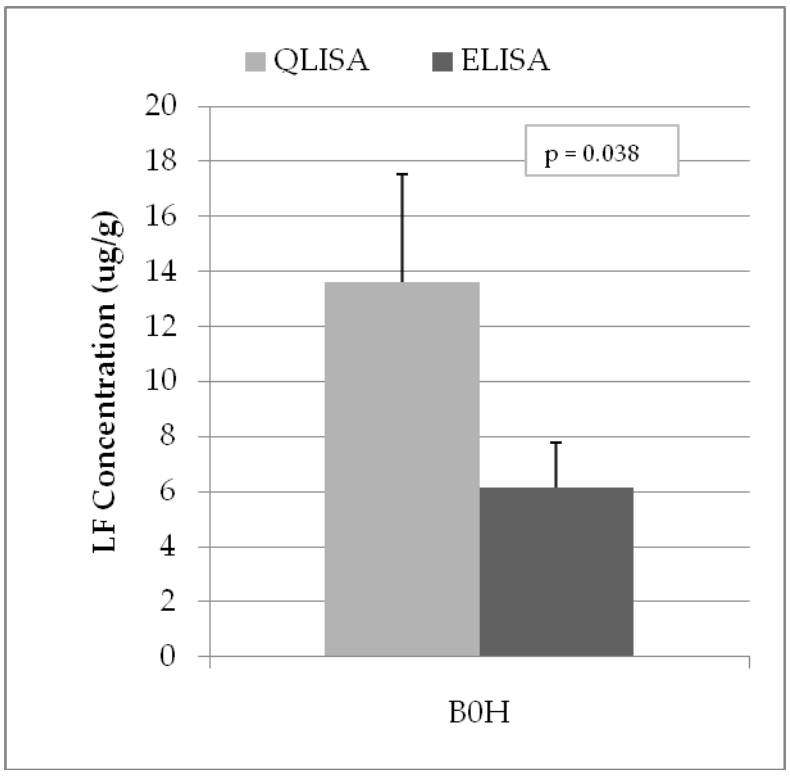

Figure 64: A comparison between myeloperoxidase levels detected in the stool sample from patient B0H using QLISA and ELISA systems. P-values from a T-test are towards the upper right corner.

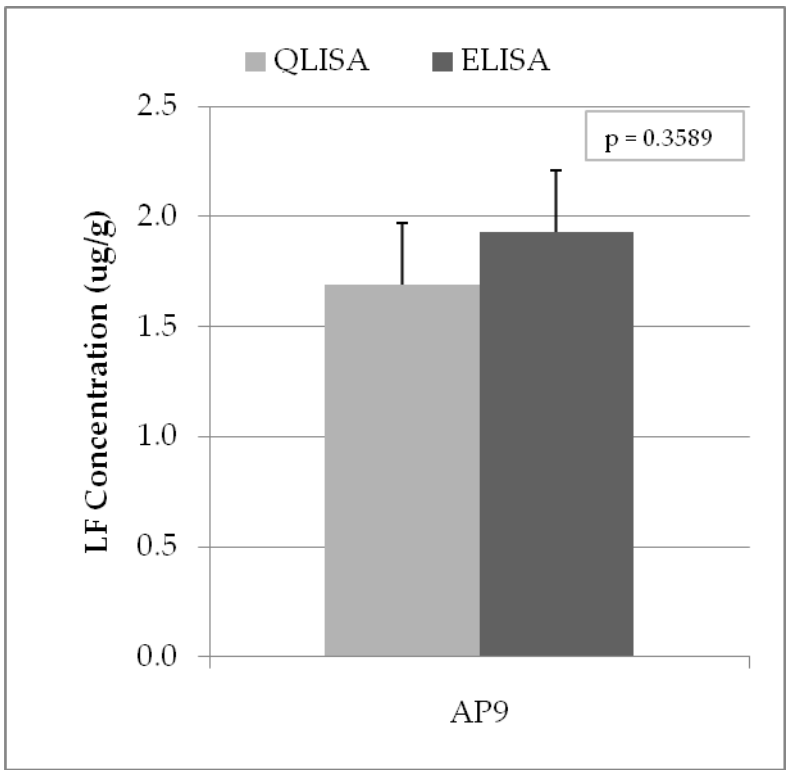

Figure 65: A comparison between myeloperoxidase levels detected in the stool sample from patient AP9 using QLISA and ELISA systems. P-values from a T-test are towards the upper right corner.

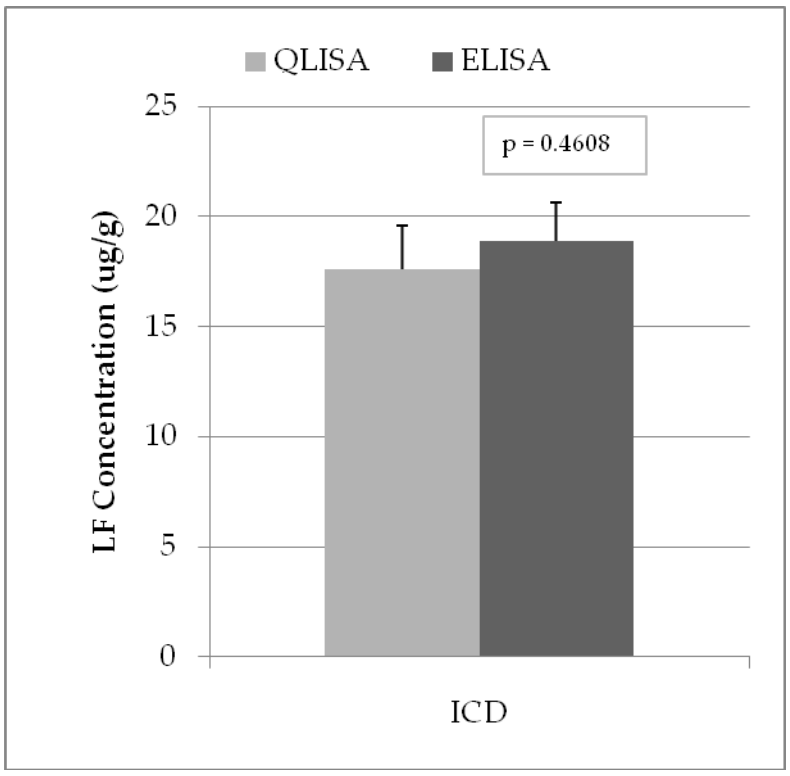

Figure 66: A comparison between myeloperoxidase levels detected in the stool sample from patient ICD using QLISA and ELISA systems. P-values from a T-test are towards the upper right corner.

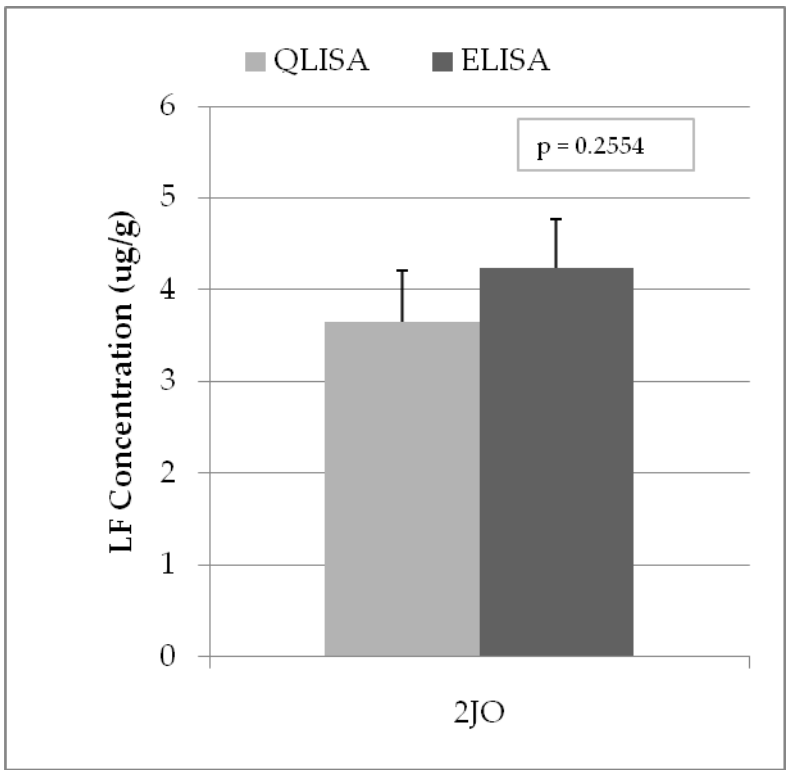

Figure 67: A comparison between myeloperoxidase levels detected in the stool sample from patient 2JO using QLISA and ELISA systems. P-values from a T-test are towards the upper right corner.

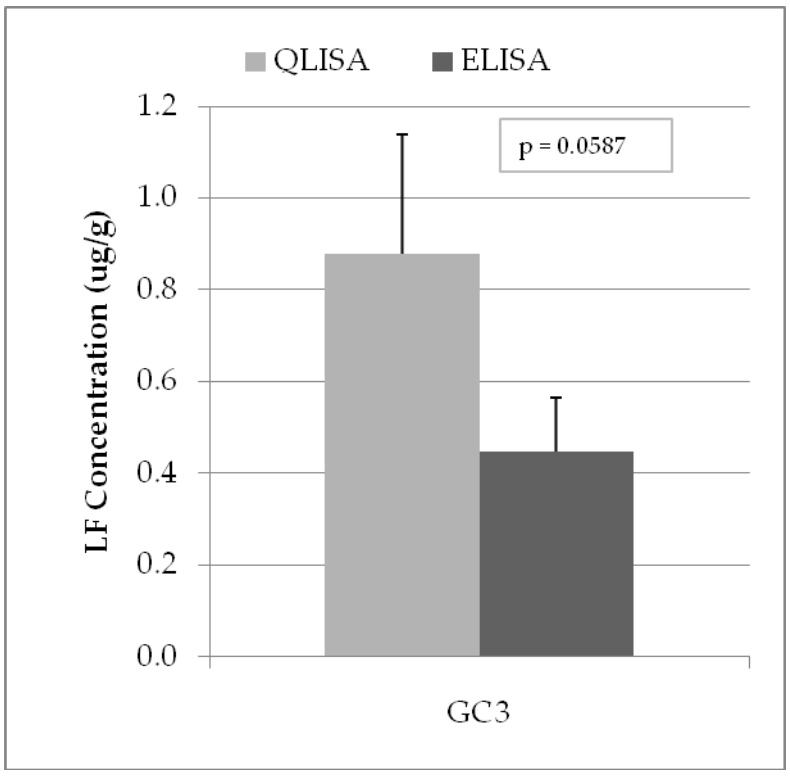

Figure 68: A comparison between myeloperoxidase levels detected in the stool sample from patient GC3 using QLISA and ELISA systems. P-values from a T-test are towards the upper right corner.

We also compare the results from QLISA and ELISA for both myeloperoxidase and lactoferrin in a graph in Figure 69. Here the x-axis is the myeloperoxidase and lactoferrin concentrations from the ELISA kits and the y-axis is the myeloperoxidase and lactoferrin concentrations from QLISA. They are each modeled with a linear regression line to compare concentrations for each sample. We find excellent agreement between the QLISA and ELISAs given the high R^2 values of 0.9880 and 0.9703 for myeloperoxidase and lactoferrin, respectively.

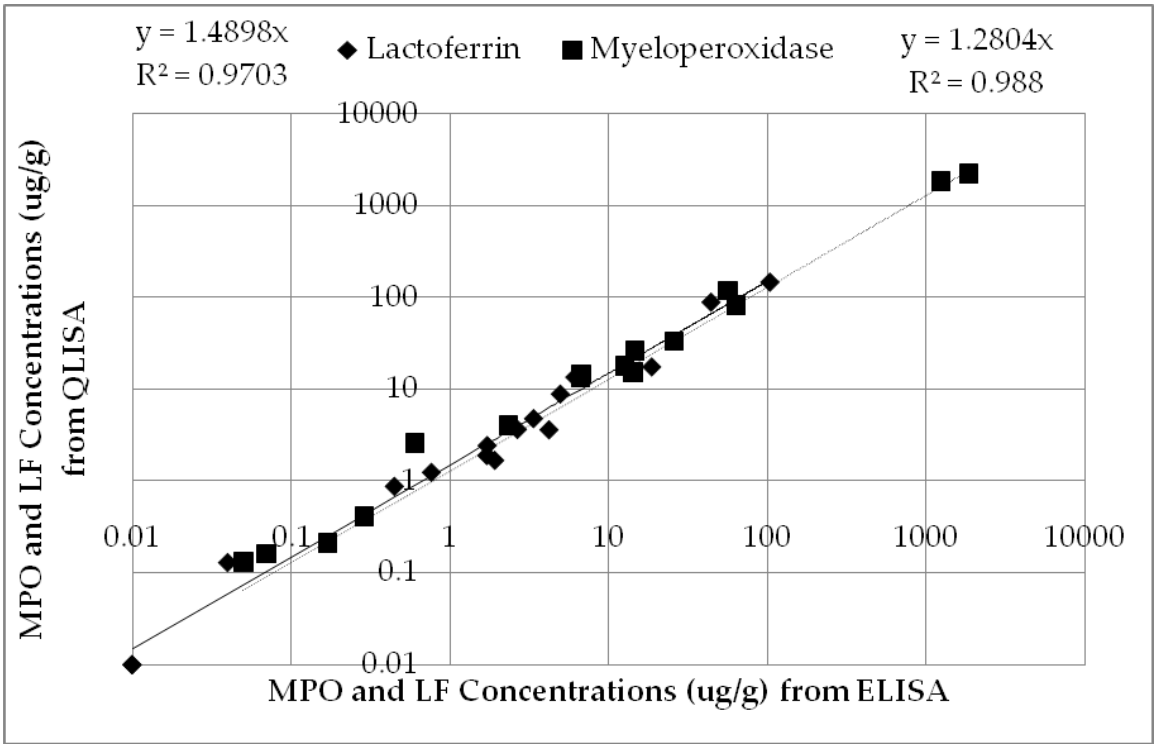

Figure 69: Linear regression lines for myeloperoxidase / lactoferrin concentrations comparing QLISA (y-axis) and ELISA (x-axis) values. R^2 values indicate a high correlation between the two immunoassays.

In addition to analysis with the 2nd generation QLISA system we also previously examined 9 of the human samples with the 1st generation QLISA, the Zen Myeloperoxidase ELISA kit (Invitrogen), and the IBD-SCAN Lactoferrin ELISA kit (IBD-SCAN) to determine myeloperoxidase and lactoferrin levels. Protocols for these immunoassays can be seen in Appendix D and E. The results showing myeloperoxidase and lactoferrin levels with QLISA and ELISA are reported and discussed in Appendix F.

3.2.4 Discussion

The discussion is broken into 2 subsections – the first discuss the comparison of QLISA and ELISA detection capabilities for both myeloperoxidase and lactoferrin and the second subsection reviews the correlation between myeloperoxidase and lactoferrin levels with clinical conditions.

3.2.4.1 QLISA – ELISA

The goal of using two different immunoassays to evaluate myeloperoxidase and lactoferrin concentrations in human stool samples is to compare the efficacy of our in-house developed immunoassay, QLISA, to a commercially available ELISA kit. We wanted to demonstrate that our system works comparably to what is currently available on the market. Statistical differences were determined using p-values found from t-test. While we use the commercial ELISA kits as a standard to measure our QLISA system we know that even the ELISA is not a perfect detection system.

Once our QLISA system was operational and we were able to regularly reproduce our standard curve we spiked healthy stool with various concentrations of myeloperoxidase and then tested those samples with QLISA.

The healthy stool samples were assumed to have little if any myeloperoxidase. Results above indicated that myeloperoxidase was recovered in expected amounts as compared to the standard curve. In other words when myeloperoxidase was added to a healthy human stool sample at a concentration of 100ng/mL, we detected about 100ng/mL of myeloperoxidase as indicated from the standard curve which measures myeloperoxidase in just buffered solutions. This is a critical finding that allows us to push forward with the unknown human samples and give us confidence in limiting any potential specificity issues of QLISA.

Above figures show concentrations of both myeloperoxidase and lactoferrin in each of the 16 human samples found with both QLISA and ELISA. We were blinded to the patient condition of the human sample and tested samples with QLISA first. The QLISA and ELISA samples for the human samples were compared individually since myeloperoxidase and lactoferrin levels were detected over a range of orders of magnitude. Simultaneous plotting would have been of limited use. When analyzing each sample, we note that myeloperoxidase and lactoferrin detection with QLISA and ELISA are statistically comparable as defined by P-values greater than 0.05. In fact myeloperoxidase detection for QLISA and ELISA was statistically similar for 9 of

the 16 patient samples and of those seven samples, only 3 had a p-value less than 0.01, indicating a relatively good correlation between QLISA and ELISA detection levels of myeloperoxidase. Even of the 3 samples with p-values less than 0.01, there is very little difference in myeloperoxidase levels. QLISA detected 1.9, 0.13, and 0.9ug/g compared to ELISA detecting 1.7, 0.04, and 0.4ug/g in the same samples, respectively. These statistical differences are seen only at the lowest end of myeloperoxidase levels and thus might be attributed to limitations of both assays lower limit of detection.

Detection of lactoferrin levels in QLISA and ELISA were also relatively similar, even more so than myeloperoxidase. In fact as seen in the Figures above there are only 3 human samples that recorded p-values less than 0.05 indicating a statistical difference between QLISA and ELISA lactoferrin detection level. Moreover there were no samples with a p-value of 0.01 or less thus indicating that even those 3 samples with different levels were only slightly statistically different. Similar to the myeloperoxidase samples that were different for QLISA and ELISA, two of the three lactoferrin samples with differences were towards the lowest detection limit and indicate small real differences in lactoferrin. The QLISA detection levels were 0.009 and 0.13ug/g and the same ELSIA samples were 0.06 and 0.04ug/g of lactoferrin, respectively. Someone reading either the

QLISA or ELISA assay would conclude that lactoferrin is not present in clinically significant concentrations.

3.2.4.2 QLISA – IBD

The major hypothesis that this research addresses is: Can fecal levels of myeloperoxidase and lactoferrin help physicians differentiate inflammatory bowel disease from healthy individuals?

There are two graphs sown in Figures 70 and 71 that show the concentration of myeloperoxidase and lactoferrin in all 16 human samples separated into 3 groups – healthy, inflammatory bowel disease (ulcerative colitis and Crohn's disease), and other inflammatory bowel disease (ischemic colitis, infectious colitis and clostridium difficile) patients. The y-axis in both graphs is plotted in a logarithmic scale which better exemplifies the range of values. Healthy patients had an average of 0.18ug/g and 0.01ug/g of myeloperoxidase and lactoferrin in their stool samples, respectively while the inflammatory bowel disease patients had 434.67ug/g and 28.91ug/g of myeloperoxidase and lactoferrin, respectively. The other inflammatory bowel disease patients had an average of 12.12ug/g and 2.23ug/g of myeloperoxidase and lactoferrin in their stool, respectively. Myeloperoxidase demonstrates a clear 2300-fold elevation in

inflammatory bowel disease patients over healthy patients. It also shows an approximate 2800-fold increase in lactoferrin levels in inflammatory bowel disease over healthy patients. Even the lowest concentration of myeloperoxidase in an inflammatory bowel disease patient shows a 12-fold increase in concentration. Using a 1ug/g myeloperoxidase cutoff as a mark between inflammatory bowel disease and healthy control would give a 100% accuracy in diagnosing inflammatory bowel disease. From this patient population we could conclude that any patient with a myeloperoxidase concentration over 1ug/g has some type of inflammatory bowel disease and any patient with a myeloperoxidase concentration below 1ug/g does not have inflammatory bowel disease. However, levels below 1ug/g for myeloperoxidase do not help rule out patients with inflammatory bowel disease given the two patients with other inflammatory bowel disease (infectious diarrhea and clostridium difficile) have myeloperoxidase levels below that threshold.

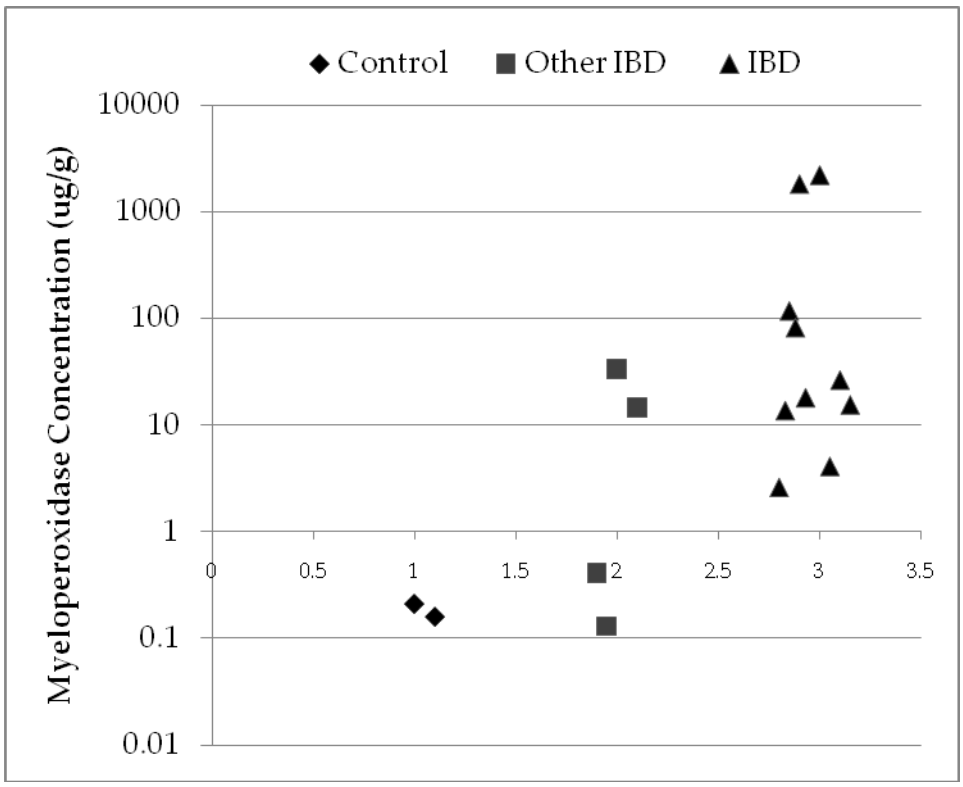

Figure 70: Myeloperoxidase levels as detected by QLISA for 16 human stool samples. The number 1 on the x-axis corresponds to healthy controls, 2 to other inflammatory bowel disease patients, and 3 to inflammatory bowel disease patients.

The lactoferrin results in also provide some clear results. Here healthy patients have extremely low levels of lactoferrin in their stool (0.01ug/g), but a cutoff lactoferrin level is less obvious. Average lactoferrin concentrations for inflammatory bowel disease (ulcerative colitis and Crohn's disease) and other inflammatory bowel disease (ischemic colitis, infectious diarrhea and clostridium difficile) patients are 28.91ug/g and 2.23ug/g, respectively. These elevations, while not as high as what we saw with myeloperoxidase, are still several orders of magnitude higher than the healthy control average of 0.01ug/g level. In fact

there is a three-fold order of magnitude increase for both myeloperoxidase and lactoferrin when comparing healthy controls to even the other inflammatory bowel disease group. However, unlike the myeloperoxidase levels in healthy controls and other inflammatory bowel disease, there is still a marked distinction between these two groups when looking at lactoferrin results, yet we still do see one Crohn's patient with a lactoferrin level below 1ug/g. This is encouraging and suggests that lactoferrin is a useful marker in helping physicians differentiating health patients from patients from the other inflammatory bowel disease patients.

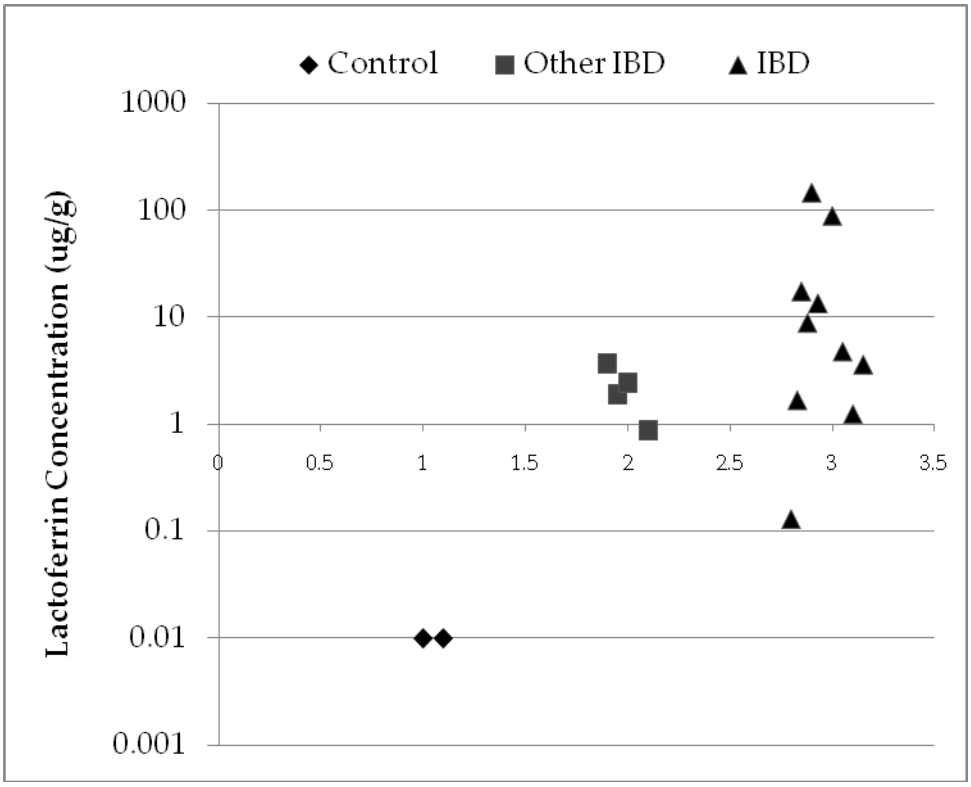

Figure 71: Myeloperoxidase levels as detected by QLISA for 16 human stool samples. The number 1 on the x-axis corresponds to healthy controls, 2 to other inflammatory bowel disease patients, and 3 to inflammatory bowel disease patients.

After determining that both myeloperoxidase and lactoferrin made good biomarkers for differentiating between inflammatory bowel disease from healthy patients, we began examining how these biomarkers correlated to specific inflammatory bowel diseases. Figures 72 and 73 show the level of myeloperoxidase and lactoferrin levels for each of the different patients. These figures demonstrate that while both markers can be used in differentiating between inflammatory bowel disease healthy individuals they do not have the ability to differentiate between types of inflammatory bowel disease. This is an

extremely small size population, so this conclusion is far from absolute. In fact we can see some higher level of both biomarkers in Crohn's disease, but this isn't true for all patients with Crohn's disease. The small sample size is due to the current number of enrolled patients (only 16) and the speed to process them. We therefore can conclude that within this small sample there is encouraging and possibly beneficial use in knowing myeloperoxidase and lactoferrin levels for differentiating inflammatory bowel disease, there is nothing that can be definitively concluded from these 16 patients and further patient analysis would be useful.

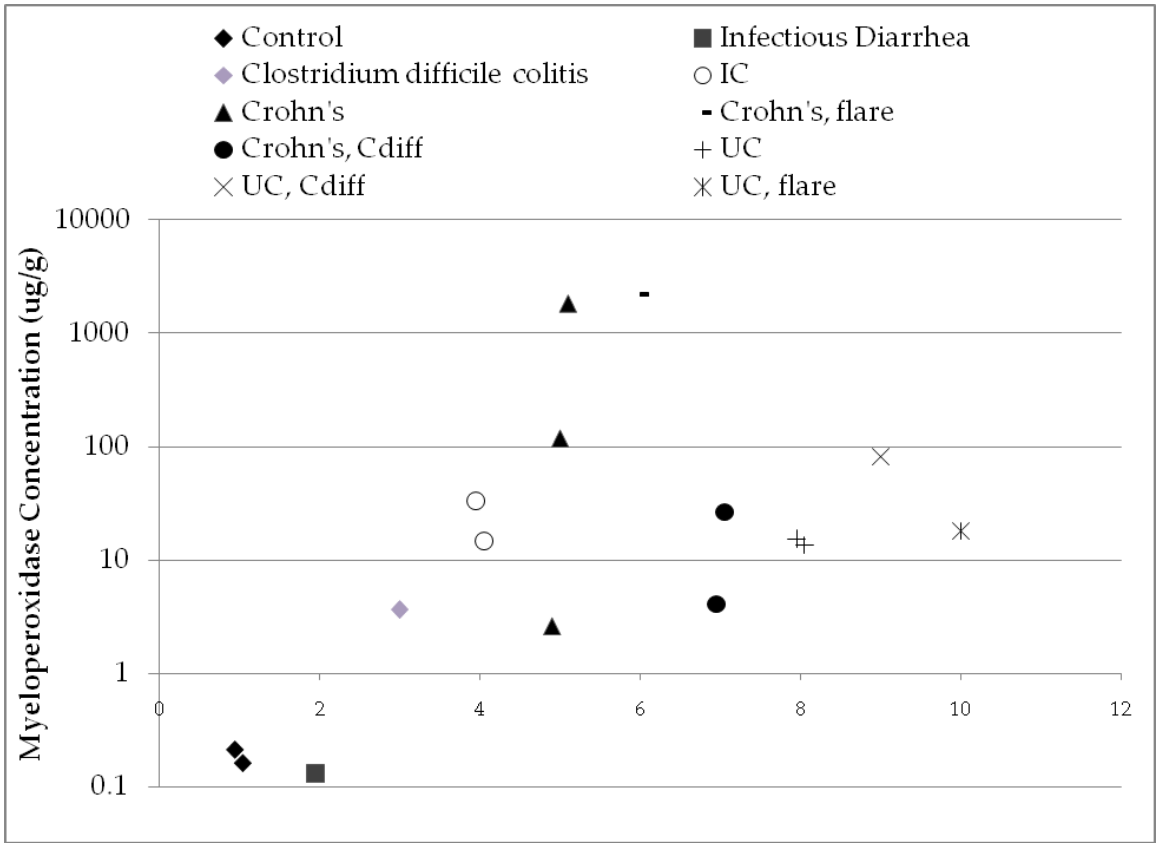

Figure 72: A graph showing myeloperoxidase concentrations in human patient samples with various conditions. The x-axis values correspond to the following: 1 – Healthy Control, 2 – Infectious Diarrhea, 3 – Clostridium difficile colits, 4 – Ischemic Colitis, 5 – Crohn's, 6 - Crohn's with flaring, 7 – Crohn's, Cdiff, 8 – Ulcerative Colitis, 9 – Ulcerative Colitis, Cdiff, 10 – Ulcerative Colitis with flaring.

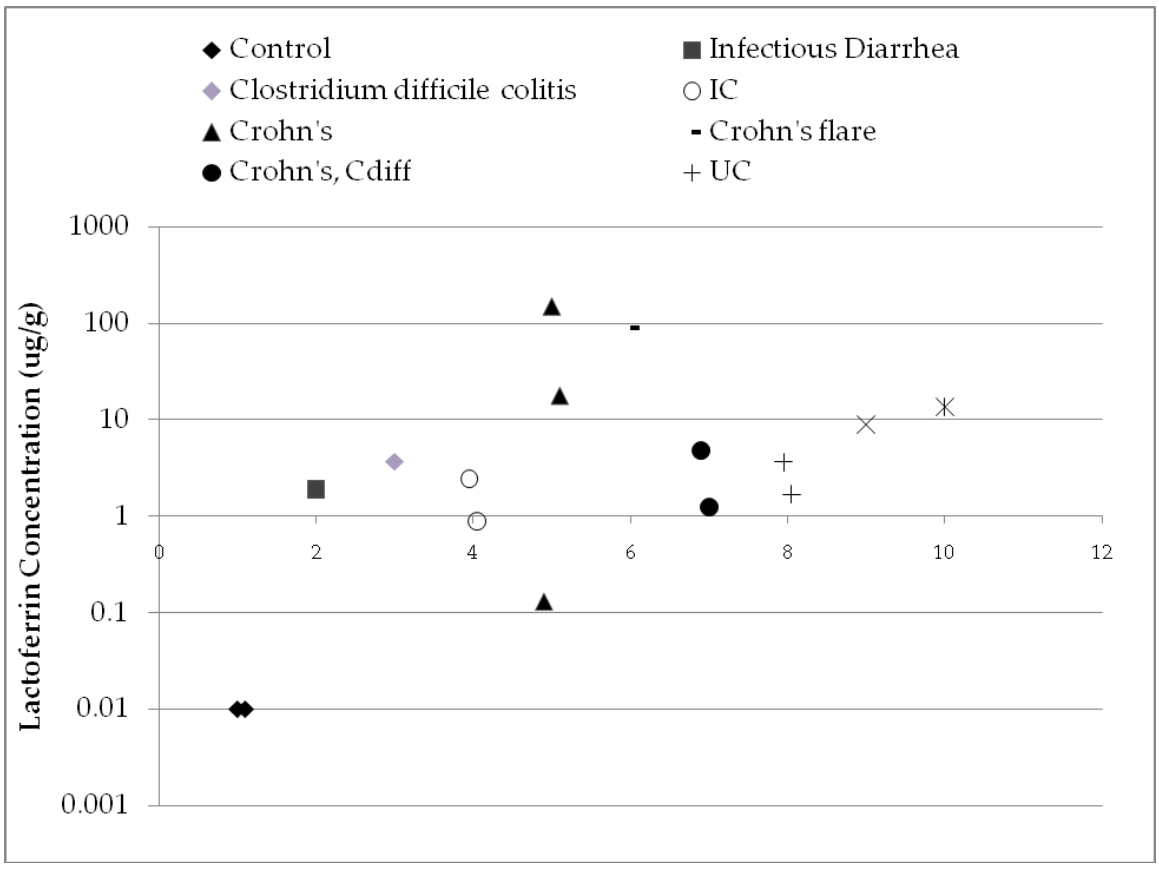

Figure 73: A graph showing lactoferrin concentrations in human patient samples with various conditions. The x-axis values correspond to the following: 1 – Healthy Control, 2 – Infectious Diarrhea, 3 – Clostridium difficile colits, 4 – Ischemic Colitis, 5 – Crohn's, 6 - Crohn's with flaring, 7 – Crohn's, Cdiff, 8 – Ulcerative Colitis, 9 – Ulcerative Colitis, Cdiff, 10 – Ulcerative Colitis with flaring.

The most important find is that high levels of myeloperoxidase and lactoferrin can rule out a healthy individual. This can better help physicians tailor their clinical decision making.

CHAPTER 4: CONCLUSIONS

The main goal of this work has been to evaluate the levels of myeloperoxidase and lactoferrin from human stool samples of patients with inflammatory bowel disease using our novel QLISA system. We have made quantifiable improvements to the QLISA system through an enhanced antibody immobilization strategy that uses a unique combination of crosslinkers. These improvements have been demonstrated with the full QLISA assay for both myeloperoxidase and lactoferrin and validated with comparisons to commercial ELISA kits.

4.1 SUMMARY OF FINDINGS

There have been several important findings from this work, which have made significant contributions. The three main findings are discussed individually below.

1. The first major achievement of this research was significantly improving the surface chemistry of the primary immobilized antibody on our PMMA

microcapillary using a unique combination of crosslinkers. Our group filed a US patent application (No.61/334,056, filed 12, May 2010, PCT international patent application No. PCT/US11/36290) for this novel surface chemistry methodology. We also reported these findings along with our direct comparison of PMMA surface activation techniques in an original research article (under review at Bioengineering and Biotechnology). This manuscript includes numerical simulations of antibody – antigen kinetics using COMSOL that support our experimental findings. In addition to this surface chemistry being novel, it provides a significant benefit to other commonly used methods, thus providing an opportunity for other immunoassay developers to improve on their own systems.

2. The next milestone in this work was showing that our QLISA system detected myeloperoxidase and lactoferrin in human stool samples at levels that were comparable to commercially available immunoassays that are marketed to do the same. We found this milestone especially rewarding as our experimental results from QLISA supported the theoretical framework it was based on. The novelty of QLISA and its potential advantages and benefits over ELISA substantiates our efforts in this

research. The two greatest advantages that QLISA has over ELISA are the small working volume (up to 100 times less than ELISA) and the multiplexing potential using different sized quantum dots for different biomarkers. The previous would be advantageous for sample collected via rectal swap or in other clinical applications like testing limited cerebrospinal fluid. The other potential advantage of using multiple quantum dots of different sizes to detect multiple biomarkers has obvious benefits given quantum dots large excitation spectra and narrow size-dependent emission spectra. Having an assay that could evaluate myeloperoxidase and lactoferrin using the same sample at the same time would have tremendous benefit, especially if three, four, or even more biomarkers could be simultaneously detected. This work, in combination with findings from our third main finding, is currently being drafted into an original research article for publication at a journal to be decided. Additionally we are in the process of writing a book chapter titled, "Quantum Dots for Bioimaging, Cellular Labeling and Biodiagnostics," for a book tentatively titled, "Quantum Dots: Applications, Synthesis and Characterization."

3. A third major accomplishment from this work was the connections we made between myeloperoxidase and lactoferrin levels in stool samples to gastrointestinal diseases like Crohn's disease, ulcerative colitis and ischemic colitis. The literature correlating these proteins to inflammatory bowel disease is lacking especially with myeloperoxidase. Our data correlating these biomarkers individually and in combination to inflammatory bowel disease is substantial in this poorly researched area. This correlation between myeloperoxidase and lactoferrin with inflammatory bowel disease will be further revealed from the continuation of this research. The more patient samples evaluated the more confident we can become in the correlations. Realizing that these are potentially critical biomarkers in helping identify inflammatory bowel disease will lend way to more research into their relationship.

In addition to these three main findings described above, we have also made other significant engineering improvement to the current QLISA technology. In addition to the improved antibody immobilization procedure described above, we have manufactured a completely new microcapillary holder. The first generation QLISA technology relied on manual focusing of the ultraviolet excitation source on the capillary. Additionally the microcapillary was held in

place with a custom made spring holder (Babu, et al., 2009). Both these methods led to variation between different microcapillary measurements and variation between the same microcapillary when measured with different users. We designed a new microcapillary holder that mounts the ultraviolet excitation source in a fixed position. We also used two steel tubes, slightly larger than the outer diameter of the microcapillary, that guide the microcapillary into the same position every time. This ensures that the microcapillaries are loaded into the same position every time, regardless of user, and that the ultraviolet source is focused on the same spot every time, regardless of user. This configuration provides a tremendous benefit over the first generation QLISA. Another improvement we made over the first generation QLISA technology was the use of a biotinylated secondary antibody that would later bind a streptavidin conjugated quantum dot. This chemistry was more reliable than the first generation QLISA technology that used a secondary antibody conjugated quantum dot. This bioconjugate chemistry was performed in our lab and subject to variability between each conjugation procedure which had to be reproduced every 3-4 weeks. As mentioned elsewhere in this dissertation, the newer biotin-streptavidin chemistry proved superior in its reliability.

4.2 CONTRIBUTIONS TO THE FIELD

We have extended and helped build on previous literature. In particular we provided a quantitative review of PMMA surface activation techniques comparing two popular methods – oxygen plasma and sodium hydroxide treatment. These two well-known techniques aren't compared and researchers frequently choose one or the other, with various parameters, with no explanation of their technique or consideration for other techniques or conditions. We built on this by quantitatively comparing surface density of several crosslinkers, which has been performed but not using all the crosslinkers we chose to use. So here we have added antibody immobilization data using unique combinations of crosslinkers. Our patent application on this contributes to this large and interesting field and could prove useful for others. Another contribution is the addition and validation of a novel biosensor - the new and improved QLISA technology. This is a unique immunoassay system that hadn't been previously tested. Lastly we help further establish the level of myeloperoxidase in stool samples of inflammatory bowel disease patients. This literature is very limited and all have very well defined patient population and testing conditions that limits their conclusions to their specific study.

4.3 FUTURE WORK

This work can be extended in several directions, all of which are exciting with high impact potential in several fields. The two most important directions would be the extension of the human sample analysis and the improved robustness of the QLISA system. The system is currently sufficient enough to evaluate human samples but is limited by the QLISA system. Clearly improving the QLISA system would make human sample analysis much easier and more efficient. Chief among the future goals of the QLISA system should be to automation of steps for improved efficacy and user-friendliness and development of a multiplexed immunoassay that took advantage of quantum dots unique excitation and emission properties. This latter goal would lead to the potential of multi-biomarker analysis in a single assay, thus increasing clinical information for the physician while reducing assay time, assay evaluation time, and money. Other potential biomarkers to use in a multi-biomarker assay would be calprotectin, perinuclear anti-neutrophil cytoplasmic antibody (pANCA), and / or anti-saccharolmyces cerevisiae antibody (ASCA). Calprotectin levels have to increase in inflammatory bowel disease patients (Rheenen, Vijver, & Fidler, 2011), and pANCA and ASCA have shown specificity

to ulcerative colitis and Crohn's disease, respectively (Bossuyt, 2006; Reese et al., 2006; Savige et al., 2003).

In my opinion, the most exciting future work is the enrollment of more patients in this study to continue the evaluation of myeloperoxidase and lactoferrin levels in their stool using QLISA with ELISA as a comparison. More patients would not only better validate the efficacy of QLISA it would also provide more meaningful correlation between myeloperoxidase and lactoferrin levels to inflammatory bowel disease. Ideally this would be on the order of hundreds of patients and to accomplish this using the current QLISA system would require a very repetitive process using several scientist running assays around the clock. A potential way to circumvent this situation would be to improve the speed and user-friendliness of the assay as addressed above.

LIST OF REFERENCES

Anderson, B. F., Baker, H. M., Dodson, E. J., Norris, G. E., Rumball, S. V., Waters, J. M., & Baker, E. N. (1987). Structure of human lactoferrin at 3.2-A resolution. *Proceedings of the National Academy of Sciences of the United States of America, 84*(7), 1769-1773.

Anderson, G. P., Jacoby, M. A., Ligler, F. S., & King, K. D. (1997). Effectiveness of protein A for antibody immobilization for a fiber optic biosensor. *Biosensors and Bioelectronics, 12*(4), 329-336.

Babu, S., Mohapatra, S., Zubkov, L., Murthy, S., & Papazoglou, E. (2009). A PMMA microcapillary quantum dot linked immunosorbent assay (QLISA). *Biosensors and Bioelectronics, 24*(12), 3467-3474.

Bai, Y., Huang, W.-C., & Yang, S.-T. (2007). Enzyme-linked immunosorbent assay of Escherichia coli O157:H7 in surface enhanced poly(methyl methacrylate) microchannels. *Biotechnology and Bioengineering, 98*(2), 328-339.

Bai, Y., Koh, C. G., Boreman, M., Juang, Y.-J., Tang, I. C., Lee, L. J., & Yang, S.-T. (2006). Surface Modification for Enhancing Antibody Binding on Polymer-Based Microfluidic Device for Enzyme-Linked Immunosorbent Assay. *Langmuir, 22*(22), 9458-9467. doi: 10.1021/la061123l

Bai, Y. L., Huang, W. C., & Yang, S. T. (2007). Enzyme-linked Immunosorbent assay of Escherichia coli O157 : H7 in surface enhanced Poly(Methyl methacrylate) microchannels. *Biotechnology and Bioengineering, 98*(2), 328-339. doi: Doi 10.1002/Bit.21429

Bai, Y. L., Koh, C. G., Boreman, M., Juang, Y. J., Tang, I. C., Lee, L. J., & Yang, S. T. (2006). Surface modification for enhancing antibody binding on polymer-based microfluidic device for enzyme-linked immunosorbent assay. *Langmuir, 22*(22), 9458-9467. doi: Doi 10.1021/La061123l

Baumgart, D. C., & Sandborn, W. J. (2007). Inflammatory bowel disease: clinical aspects and established and evolving therapies. *Lancet, 369*(9573), 1641-1657. doi: S0140-6736(07)60751-X [pii]

10.1016/S0140-6736(07)60751-X

Blair-Johnson, M., Fiedler, T., & Fenna, R. (2001). Human Myeloperoxidase: Structure of a Cyanide Complex and Its Interaction with Bromide and Thiocyanate Substrates at 1.9 Å Resolution&#x2020. *Biochemistry, 40*(46), 13990-13997. doi: doi:10.1021/bi0111808

Bossuyt, X. (2006). Serologic Markers in Inflammatory Bowel Disease. *Clin Chem, 52*(2), 171-181. doi: 10.1373/clinchem.2005.058560

Butler, J. E., Ni, L., Brown, W. R., Joshi, K. S., Chang, J., Rosenberg, B., & Voss, J. E. W. (1993). The immunochemistry of sandwich elisas--VI. Greater than 90% of monoclonal and 75% of polyclonal anti-fluorescyl capture antibodies (CAbs) are denatured by passive adsorption. *Molecular Immunology, 30*(13), 1165-1175.

Butler, J. E., Ni, L., Nessler, R., Joshi, K. S., Suter, M., Rosenberg, B., . . . Cantarero, L. A. (1992). The physical and functional behavior of capture antibodies adsorbed on polystyrene. *Journal of Immunological Methods, 150*(1-2), 77-90.

Carpena, X., Vidossich, P., Schroettner, K., Calisto, B. M., Banerjee, S., Stampler, J., . . . Obinger, C. (2009). Essential Role of Proximal Histidine-Asparagine Interaction in Mammalian Peroxidases. *Journal of Biological Chemistry, 284*(38), 25929-25937. doi: 10.1074/jbc.M109.002154

Chang, L., & Heitkemper, M. M. (2002). Gender differences in irritable bowel syndrome. *Gastroenterology, 123*(5), 1686-1701. doi: S0016508502003025 [pii]

Choi, S.-M., Yang, W.-K., Yoo, Y.-W., & Lee, W.-K. (2010). Effect of surface modification on the in vitro calcium phosphate growth on the surface of poly(methyl methacrylate) and bioactivity. *Colloids and Surfaces B: Biointerfaces, 76*(1), 326-333. doi: DOI: 10.1016/j.colsurfb.2009.11.012

Chung, J. W., Park, J. M., Bernhardt, R., & Pyun, J. C. (2006). Immunosensor with a controlled orientation of antibodies by using NeutrAvidin-protein A complex at immunoaffinity layer. *Journal of Biotechnology, 126*(3), 325-333.

Dai, J., Liu, W.-Z., Zhao, Y.-P., Hu, Y.-B., & Ge, Z.-Z. (2007). Relationship between fecal lactoferrin and inflammatory bowel disease. *Scandinavian Journal of Gastroenterology, 42*(12), 1440-1444. doi: doi:10.1080/00365520701427094

Della-Penna, D., Christoffersen, R. E., & Bennett, A. B. (1986). Biotinylated proteins as molecular weight standards on Western blots. *Analytical Biochemistry, 152*(2), 329-332. doi: 10.1016/0003-2697(86)90417-3

Everhart, J. E., & Ruhl, C. E. (2009). Burden of Digestive Diseases in the United States Part II: Lower Gastrointestinal Diseases. *Gastroenterology, 136*(3), 741-754.

Fan, R., Vermesh, O., Srivastava, A., Yen, B. K. H., Qin, L., Ahmad, H., . . . Heath, J. R. (2008). Integrated barcode chips for rapid, multiplexed analysis of proteins in microliter quantities of blood. [10.1038/nbt.1507]. *Nat Biotech, 26*(12), 1373-1378. doi: http://www.nature.com/nbt/journal/v26/n12/suppinfo/nbt.1507_S1.html

Fenna, R. E., Zeng, J., & Davey, C. A. (1995). Structure of the Green Heme in Myeloperoxidase. *Archives of Biochemsitry and Biophysics, 316*(1), 653-657. doi: doi:10.1006/abbi.1995.1086 <http://dx.doi.org/10.1006/abbi.1995.1086>

Fiedler, T. J., Davey, C. A., & Fenna, R. E. (2000). X-ray Crystal Structure and Characterization of Halide-binding Sites of Human Myeloperoxidase at 1.8 A Resolution. *J. Biol. Chem., 275*(16), 11964-11971. doi: 10.1074/jbc.275.16.11964

Fowler, J. M., Stuart, M. C., & Wong, D. K. Y. (2006). Self-Assembled Layer of Thiolated Protein G as an Immunosensor Scaffold. *Analytical Chemistry, 79*(1), 350-354. doi: 10.1021/ac061175f

Ghose, S., Hubbard, B., & Cramer, S. M. (2007). Binding capacity differences for antibodies and Fc-fusion proteins on protein A chromatographic materials. *Biotechnology and Bioengineering, 96*(4), 768-779.

Green, N. M. (1990). *Avidin and streptavidin* (Vol. 184). San Diego, CA, ETATS-UNIS: Elsevier.

Groves, M. L. (1960). The Isolation of a Red Protein from Milk2. *Journal of the American Chemical Society, 82*(13), 3345-3350. doi: 10.1021/ja01498a029

Guss, B., Uhlen, M., Nilsson, B., Lindberg, M., Sjoquist, J., & Sjodahl, J. (1984). Region X, the cell-wall-attachment part of staphylococcal protein A. *European Journal of Biochemistry, 138*(2), 413-420.

Hampton, M. B., Kettle, A. J., & Winterbourn, C. C. (1998). Inside the Neutrophil Phagosome: Oxidants, Myeloperoxidase, and Bacterial Killing. *Blood, 92*(9), 3007-3017.

Hermanson, G. T. (2008). *Bioconjugate Techniques* (2nd ed.). San Diego: Academic Press.

Hu, J., Li, S., & Liu, B. (2006). Properties of immobilized pepsin on Modified PMMA microspheres. *Biotechnology Journal, 1*(1), 75-79. doi: 10.1002/biot.200500022

Hulisz, D. (2004). The burden of illness of irritable bowel syndrome: current challenges and hope for the future. *J Manag Care Pharm, 10*(4), 299-309. doi: 2004(10)4: 299-309 [pii]

Jagannath, C., & Sehgal, S. (1989). Enhancement of the antigen-binding capacity of incomplete IgG antibodies to Brucella melitensis through Fc region interactions with staphylococcal protein A. *Journal of Immunological Methods, 124*(2), 251-257.

Jendeberg, L., Tashiro, M., Tejero, R., Lyons, B. A., Uhlen, M., Montelione, G. T., & Nilsson, B. (1996). The Mechanism of Binding Staphylococcal Protein A to Immunoglobin G Does Not Involve Helix Unwinding. *Biochemistry, 35*(1), 22-31. doi: 10.1021/bi9512814

Johnson, C. P., Jensen, I. E., Prakasam, A., Vijayendran, R., & Leckband, D. (2003). Engineered Protein A for the Orientational Control of Immobilized Proteins. *Bioconjugate Chemistry, 14*(5), 974-978. doi: 10.1021/bc034063t

Kane, S. V., Sandborn, W. J., Rufo, P. A., Zholudev, A., Boone, J., Lyerly, D., . . . Hanauer, S. B. (2003). Fecal Lactoferrin Is a Sensitive and Specific Marker in Identifying Intestinal Inflammation. *Am J Gastroenterol, 98*(6), 1309-1314.

Kappelman, M. D., Rifas-Shiman, S. L., Porter, C. Q., Ollendorf, D. A., Sandler, R. S., Galanko, J. A., & Finkelstein, J. A. (2008). Direct health care costs of Crohn's disease and ulcerative colitis in US children and adults. *Gastroenterology, 135*(6), 1907-1913. doi: S0016-5085(08)01675-2 [pii]
10.1053/j.gastro.2008.09.012

Kimura, S., & Ikeda-Saito, M. (1988). Human myeloperoxidase and thyroid peroxidase, two enzymes with separate and distinct physiological functions, are evolutionarily related members of the same gene family. *Proteins: Structure, Function, and Genetics, 3*(2), 113-120.

Klebanoff, S. J. (2005). Myeloperoxidase: friend and foe. *Journal of Leukocyte Biology, 77*(5), 598-625. doi: 10.1189/jlb.1204697

LÃ¶nnerdal, B., & Iyer, S. (1995). Lactoferrin: Molecular Structure and Biological Function. *Annual Review of Nutrition, 15*(1), 93-110. doi: doi:10.1146/annurev.nu.15.070195.000521

Langhorst, J., Elsenbruch, S., Koelzer, J., Rueffer, A., Michalsen, A., & Dobos, G. J. (2008). Noninvasive Markers in the Assessment of Intestinal Inflammation in Inflammatory Bowel Diseases: Performance of Fecal Lactoferrin, Calprotectin, and PMN-Elastase, CRP, and Clinical Indices. *The American Journal of Gastroenterology, 103*(1), 162-169.

Lefkowitz, D. L., & Lefkowitz, S. S. (2001). Macrophage-neutrophil interaction: A paradigm for chronic inflammation revisited. *Immunol Cell Biol, 79*(5), 502-506.

LettesjÃ¶, H., Hansson, T., Peterson, C., Ung, K.-A., RingstrÃ¶m, G., Abrahamsson, H., & SimrÃ©n, M. (2006). Detection of inflammatory markers in stools from patients with irritable bowel syndrome and collagenous colitis. *Scandinavian Journal of Gastroenterology, 41*(1), 54-59. doi: doi:10.1080/00365520510023909

Li, S., Hu, J., & Liu, B. (2004). Use of chemically modified PMMA microspheres for enzyme immobilization. *Biosystems, 77*(1-3), 25-32. doi: 10.1016/j.biosystems.2004.03.001

Lin, Z., Wang, X., Li, Z.-J., Ren, S.-Q., Chen, G.-N., Ying, X.-T., & Lin, J.-M. (2008). Development of a sensitive, rapid, biotin-streptavidin based chemiluminescent enzyme immunoassay for human thyroid stimulating hormone. *Talanta, 75*(4), 965-972. doi: 10.1016/j.talanta.2007.12.043

Liu, J., Pan, T., Woolley, A. T., & Lee, M. L. (2004). Surface-Modified Poly(methyl methacrylate) Capillary Electrophoresis Microchips for Protein and Peptide Analysis. *Analytical Chemistry, 76*(23), 6948-6955. doi: 10.1021/ac040094l

Liu, R., Liu, J., Xie, L., Wang, M., Luo, J., & Cai, X. (2010). A fast and sensitive enzyme immunoassay for brain natriuretic peptide based on micro-magnetic probes strategy. *Talanta, 81*(3), 1016-1021. doi: 10.1016/j.talanta.2010.01.051

Magalhães, M. L. B., Czekster, C. M., Guan, R., Malashkevich, V. N., Almo, S. C., & Levy, M. (2011). Evolved streptavidin mutants reveal key role of loop residue in high-affinity binding. *Protein Science, 20*(7), 1145-1154. doi: 10.1002/pro.642

Marie-Madeleine CALS, P. M., Ghislaine BRIGNON, Patricia ANGLADE, Bruno Ribadeau DUMAS,. (1991). Primary structure of bovine lactoperoxidase, a fourth member of a mammalian heme peroxidase family. *European Journal of Biochemistry, 198*(3), 733-739.

Mayer, E. A. (2008). Clinical practice. Irritable bowel syndrome. *N Engl J Med, 358*(16), 1692-1699. doi: 358/16/1692 [pii]

10.1056/NEJMcp0801447

McFarland, L. V. (2008). State-of-the-art of irritable bowel syndrome and inflammatory bowel disease research in 2008. *World J Gastroenterol, 14*(17), 2625-2629.

Medintz, I. L., Uyeda, H. T., Goldman, E. R., & Mattoussi, H. (2005). Quantum dot bioconjugates for imaging, labelling and sensing. [10.1038/nmat1390]. *Nat Mater, 4*(6), 435-446.

Mehne, J., Markovic, G., Pröll, F., Schweizer, N., Zorn, S., Schreiber, F., & Gauglitz, G. (2008). Characterisation of morphology of self-assembled PEG monolayers: a comparison of mixed and pure coatings optimised for biosensor applications. *Analytical and Bioanalytical Chemistry, 391*(5), 1783-1791. doi: 10.1007/s00216-008-2066-0

Merlie, J., Fagan, D., Mudd, J., & Needleman, P. (1988). Isolation and characterization of the complementary DNA for sheep seminal vesicle prostaglandin endoperoxide synthase (cyclooxygenase). *J. Biol. Chem., 263*(8), 3550-3553.

Mohanty, S. P., & Kougianos, E. (2006). Biosensors: a tutorial review. *Potentials, IEEE, 25*(2), 35-40.

Molecular Probes, I. (2006). AlexaFluor 488 Protein Labeling Kit.

Nicholls, S. J., & Hazen, S. L. (2005). Myeloperoxidase and Cardiovascular Disease. *Arteriosclerosis, Thrombosis, and Vascular Biology, 25*(6), 1102-1111. doi: 10.1161/01.ATV.0000163262.83456.6d

Niemeyer, C. M., Adler, M., & Wacker, R. (2007). Detecting antigens by quantitative immuno-PCR. [10.1038/nprot.2007.267]. *Nat. Protocols, 2*(8), 1918-1930.

Otten, C. M. T., Kok, L., Witteman, B. J. M., Baumgarten, R., Kampman, E., Moons, K. G. M., & de Wit, N. J. (2008). Diagnostic performance of rapid tests for detection of fecal calprotectin and lactoferrin and their ability to discriminate inflammatory from irritable bowel syndrome. *Clinical Chemistry and Laboratory Medicine, 46*(9), 1275-1280. doi: 10.1515/cclm.2008.246

Owaku, K., Goto, M., Ikariyama, Y., & Aizawa, M. (1995). Protein A Langmuir-Blodgett Film for Antibody Immobilization and Its Use in Optical Immunosensing. *Analytical Chemistry, 67*(9), 1613-1616. doi: 10.1021/ac00105a021

Ozcan, C., Zorlutuna, P., Hasirci, V., & Hasirci, N. (2008). Influence of Oxygen Plasma Modification on Surface Free Energy of PMMA Films and Cell Attachment. *Macromolecular Symposia, 269*(1), 128-137. doi: 10.1002/masy.200850916

Pan, Y., Sonn, G. A., Sin, M. L. Y., Mach, K. E., Shih, M.-C., Gau, V., . . . Liao, J. C. (2010). Electrochemical immunosensor detection of urinary lactoferrin in clinical samples for urinary tract infection diagnosis. *Biosensors and Bioelectronics, 26*(2), 649-654. doi: 10.1016/j.bios.2010.07.002

Patel, S., Thakar, R. G., Wong, J., McLeod, S. D., & Li, S. (2006). Control of cell adhesion on poly(methyl methacrylate). *Biomaterials, 27*(14), 2890-2897.

Peterson, C. G. B., Eklund, E., Taha, Y., Raab, Y., & Carlson, M. (2002). A new method for the quantification of neutrophil and eosinophil cationic proteins in feces: establishment of normal levels and clinical application in patients with inflammatory bowel disease. *Am J Gastroenterol, 97*(7), 1755-1762.

Raab, Y., Gerdin, B., Ahlstedt, S., & HÃ¤llgren, R. (1993). Neutrophil mucosal involvement is accompanied by enhanced local production of interleukin-8 in ulcerative colitis. *Gut, 34*(9), 1203-1206. doi: 10.1136/gut.34.9.1203

Rauf, S., Glidle, A., & Cooper, J. M. (2010). Application of quantum dot barcodes prepared using biological self-assembly to multiplexed immunoassays. *Chemical Communications, 46*(16), 2814-2816.

Reese, G. E., Constantinides, V. A., Simillis, C., Darzi, A. W., Orchard, T. R., Fazio, V. W., & Tekkis, P. P. (2006). Diagnostic Precision of Anti-Saccharomyces cerevisiae Antibodies and Perinuclear Antineutrophil Cytoplasmic Antibodies in Inflammatory Bowel Disease. *Am J Gastroenterol, 101*(10), 2410-2422.

Rehák, M., Snejdárková, M., & Otto, M. (1994). Application of biotin-streptavidin technology in developing a xanthine biosensor based on a self-assembled phospholipid membrane. *Biosensors and Bioelectronics, 9*(4-5), 337-341. doi: 10.1016/0956-5663(94)80033-2

Rheenen, P., Vijver, E. V. d., & Fidler, V. (2011). Review: Fecal calprotectin is accurate for screening for suspected IBD in adults but less so in children. *Annals of Internal Medicine, 154*(2), JC1-12. doi: 10.1059/0003-4819-154-2-201101180-02012

Saiki, T. (1998). Myeloperoxidase concentrations in the stool as a new parameter of inflammatory bowel disease. *Kurume Med J, 45*(1), 69-73.

Savige, J., Dimech, W., Fritzler, M., Goeken, J., Hagen, E. C., Jennette, J. C., . . . Antibodies, R. o. A. C. (2003). Addendum to the International Consensus Statement on Testing and Reporting of Antineutrophil Cytoplasmic Antibodies. *American Journal of Clinical Pathology, 120*(3), 312-318. doi: 10.1309/waepadw0k4lpuhfn

Schmalenberg, K. E., Buettner, H. M., & Uhrich, K. E. (2004). Microcontact printing of proteins on oxygen plasma-activated poly(methyl methacrylate). *Biomaterials, 25*(10), 1851-1857. doi: DOI: 10.1016/j.biomaterials.2003.08.048

Schoepfer, A., Trummler, M., Seeholzer, P., Criblez, D., & Seibold, F. (2007). Accuracy of Four Fecal Assays in the Diagnosis of Colitis. *Diseases of the Colon & Rectum, 50*(10), 1697-1706.

Schoepfer, A. M., Trummler, M., Seeholzer, P., Criblez, D. H., & Seibold, F. (2007). Accuracy of four fecal assays in the diagnosis of colitis. *Diseases of the colon and rectum, 50*(10), 10.

Schoepfer, A. M., Trummler, M., Seeholzer, P., Seibold-Schmid, B., & Seibold, F. (2008). Discriminating IBD from IBS: Comparison of the test performance of fecal markers, blood leukocytes, CRP, and IBD antibodies. *Inflammatory Bowel Diseases, 14*(1), 32-39.

Scholtz, J., & Kaminker, K. (1962). Myeloperoxidase of the leucocyte of normal human blood. 1: Content and localization. *Archives of Biochemsitry and Biophysics, 96*, 465-467.

Shukla, P. K., Sinha, M., Kaur, P., Sharma, S., Singh, T.P. (2011). *Crystal Structure of C-lobe of Bovine lactoferrin Complexed with Lipopolysaccharide at 2.0 A Resolution*.

Sipponen, T., Savilahti, E., Kolho, K.-L., Nuutinen, H., Turunen, U., & Färkkilä, M. (2008). Crohn's disease activity assessed by fecal calprotectin and lactoferrin: Correlation with Crohn's disease activity index and endoscopic findings. *Inflammatory Bowel Diseases*, *14*(1), 40-46.

Situma, C., Moehring, A. J., Noor, M. A. F., & Soper, S. A. (2007). Immobilized molecular beacons: A new strategy using UV-activated poly(methyl methacrylate) surfaces to provide large fluorescence sensitivities for reporting on molecular association events. *Analytical Biochemistry, 363*(1), 35-45. doi: DOI: 10.1016/j.ab.2006.12.029

Staros, J. V., Wright, R. W., & Swingle, D. M. (1986). Enhancement by N-Hydroxysulfosuccinimide of Water-Soluble Carbodiimide-Mediated Coupling Reactions. *Analytical Biochemistry, 156*(1), 220-222.

Stayton PS, Freitag S, Klumb LA, Chilkoti A, Chu V, Penzotti JE, . . . RE, S. (1999). Streptavidin-biotin binding energetics. *Biomolecular Engineering, 16*(1-4), 6.

Steinhoff, J., Einecke, G., Niederstadt, C., Fricke, L., Rob, P. M., & Sack, K. (1997). Myeloperoxidase in urine: A new marker for distinction between rejection and urinary tract infection after renal transplantation. *Transplantation proceedings, 29*(7), 3098.

Ting Cao, A. W., Xuemei Liang, Haiying Tang, Gregory W. Auner, Steven O. Salley, K.Y. Simon Ng,. (2007). Investigation of spacer length effect on immobilized <I>Escherichia coli</I> pili-antibody molecular recognition by AFM. *Biotechnology and Bioengineering, 98*(6), 1109-1122.

Trinder, D., Fox, C., Vautier, G., & Olynyk, J. K. (2002). Molecular pathogenesis of iron overload. *Gut, 51*(2), 290-295. doi: 10.1136/gut.51.2.290

Turkay, C., & Kasapoglu, B. (2010). Noninvasive methods in evaluation of inflammatory bowel disease: where do we stand now? An update. *Clinics, 65*, 221-231.

Uchida, E., Uyama, Y., & Ikada, Y. (1993). Sorption of low-molecular-weight anions into thin polycation layers grafted onto a film. *Langmuir, 9*(4), 1121-1124. doi: 10.1021/la00028a040

Wagner, M., Peterson, C. G., Ridefelt, P., Sangfelt, P., & Carlson, M. (2008). Fecal markers of inflammation used as surrogate markers for treatment outcome in relapsing inflammatory bowel disease. *World Journal of Gastroenterology, 14*(36), 6.

Wang, L., Zhang, Y., Gao, X., Duan, Z., & Wang, S. (2010). Determination of Chloramphenicol Residues in Milk by Enzyme-Linked Immunosorbent Assay: Improvement by Biotin−Streptavidin -Amplified System. *Journal of Agricultural and Food Chemistry, 58*(6), 3265-3270. doi: 10.1021/jf903940h

Weber, P., Ohlendorf, D., Wendoloski, J., & Salemme, F. (1989). Structural origins of high-affinity biotin binding to streptavidin. *Science, 243*(4887), 85-88. doi: 10.1126/science.2911722

Wen, X., He, H., & Lee, L. J. (2009). Specific antibody immobilization with biotin-poly(l-lysine)-g-poly(ethylene glycol) and protein A on microfluidic chips. *Journal of Immunological Methods, 350*(1-2), 97-105.

Wilchek, M., Bayer, E. A., & Livnah, O. (2006). Essentials of biorecognition: The (strept)avidin-biotin system as a model for protein-protein and protein-ligand interaction. *Immunology Letters, 103*(1), 27-32. doi: 10.1016/j.imlet.2005.10.022

Yu, X., Hartmann, M., Wang, Q., Poetz, O., Schneiderhan-Marra, N., Stoll, D., . . . Joos, T. O. (2010). μFBI: A Microfluidic Bead-Based Immunoassay for Multiplexed Detection of Proteins from a μL Sample Volume. *PLoS One, 5*(10), e13125.

Yuan, Y., He, H., & Lee, L. J. (2009). Protein A-based antibody immobilization onto polymeric microdevices for enhanced sensitivity of enzyme-linked immunosorbent assay. *Biotechnology and Bioengineering, 102*(3), 891-901.

Yuan, Y., Yuan, R., Chai, Y., Zhuo, Y., Bai, L., & Liao, Y. (2010). An electrochemical enzyme bioaffinity electrode based on biotin-streptavidin conjunction and bienzyme substrate recycling for amplification. *Analytical Biochemistry, 405*(1), 121-126. doi: 10.1016/j.ab.2010.05.025

Zeng, J., & Fenna, R. E. (1992). X-ray crystal structure of canine myeloperoxidase at 3 Å resolution. *Journal of Molecular Biology, 226*(1), 185-207.

Appendix A: Standard Operating Procedures

Included in this list of appendices are several of the most critical protocols used in this thesis. Many are adapted directly from vendors to ensure that readers can follow these vital procedures.

Appendix B: AlexaFluor 488 – Antibody Conjugation

This protocol is taken directly from Invitrogen – MP 10235

Labeling the Protein

1.1 Prepare a 1 M solution of sodium bicarbonate by adding 1 mL of deionized water (dH2O) to the provided vial of sodium bicarbonate (Component B). Vortex or pipet up and down until fully dissolved. The bicarbonate solution, which will have a pH ~9.0, can be stored at 4°C for up to two weeks.

1.2 If the protein concentration is greater than 2 mg/mL, the protein should be diluted to 2 mg/mL in a suitable buffer, e.g. PBS or 0.1 M sodium bicarbonate.

1.3 To 0.5 mL of the 2 mg/mL protein solution, add 50 μL of 1 M bicarbonate (prepared in step 1.1).

Note: Bicarbonate, pH ~8.3, is added to raise the pH of the reaction mixture, since TFP esters react efficiently at alkaline pH.

1.4 Allow a vial of reactive dye to warm to room temperature. Transfer the protein solution from step 1.3 to the vial of reactive dye. This vial contains a magnetic stir bar. Cap the vial and invert a few times to fully dissolve the dye. Stir the reaction mixture for 1 hour at room temperature. Because preparation of the purification column takes ~15 minutes, you may wish to begin pouring the column (see *Purifying the Labeled Protein*) during the labeling reaction.

Purifying the Labeled Protein

2.1 Assemble the column and position it upright (see Figure 2): Attach a funnel to the top of a column. Gently insert the column through the X-cut in one of the provided foam holders to avoid damaging the column. Using the foam holder, secure the column with a clamp to a ringstand. Carefully remove the cap from the bottom of the column.

2.2 Prepare elution buffer by diluting the room temperature 10X stock (Component D) 10-fold in dH2O. Typically, less than 10 mL will be required for each purification. Set aside until step 2.5.

Note: The 10X elution buffer (10X PBS) contains 0.1 M potassium phosphate, 1.5 M NaCl, pH 7.2, with 2 mM sodium azide. The 10X stock should be warmed to

room temperature prior to use to ensure that the buffer is fully dissolved. Sufficient elution buffer is included to allow washing of the columns for reuse, if desired.

2.3 Using one of the provided pipets, stir the purification resin (Component C) thoroughly to ensure a homogeneous suspension. Pipet the resin into the column, allowing excess buffer to drain away into a small beaker or other container. Resin should be packed into the column until the resin is ~3 cm from the top of the column. Component C, Bio-Rad BioGel P-30 Fine size exclusion purification resin, is designed to separate free dye from proteins with MW > 40,000. This is packaged in PBS containing 2 mM sodium azide. For smaller proteins, gel filtration media of a suitable molecular weight cutoff should be selected. Labeled peptides may be separated from free dye by TLC or HPLC.

2.4 Allow the excess buffer to drain into the column bed. Do not worry about the column drying out, since the matrix will remain hydrated. Make certain the buffer elutes through the column with a consistently even flow prior to adding the reaction mixture. If the flow of buffer is slow or stalled, repack the column. Carefully load the reaction mixture from step 1.4 onto the column. You may wish to remove the column funnel to load the sample. Allow the mixture to enter the

column resin. Rinse the reaction vial with ~100 μL of elution buffer and apply to the column. Allow this solution to enter the column.

2.5 Replace the funnel if it was removed for sample loading. Slowly add elution buffer (prepared in step 2.2), taking care not to disturb the column bed. Continue adding elution buffer until the labeled protein has been eluted (typically about 30 minutes).

Important

Collect, and retain as fractions, all of the eluted buffer.

2.6 As the column runs, periodically illuminate the column with a handheld UV lamp. You should observe two colored bands, which represent the separation of labeled protein from unincorporated dye. Collect the first colored band, which contains the labeled protein, into one of the provided collection tubes. If desired, a foam holder can be used to support the collection tube. Add elution buffer to the column as necessary. Do not collect the slower moving band, which consists of unincorporated dye.

Once the fraction containing the labeled protein has been successfully collected, all other fractions of eluted buffer may be discarded. In rare instances where there is no discernable band corresponding to labeled protein, the retained fractions can be used to recover any unlabeled protein.

Determining the Degree of Labeling

3.1 Measure the absorbance of the conjugate solution at 280 nm and 494 nm (A280 and A494) in a cuvette with a 1 cm pathlength.

Note: Dilution of the sample may be necessary.

3.2 Calculate the concentration of protein in the sample:

protein concentration (M) = [A280 - (A494 × 0.11)] × dilution factor 203,000

where 203,000 cm-1M-1 is the molar extinction coefficient of a typical IgG and 0.11 is a correction factor to account for absorption of the dye at 280 nm.

Non-IgG proteins will likely have significantly different molar extinction coefficients.

3.3 Calculate the degree of labeling:

moles dye per mole protein = A494 × dilution factor / (71,000 × protein concentration (M))

where 71,000 cm-1M-1 is the approximate molar extinction coefficient of the Alexa Fluor® 488 dye at 494 nm. For IgGs, we find that labeling with 4–9 moles of Alexa Fluor® 488 dye per mole of antibody is optimal.

Storing and Handling the Conjugates

Store the labeled protein—which will be in PBS, pH 7.2, containing ~2 mM sodium azide—at 2–6°C, protected from light. If the final concentration of purified protein conjugate is less than 1 mg/mL, add bovine serum albumin (BSA) or other stabilizing protein to 1–10 mg/mL. The conjugate should be stable at 4°C for several months. For long-term storage, divide the solution into small aliquots and freeze at ≤–20°C. AVOID REPEATED FREEZING AND THAWING. PROTECT FROM LIGHT.

It is a good practice to centrifuge solutions of conjugates in a microcentrifuge before use; only the supernatant should then be used in the experiment. This step will remove any aggregates that may have formed during storage.

Tips for Using the Kit with Other Proteins and/or Concentrations

Proteins at less than 2 mg/mL

Proteins at concentrations less than 2 mg/mL will not label as efficiently. If the protein cannot be concentrated to ~2 mg/mL, you may wish to use less than 1 mg protein per reaction to increase the molar ratio of dye to protein. In addition, using a dilute protein solution, especially at <1 mg/mL, will make it more difficult to efficiently remove the unconjugated dye from the dye-labeled protein with acceptable yields, since the provided purification columns are designed to purify conjugates from a total volume of less than 1 mL. For reaction volumes greater than 1 mL, you can divide the solution of the conjugate and apply it to multiple purification columns or, to avoid further dilution of the conjugate, you can remove free dye by extensive dialysis.

Proteins with MW other than ~145,000

Typically, lower MW proteins require fewer dye molecules and higher MW proteins require more dye molecules per protein for optimal labeling. For this reason, we recommend initially performing the reaction with 0.5 mL of 2 mg/mL protein solution, as described for IgGs. The labeling conditions can then be optimized based on the initial results, if desired.

Troubleshooting

Under-Labeling

If calculations indicate that the protein is labeled with significantly less than four moles of fluorophore per mole of 145,000 dalton protein, your protein could possibly be under-labeled. A number of conditions can cause a protein to label inefficiently:

Trace amounts of primary amine–containing components in the buffer will react with the dye and decrease the efficiency of protein labeling. If your protein has been in amine containing buffers (e.g. Tris or glycine), dialyze *extensively* versus PBS before labeling.

Dilute solutions of protein (≤1 mg/mL) will not label efficiently. Please see *Proteins at Less Than 2 mg/mL.*

The addition of sodium bicarbonate (step 1.3) is designed to raise the pH of the reaction mixture to ~8, as TFP esters react most efficiently with primary amines at slightly alkaline pH. If the protein solution is strongly buffered at a lower pH, the addition of bicarbonate will not raise the pH to the optimal level. Either more bicarbonate can be added, or the buffer can be exchanged with PBS, which is only weakly buffered, or with 0.1 M sodium bicarbonate, pH 8.3, by dialysis or other method prior to starting the reaction.

Because proteins, including different antibodies, react with fluorophores at different rates and retain biological activity at different degrees of dye labeling, the standard protocol may not always result in optimal labeling. To increase the amount of labeling, you can relabel the same protein sample, or you can label a new protein sample using either less protein or more reactive dye per reaction. To increase the amount of dye in the reaction, you can combine the contents of two vials of reactive dye together. Some researchers obtain better labeling with overnight incubations at 4°C after an initial incubation of one hour at room temperature.

Over-Labeling

If calculations indicate that the protein conjugate is labeled with significantly more than nine moles of fluorophore per mole of 145,000 dalton protein, your protein is probably overlabeled. Although conjugates with a high number of attached dye molecules may be acceptable for use, over-labeling can cause aggregation of the protein conjugate and can also reduce the antibody's specificity for its antigen—both of which can lead to nonspecific staining. Over-labeling can also cause fluorescence quenching of the attached dyes, which will decrease the fluorescence of the conjugate. To reduce the amount of labeling next time, you can either add more protein to your reaction to decrease the molar ratio of dye to protein or allow the reaction to proceed for a shorter time.

Inefficient Removal of Free Dye

Although we have had good success in removing free dye from protein conjugates with the provided columns, it is possible that trace amounts of free dye will remain in the conjugate solution after purification, particularly if a low molecular weight protein is labeled. The presence of free dye, which can be determined by thin layer chromatography, will result in erroneously high calculated values for the degree of labeling (see *Determining the Degree of*

Labeling). Remaining traces of free dye can be removed by applying the conjugate to another column or by extensive dialysis.

Appendix C: Quantum Dot – Antibody Conjugation

This protocol is taken directly from Invitrogen – MP 19010)

Preparing for the Conjugation Reaction

1.1 Thaw 1 **new** vial of SMCC solution (Component B) at 37ºC for at least 15 minutes before use (see step 2.1 below).

1.2 Prepare 300 µL of a 1 mg/mL antibody solution in PBS by dilution or concentration. For example, if the antibody is at a concentration of 0.5 mg/mL, concentrate 600 µL to a final volume of 300 µL at 1 mg/mL using 50 KDa molecular weight cutoff centrifuge concentrators (not included in kit).

1.3 The first time you use a new Qdot® Antibody Conjugation Kit, add 40 µL of distilled water to supplied dye labeled marker (Component G) and mix. This makes enough dye labeled marker for two conjugation reactions. Store at 2–6˚C when not in use.

Activating Qdot® Nanocrystals

2.1 Pipette 14 µL of thawed SMCC solution into a centrifugation tube (Component L).

2.2 To the tube containing the SMCC, add 125 µL of Qdot® nanocrystals (Component A). Vortex briefly to mix.

Note: When activating Qdot® nanocrystals, always use SMCC from a new vial. After the aliquot of Qdot® nanocrystals is added to the aliquot of thawed SMCC, throw the rest of the vial of SMCC away. **Do not reuse SMCC**.

2.3 Incubate for 1 hour at room temperature to activate the nanocrystals.

2.4 Start the protocol **Reducing the Antibody Sample** (below) when there are 30 minutes remaining for the Qdot® activation reaction.

Note: Do not store activated Qdot® nanocrystals and reduced antibody. It is important to proceed with the desalting and conjugation reactions as soon as the Qdot® nanocrystals and antibody sample are ready.

Reducing the Antibody Sample

3.1 Pipette 300 μL of antibody at 1 mg/mL (see step 1.2) into a centrifugation tube (Component L).

3.2 Add 6.1 μL of DTT solution (Component C) to antibody and mix briefly.

3.3 Incubate for 30 minutes at room temperature.

3.4 Prepare the desalting columns while the antibody reduction step is proceeding.

Note: If desired, the desalting columns can be equilibrated with exchange buffer and capped before performing the **Activating the Qdot® Nanocrystals** step and **Reducing the Antibody Sample** step.

Equilibrating the Desalting Column

Prepare two desalting columns with exchange buffer prior to the end of the antibody reduction.

4.1 Label two desalting columns (Component M). Mark one "reduced antibody" and the other "activated Qdot® nanocrystals".

4.2 Remove top and bottom caps from both columns and just as the liquid in each column is approaching the top of the column gel bed, begin adding exchange buffer (see step 4.3).

4.3 Equilibrate each column gel bed with 10 mL (3 column volumes) of exchange buffer (Component E).

4.4 While there is still exchange buffer visible above the gel bed on each column, cap the bottom of each column and set aside until the antibody reduction is completed.

Desalting and Collecting the Reduced Antibody

5.1 Add 500 µL of water to a centrifugation tube (Component L) and mark the outside of the tube at the meniscus. Add another 500 µL of water and make a second mark on the outside of the tube corresponding to the new volume. Discard the water.

Note: This tube is used to collect the reduced antibody in step 5.6 and the activated Qdot® nanocrystals in step 6.4.

5.2 When the antibody reduction is completed, add 20 μL of dye labeled marker (prepared in step 1.3) to the reduced antibody.

5.3 Uncap the desalting column labeled "reduced antibody" and allow remaining exchange buffer to enter gel bed and as soon as it has done so, immediately add reduced antibody mixture (prepared in step 5.1) to the top of the gel bed.

5.4 Allow the reduced antibody mixture to completely enter the gel.

5.5 Add 1 mL of exchange buffer to the top of the gel bed to elute the antibody.

5.6 Begin collecting reduced antibody into a centrifugation tube (marked in step 5.1) when the first colored drop elutes; collect no more than 500 μL (to the lower marked line from step 5.1). Do not attempt to collect more than 500 μL as it may contain residual DTT that will interfere with the conjugation.

Desalting and Collecting the Activated Qdot® Nanocrystals

6.1 Uncap the desalting column labeled "activated Qdot® nanocrystals" allow remaining exchange buffer to enter gel bed and as soon as it has done so, immediately add the activated Qdot® nanocrystals (from step 2.3) to the top of the gel bed.

6.2 Allow the activated Qdot® nanocrystals mixture to completely enter the gel.

6.3 Add 1 mL of exchange buffer to top of gel bed to elute the Qdot® nanocrystals

6.4 When the first drop of colored material elutes from the column, begin collecting directly into the centrifugation tube containing the reduced and desalted antibody.

6.5 Stop collecting when the final volume reaches 1 mL (up to the top line marked in step 5.1; 500 μL of activated Qdot® nanocrystals).

6.6 Mix briefly.

Conjugation Reaction

7.1 Allow the reduced antibody and activated Qdot® nanocrystals to react for 1 hour at room temperature.

7.2 During the conjugation reaction or quenching step, prepare the separation column (see **Preparing the Separation Column**).

Quenching the Conjugation Reaction

8.1 Prepare a 10 mM working solution of 2-mercaptoethanol just before using. To do this, add 3 µL of 2-mercaptoethanol (Component D) to 4 mL distilled water.

8.2 Add 10 µL of diluted 2-mercaptoethanol to the conjugation reaction from step 7.1.

8.3 Incubate for 30 minutes at room temperature.

Preparing the Separation Column

During the conjugation or quenching step, prepare the separation column. The separation media (Component F) is supplied as a suspension containing 20% ethanol as a preservative.

9.1 Remove and save the top and bottom column caps from a new separation column (Component I).

9.2 Suspend the separation media (Component F) in the bottle with gentle shaking or vortexing. Ensure the media is fully suspended (some may be stuck to the underside of the cap) before starting column preparation.

9.3 Mark the column with two lines, one at 45 mm above the top of the frit, and a second at 55 mm above the frit.

Note: These two marks serve to indicate how much suspended separation media to add and, consequently, the height of the packed gel bed. A uniform suspension of separation media added to the 55 mm mark should settle into a packed gel bed about 45 mm high.

9.4 After ensuring that the separation media is a uniform suspension, load media into the column with a 1 mL pipette to the second line at 55 mm mark. The column begins to drip at the bottom.

9.5 Gently add 0.5 mL distilled water to top off the gel while maintaining a level bed surface.

9.6 Attach one end of the tubing (Component J) to the tip of the column, and attach the other end to the syringe (Component H) that has the plunger completely depressed.

9.7 By **slowly** drawing the syringe plunger out, withdraw the solvent from the column. Do not allow the solvent to drain below the top of the gel bed.

9.8 As the solvent level drops to near the top of the settled gel bed, fill the column with PBS pH 7.2 and, using the syringe, draw the PBS level down to just above the top of the gel bed. Repeat this PBS fill and drain two more times, using the syringe to draw the PBS through.

9.9 When you have drawn the PBS from the last fill down to a level 2 to 3 mm above the top of the settled gel bed line, remove the syringe and replace the bottom and top caps.

Concentrating the Sample

10.1 Split the volume of the quenched conjugation reaction (from step 8.3) into two ultrafiltration devices (Component K).

10.2 Concentrate each half reaction to ~20 µL by centrifuging at 4000 *g* for approximately 10 to 15 minutes. This corresponds to ~7,000 rpm in most benchtop microcentrifuges.

10.3 If the volume is larger than 20 µL after this initial centrifugation, continue centrifuging for another 5 minutes.

Separating the Conjugated Antibody from Unconjugated Antibody

11.1 Uncap the separation column (from step 9.9) and allow the PBS to elute by gravity so that it is just at the top of the column bed.

11.2 Immediately add to the gel bed the concentrated conjugate reaction from the two ultrafiltration devices (~40 µL total volume).

11.3 Allow the conjugate to enter gel and then gently add 50 µL of PBS pH 7.2 and allow that to run into the gel bed.

11.4 Gently fill the reservoir above the column with PBS and allow the sample to elute by gravity. Visually monitor the "dead space" between the frit and the column tip.

11.5 When color appears in the "dead space," collect the first ten drops only of colored conjugate in a centrifugation tube (Component L). **Do not collect more than the first ten drops from the column**. Subsequent drops contain unconjugated antibody that will interfere with the application the conjugate is used for.

Note: The second colored band above the Qdot® conjugate comes from the dye marker added to the antibody reduction reaction. This is **NOT** an indication of where the free antibody runs as free antibody will elute much closer to the actual conjugate.

11.6 Add sodium azide to the collected conjugate at a final concentration of 0.01% (w/v) to serve as a preservative, if desired.

11.7 Store the conjugate at 4˚C. **Do not freeze** the conjugate.

Conjugate collected from the separation column is typically in the 1 to 2 micromolar range. If desired, the conjugate concentration can be determined by measuring the optical density of the conjugate at the specified wavelength and then using the formula $A = \varepsilon cL$, where A is the absorbance, ε is the molar extinction coefficient (Qdot 605 nanocrystals = 650,000 M^{-1} cm^{-1}), c is the molar concentration, and L is the path length.

For example, for a Qdot® 655 antibody conjugate, if material eluting from the final column has A = 0.65 measured in a cuvette with 1 cm path length, then $c = A/\varepsilon = 0.65/800{,}000 = 0.812$ μM conjugate, based on nanocrystal absorbance.

Determine optimal working concentrations by performing a titration series for the application of interest. We typically use a conjugate concentration of 10 nM for immunocytochemistry applications. Recommended protocols on use of Qdot®antibody conjugates are available from probes.invitrogen.com.

Appendix D: ELISA – Myeloperoxidase

This protocol is taken directly from Invitrogen – MP 33857.

Solution Preparation Before opening any vial in this kit, allow its contents to warm to room temperature.

Caution: Components B, D, and E are irritants, and Component E is a potential mutagen. Follow safe laboratory practices, and handle these chemicals with appropriate precautions.

1.1 Prepare 500 mL of 1X PBS by adding 50 mL of 10X PBS (Component C) to 450 mL of distilled and deionized water. This 1X PBS will be used in the preparation of other buffers, as well as in the final Amplex® UltraRed reaction.

1.2 Prepare 300 mL of 1X PBST by adding 300 µL of Tween 20 (Component I) to 300 mL of 1X PBS. Shake well to mix. This solution is sufficient for 100 assays using the protocol described here. Solution left over can be stored at 4°C for future assays.

1.3 Prepare 100 mL of 1X PBS-BSA by adding 1 g of BSA (Component H) to 100 mL of 1X PBS. Dissolve completely. Store at 4°C when not in use.

1.4 Prepare 50 mL of 0.1X PBS-BSA by mixing 5 mL of 1X PBS-BSA with 45 mL of 1X PBS.

1.5 Dilute the MPO standard (component G) 1:100 in 0.1X PBS-BSA to make a 100 ng/mL MPO stock solution. Divide this MPO stock solution into aliquots (e.g., 500 μL) and store at 4°C when not in use.

1.6 Reconstitute the goat anti–rabbit IgG HRP conjugate (Component D) by adding 0.5 mL of 1X PBS-BSA directly to the Component D vial, to create a 200 μg/mL stock solution. This stock solution may be stored at 4°C after adding thimerosal (not included in the kit) to a final concentration of 0.02%. Alternatively, the stock solution can be frozen, without thimerosal.

1.7 Prepare an Amplex® UltraRed reagent solution by adding 60 μL of DMSO (Component B) to one vial of Amplex® UltraRed reagent (Component A). Vortex well to dissolve. Protect this solution from light and store at –20°C when not in use.

1.8 Prepare 10 mL of Amplex® stop solution by adding 1 mL of 1 M NaOH to the vial of Amplex® stop reagent (Component E), and then once it is fully dissolved, adding it to 9 mL of 1X PBS. This solution is stable for one month at 4°C when protected from light. Discard this solution if it starts to turn amber in color.

Experimental Protocol

The following protocol describes a typical sandwich ELISA in 96-well format designed for use with a fluorescence microplate reader. This protocol is provided for your convenience but may be replaced with any standard sandwich ELISA protocol at your discretion. However, steps 2.9–2.15 of this protocol should be followed as written.

2.1 Hydrate the Zen™ microplate plate by dispensing 200 µL 1X PBST into each well. Incubate the plate on a plate shaker at room temperature for 5 minutes at ~500 rpm.

2.2 Following the hydration, empty the wells. The wells can be emptied by simply inverting the plate over a sink or waste receptacle. For optimal assay sensitivity, remove as much fluid as possible (for example, by pipetting the fluid

out carefully, without touching the bottoms of the wells). As a final measure, invert the plate on a paper towel, and firmly tap the plate to remove any remaining buffer.

2.3 Prepare a 500 ng/mL solution of the mouse anti-MPO primary capture antibody. For 100 assays, make 10 mL by adding 100 μL of Component J to 10 mL of 0.1X PBS-BSA. For each sample, dispense 100 μL of the primary capture antibody solution into a well of the Zen™ plate. Incubate the plate on a plate shaker for 1 hour at ~500 rpm at room temperature.

2.4 Near the end of the 1 hour incubation, prepare a series of MPO standards from the MPO stock solution made in step 1.5 and using 0.1X PBS-BSA as a diluent, ranging from 100 ng/mL to 0 ng/mL. We recommend 8 to 10 MPO concentrations—e.g., 100, 50, 25, 12.5, 6.25, 3.125, 1.5, 0.75, 0.375, and 0 ng/mL—and duplicates for each concentration. Each assay well uses 100 μL of MPO-containing sample or standard (see step 2.6), so one 500 μL aliquot of the 100 ng/mL MPO stock solution is sufficient to make duplicate sets of the concentrations listed above. Keep the diluted standards on ice until step 2.6.

2.5 Dilute your samples (sera or cell lysates) 1:1, 1:10, 1:100, and 1:1,000 in 0.1X PBS-BSA. The goal is to obtain at least one dilution that contains an amount of MPO that falls within the dynamic range of the assay. If you know from past experience the approximate MPO content of samples that you work with often, the samples can be diluted at different ratios at your discretion.

2.6 Following the 1 hour incubation, empty the wells and wash three times with 200 μL of 1X PBST. After the final wash, invert the plate over a paper towel and firmly tap the plate to remove any solution from the wells.

Dispense 100 μL each of the MPO standards and diluted samples into microplate wells. Incubate on a plate shaker for 1 hour at ~500 rpm at room temperature.

2.7 Empty the wells and wash them three times with 200 μL of 1X PBST. After the final wash, invert the plate on a paper towel, and firmly tap the plate to remove any remaining buffer from the wells.

2.8 Prepare a 1.0 μg/mL solution of the rabbit anti-MPO secondary capture antibody. For 100 assays, make 10 mL by adding 1 mL of Component K to 9 mL of 0.1X PBS-BSA. Dispense 100 μL of the secondary capture antibody solution

into each assay well. Incubate on a plate shaker for 30 minutes at ~500 rpm at room temperature.

2.9 Empty the wells and wash them three times with 200 μL of 1X PBST. After the final wash, invert the plate on a paper towel, and firmly tap the plate to remove any remaining buffer from the wells.

2.10 Make 10 mL of 100 ng/mL goat anti–rabbit IgG-HRP by adding 5 μL of the goat anti–rabbit IgG-HRP stock solution (prepared in step 1.6) to 10 mL of 0.1X PBS-BSA.

Add 100 μL of this solution to each microplate well. Incubate on a plate shaker for 30 minutes at ~500 rpm at room temperature.

2.11 Empty the wells and wash them three times with 200 μL of 1X PBST. The stringency of the assay may be adjusted by washing more or fewer times with 1X PBST, or by agitating the 1X PBST in the wells during the wash steps. After the final wash, empty the wells, invert the plate on a paper towel, and firmly tap the plate to remove any remaining buffer from the wells.

To obtain optimal sensitivity from the assay, **protect the plate from light after the final wash**. Antibodies exposed to UV light can produce trace amounts of singlet oxygen, which can interfere with detection of Amplex® UltraRed reagent.

2.12 Make 10 mL of reagent mix by adding 50 µL of the Amplex® UltraRed reagent stock solution (prepared in step 1.7) and 22.7 µL of 3% H2O2 (Component F; check the label for the actual H2O2 concentration, and adjust as necessary) to 10 mL of 1X PBS. Protect the reagent mix from light and use it within 1 hour.

2.13 Using a multichannel pipet, add 100 µL of the reagent mix to each assay well. This initiates the detection reaction.

2.14 Incubate the plate at room temperature or 37°C, protected from light until the fluorescence measurement is taken. For most reactions, a 30 minute incubation is sufficient. The plate can also be read continuously for up to an hour. If desired, 20 µL of Amplex® stop solution (prepared in step 1.8) may be added to each assay well. This will arrest the reactions, providing a stable signal that may be read for at least 2 hours if the plate is protected from light and kept at room temperature.

2.15 Read the fluorescence of the microplate wells using filters for 530 nm (excitation) and 590 nm (emission).

2.16 Determine the MPO concentrations of your experimental samples from your own standard curve. Figure 2 shows a typical standard curve for this assay.

Appendix D: ELISA – Lactoferrin

This protocol is taken directly from IBD-SCAN ELISA kit for lactoferrin (Catalog No. T5009) and includes only the most relevant parts.

PRELIMINARY PREPARATIONS

1. Remove all reagents from the kit box to warm to room temperature before use.

2. **Prepare 1X *Wash Solution.*** The *Wash Solution* is supplied as a 20X concentrate (a precipitate may be noticed). It should be mixed and diluted to a total volume of 1 liter by adding 50 mL of the concentrate to 950 mL of deionized water. Label the bottle. Store any unused 1X *Wash Solution* between 2° and 8°C.

3. **Prepare 1X *Diluent*.** The *Diluent* is supplied as a 10X concentrate (a precipitate may be noticed). It should be mixed and diluted to a total volume of 400 mL by adding 40 mL of the concentrate to 360 mL of deionized water. Label the bottle. Store any unused 1X *Diluent* between 2° and 8°C.

4. ***Microassay Plate*** **Preparation.** Each Strip contains 8 wells coated with polyclonal antibody specific for lactoferrin. Each specimen or control will require one of these coated wells. Avoid contact with the bottom of the wells because this is the optical window for ELISA readers. Microassay wells not used must be returned to the foil bag and carefully resealed with desiccant.

TEST PROCEDURES

1. Designate and use 2 wells for each *Standard*, 1 well for the negative control (1X *Diluent*), 1 well for the 1:200 dilution of *Positive Control* and 1 well for specimen dilutions 1:100 and 1:1000. See the table under QUALITY CONTROL for example of well locations.

2. Using a calibrated pipette, add 100 μL of each *Standard* LS1-LS5 to duplicate wells and 100 μL of the 1X *Diluent* and *Positive Control* to designated wells.

3. Add 100 μL from each specimen dilution (1:100 and 1:1000) to separate wells.

4. Cut the adhesive plastic sheet to the size necessary to cover the wells. Cover the wells and incubate them at 37°C ± 2°C for 30 minutes stationary.

5. Shake out the contents of the assay wells into a discard pan.

6. Wash each well 5 times using the 1X *Wash Solution* in a squirt bottle with a fine tipped nozzle, directing the *Wash Solution* to the bottom of the well with force (i.e. fill the wells, then shake the *Wash Solution* out of the wells into a discard pan).

Slap the inverted plate on a dry paper towel and repeat **four times** using a dry paper towel each time. If any particulate matter is seen in the wells, continue washing until all the matter is removed.

7. Add 1 drop of *Conjugate* (red cap) to each well. Incubate the wells at 37°C ± 2°C for 30 minutes stationary.

8. Repeat step #6. *Dispose of paper towels and specimen containers properly.*

9. Add 2 drops of *Substrate* (blue cap) to each well. Gently tap the wells to mix the contents. Incubate the wells at room temperature for 15 minutes. Gently tap the wells 1 or 2 times during this incubation period.

10. Add 1 drop of *Stop Solution* (yellow cap) to each well. Gently tap the wells to mix and wait 2 minutes before reading. The addition of the *Stop Solution* converts the blue color to a yellow color which may be quantitated by measuring the optical density at 450 nm or 450/620 nm on a microplate ELISA reader. Wipe the underside of each well with a soft paper towel before measuring the optical density. Read within two to ten minutes after adding *Stop Solution.*

11. Record absorbance values for the positive control dilution, for the negative control, for each specimen dilution, and for the standards.

12. Average the acceptable readings of duplicate wells before interpreting results.

CALCULATION OF RESULTS

The results in this insert were determined using a Linear Trend/Regression Type analysis. Other data reduction methods may give slightly different results.

1. An appropriate data reduction computer program, using Linear Trend/Regression Type analysis, should be used for optimal estimation of

sample values. If a computer program is not available, the data may be plotted using graph paper.

2. Choose the most diluted specimen that gives an OD450 orOD450/620 value within the standard curve and OD >0.100 or 0.060, respectively. If both sample dilutions have absorbance readings greater than the highest concentration of standard, repeat using additional 1:10 dilutions. Conversely, any sample having an absorbance reading less than the lowest concentration of standard should be retested using the 1:10 dilution and if found negative recorded as <1 μg/g wet weight.

3. Plot the average absorbance values of the *Standards* on the y-axis versus the concentration on the x-axis.

4. Perform the Linear Trend/Regression Type analysis and determine if the R^2 value is > 0.98.

5. Instruct the program to produce the equation for the plotted line. The equation should fit the equation of a line which is Y = MX + B, where Y = OD450 or

OD450/620 of the sample, M = Slope, B = Y-intercept and X = Concentration of the unknown sample.

6. Solve the equation for X to determine the concentration of lactoferrin in the specimen.

7. Multiply the value of the unknown sample by the dilution factor.

8. Divide by 1000 to convert ng/mL to μg/mL (approximately μg/g wet weight).

Appendix F: QLISA – 1st Generation Data / Results

This appendix includes data generated using the 1st generation QLISA system that was previously described. The data is presented in a format identical to the data for the 2nd Generation QLISA so comparisons can readily be made. The 1st generation QLISA showed promise in detecting quantities of myeloperoxidase and lactoferrin in quantities that were statistically similar ($P > 0.05$) for most of the human patient samples. One drawback is the relatively large standard deviations found when using QLISA, which could be a contributing factor to statistical similarities despite variation in mean. Regardless, were encouraged with these results yet strived to further improve, which we did with the 2nd generation QLISA system.

Another point to highlight is the differences in detected biomarker concentrations between even commercial ELISA assays. When reviewed we see significant differences within these commercially available products. The first generation QLISA was compared to ELISA kits from Invitrogen (myeloperoxidase) and IBD-SCAN (lactoferrin) while the second generation QLISA was compared to ELISA kits from Hycult Biotech (myeloperoxidase and lactoferrin). This was originally done because of ELISA kit availability

(Invitrogen and IBD-SCAN were months until shipping), but resulted in some interesting findings. All ELISA kits come from reputable commercial companies yet we found variation within these results. These findings perhaps substantiate or at least lend reason to why we see variations within even different immunoassays like 1st and 2nd generation QLISAs. Irrespective of these findings and conclusions we were able to improve the repeatability in the 2nd generation QLISA system.

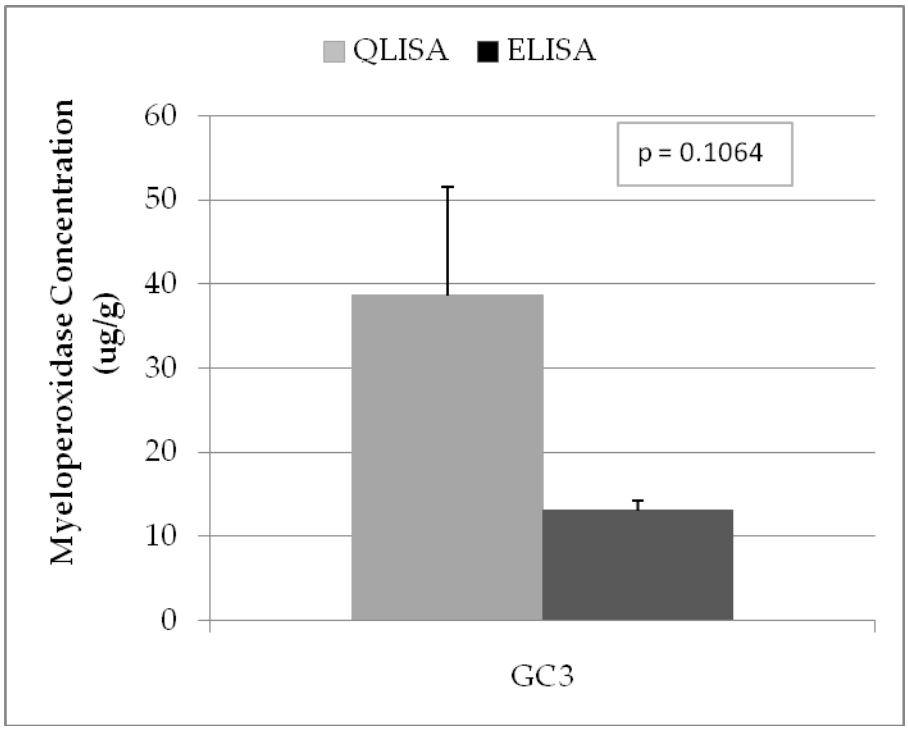

Figure 74: A comparison between myeloperoxidase levels detected in the stool sample from patient GC3 using QLISA and ELISA systems. P-values from a T-test are towards the upper right corner.

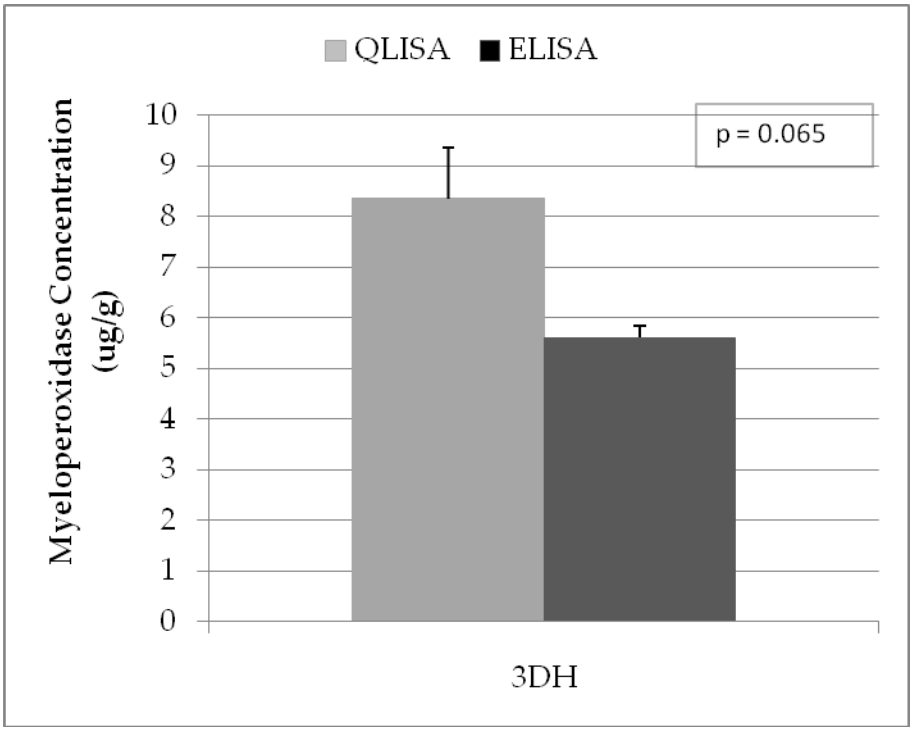

Figure 75: A comparison between myeloperoxidase levels detected in the stool sample from patient 3DH using QLISA and ELISA systems. P-values from a T-test are towards the upper right corner.

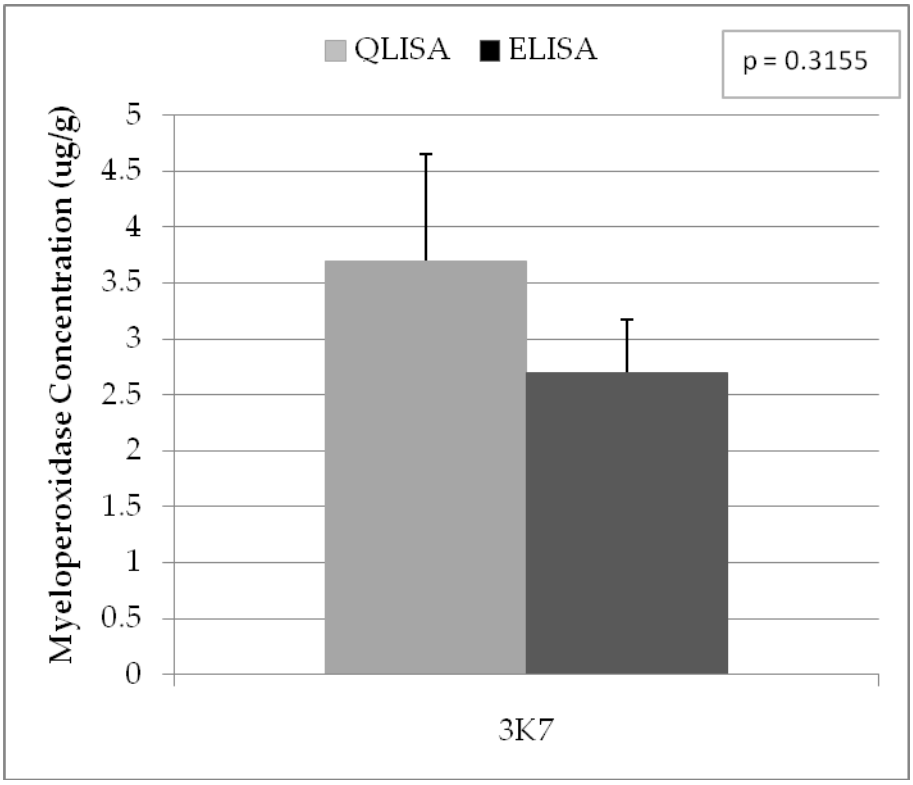

Figure 76: A comparison between myeloperoxidase levels detected in the stool sample from patient 3K7 using QLISA and ELISA systems. P-values from a T-test are towards the upper right corner.

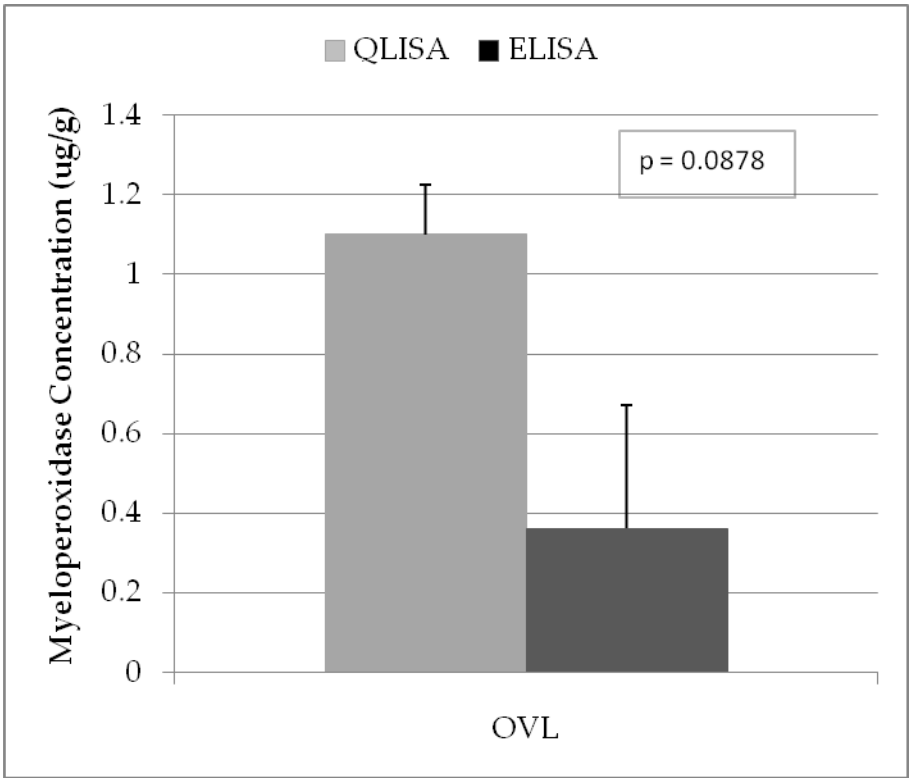

Figure 77: A comparison between myeloperoxidase levels detected in the stool sample from patient OVL using QLISA and ELISA systems. P-values from a T-test are towards the upper right corner.

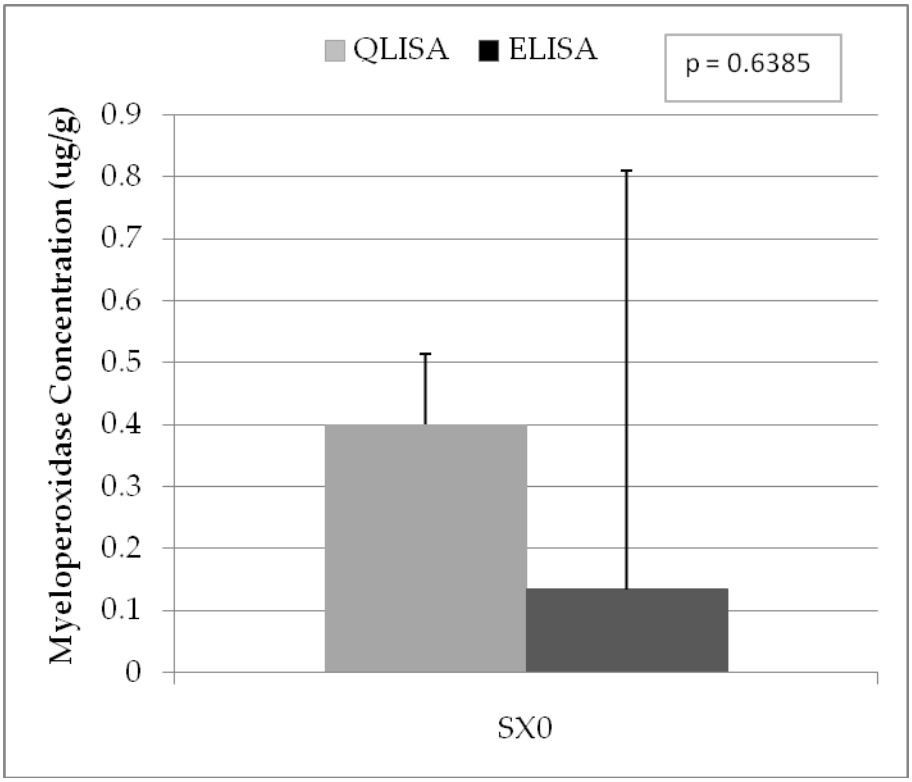

Figure 78: A comparison between myeloperoxidase levels detected in the stool sample from patient SX0 using QLISA and ELISA systems. P-values from a T-test are towards the upper right corner.

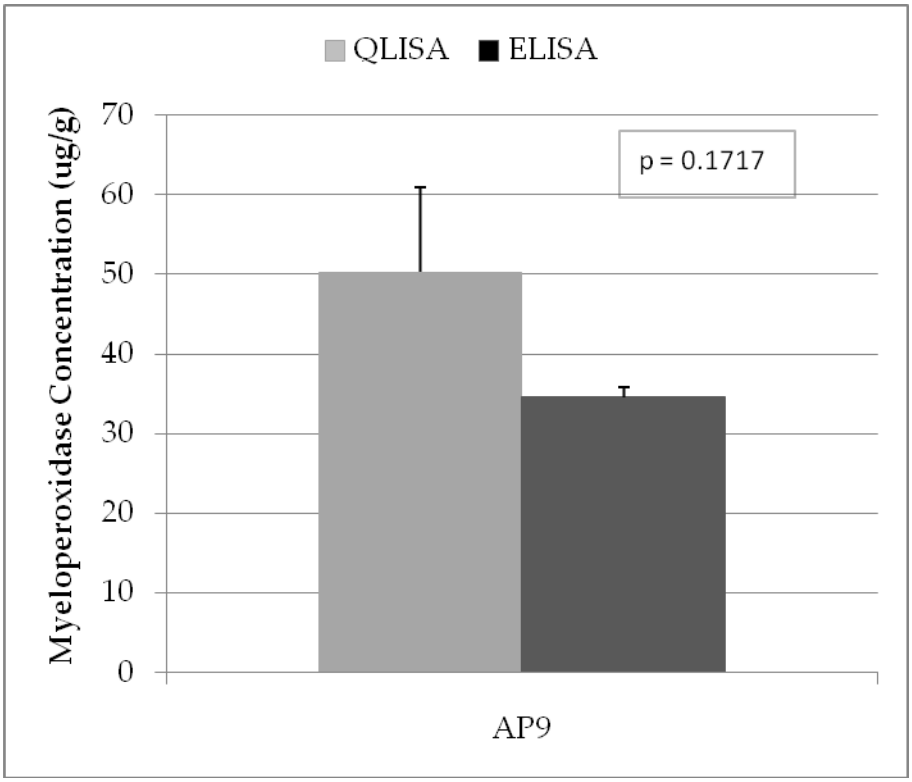

Figure 79: A comparison between myeloperoxidase levels detected in the stool sample from patient AP9 using QLISA and ELISA systems. P-values from a T-test are towards the upper right corner.

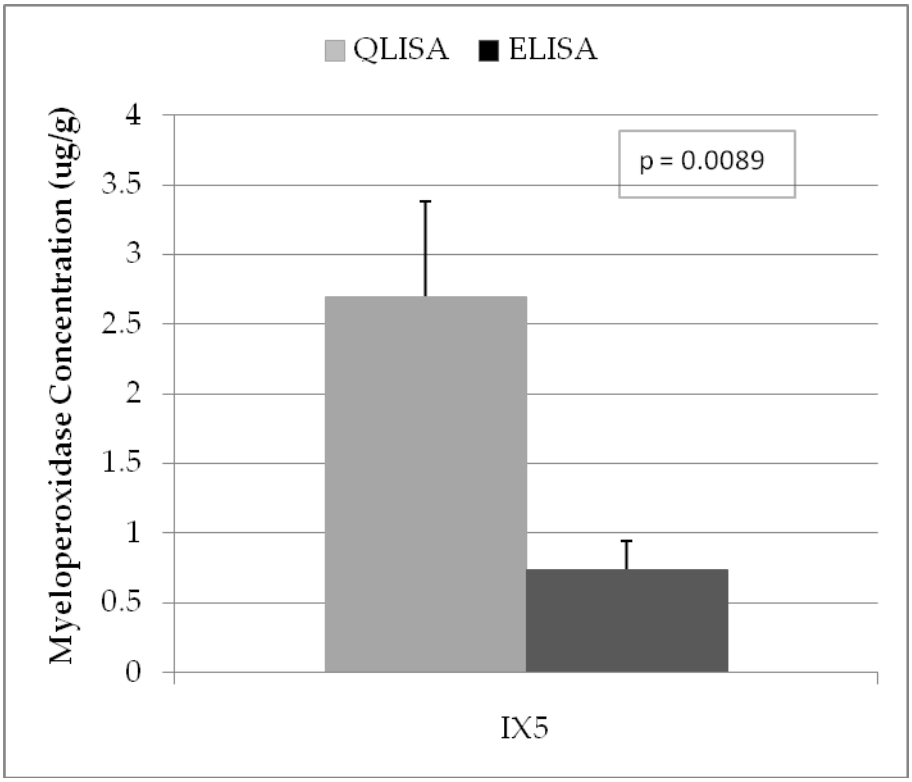

Figure 80: A comparison between myeloperoxidase levels detected in the stool sample from patient IX5 using QLISA and ELISA systems. P-values from a T-test are towards the upper right corner.

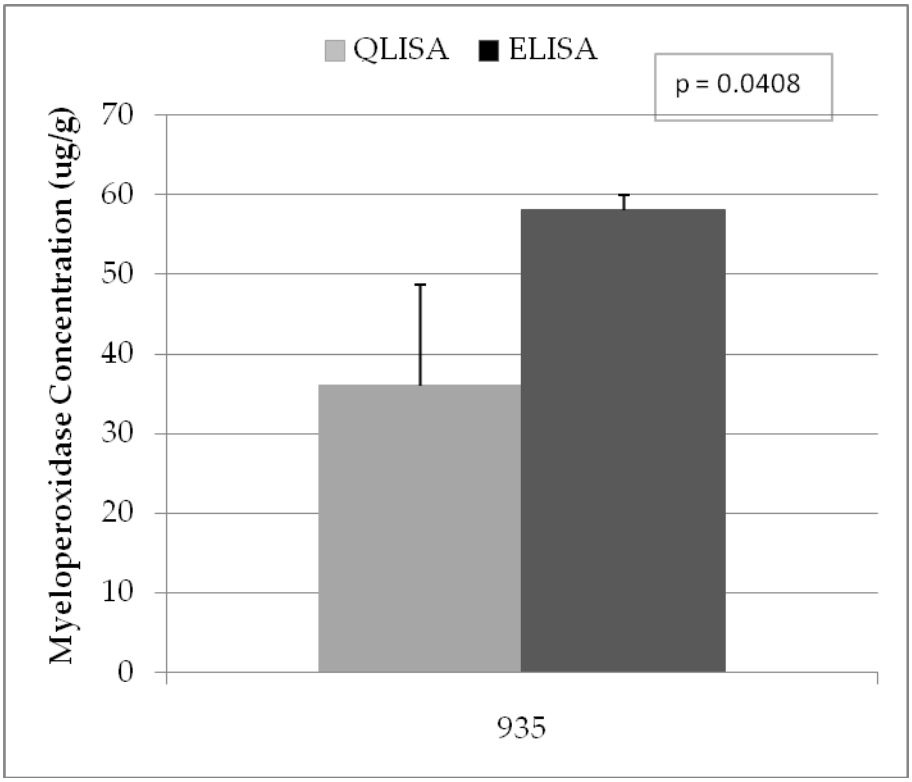

Figure 81: A comparison between myeloperoxidase levels detected in the stool sample from patient 935 using QLISA and ELISA systems. P-values from a T-test are towards the upper right corner.

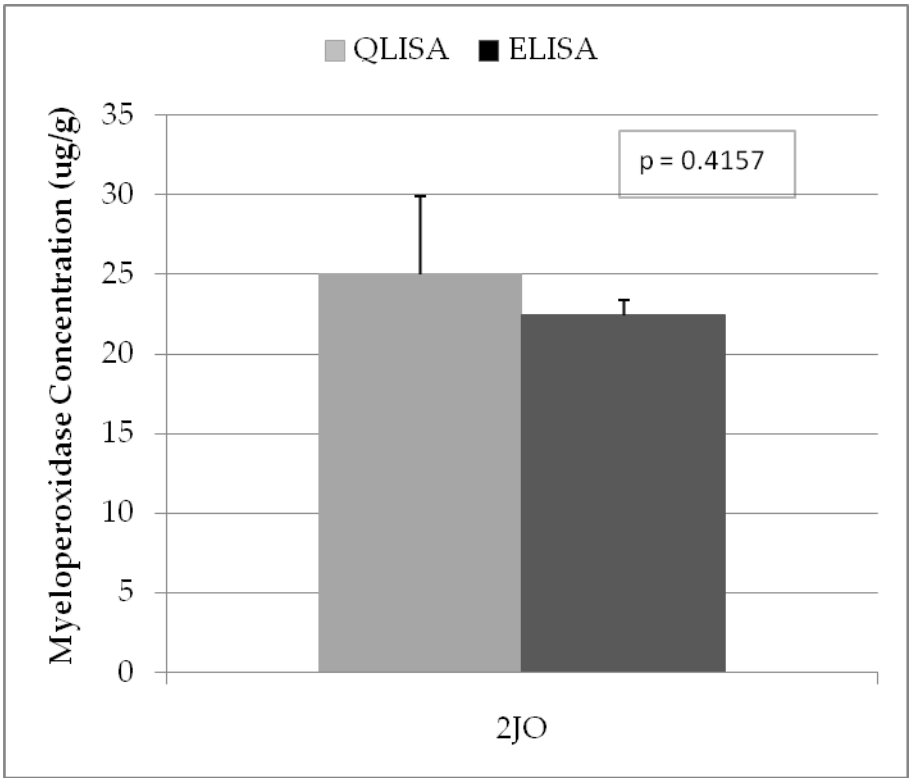

Figure 82: A comparison between myeloperoxidase levels detected in the stool sample from patient 2JO using QLISA and ELISA systems. P-values from a T-test are towards the upper right corner.

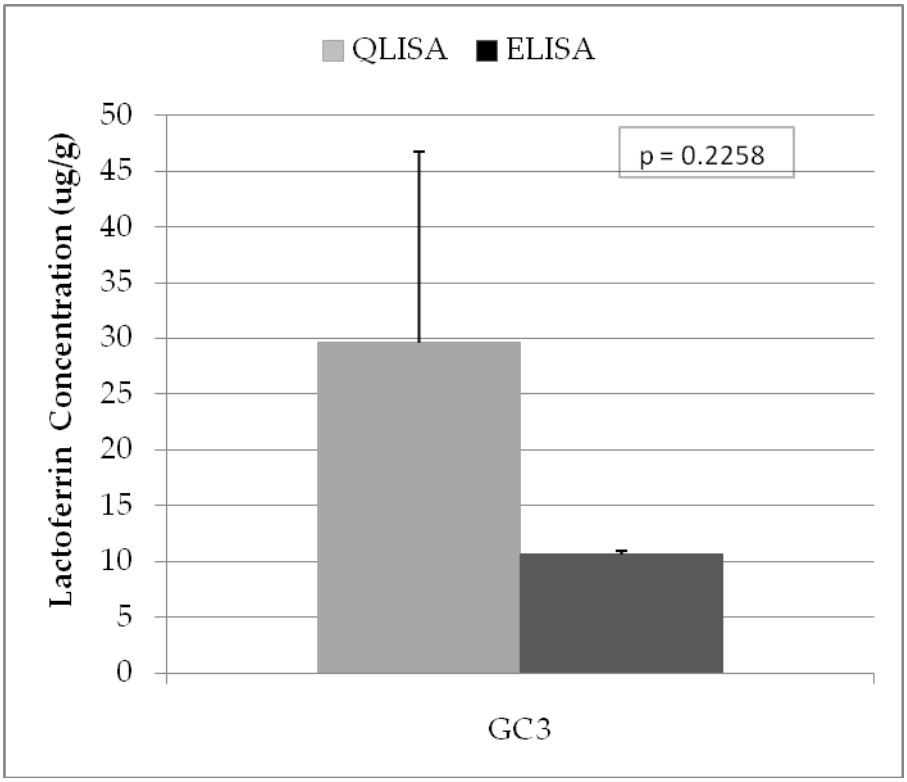

Figure 83: A comparison between lactoferrin levels detected in the stool sample from patient GC3 using QLISA and ELISA systems. P-values from a T-test are towards the upper right corner.

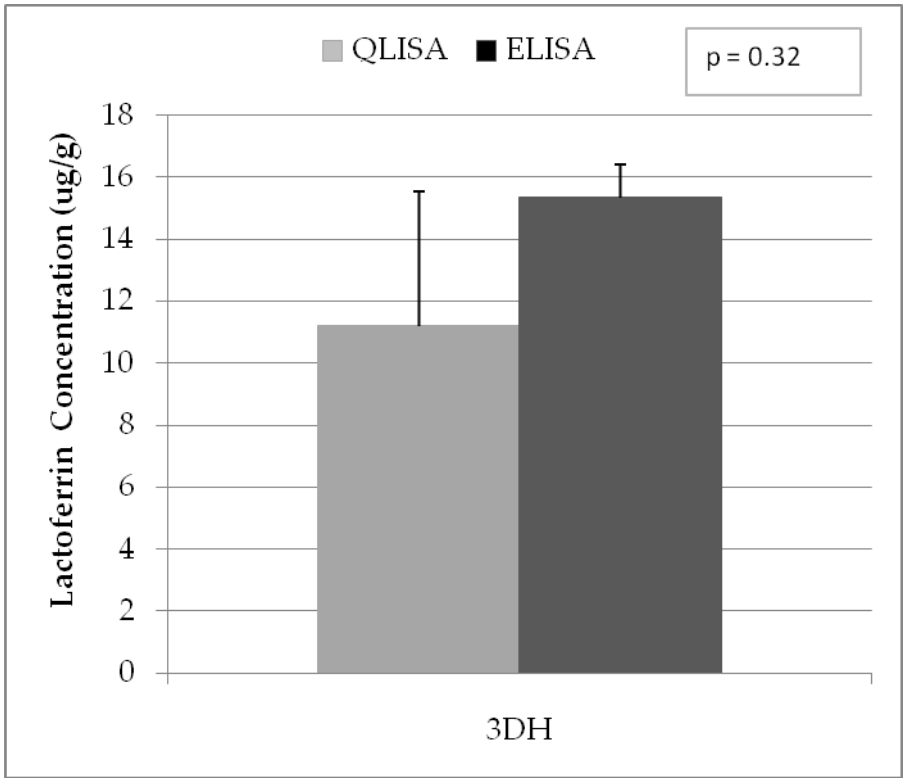

Figure 84: A comparison between lactoferrin levels detected in the stool sample from patient 3DH using QLISA and ELISA systems. P-values from a T-test are towards the upper right corner.

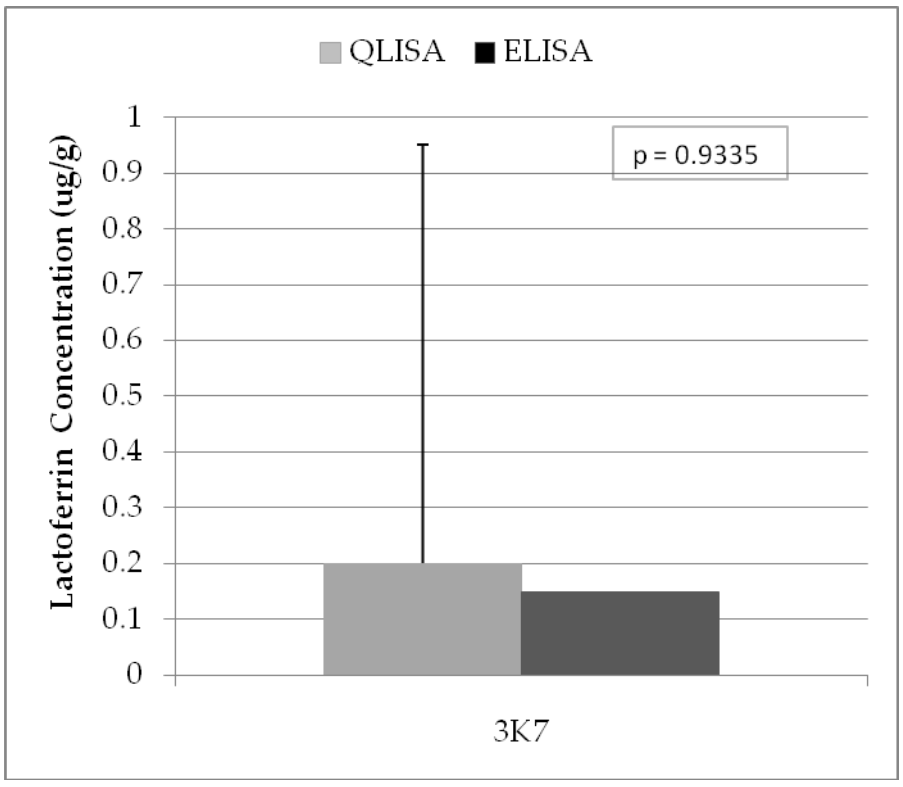

Figure 85: A comparison between lactoferrin levels detected in the stool sample from patient 3K7 using QLISA and ELISA systems. P-values from a T-test are towards the upper right corner.

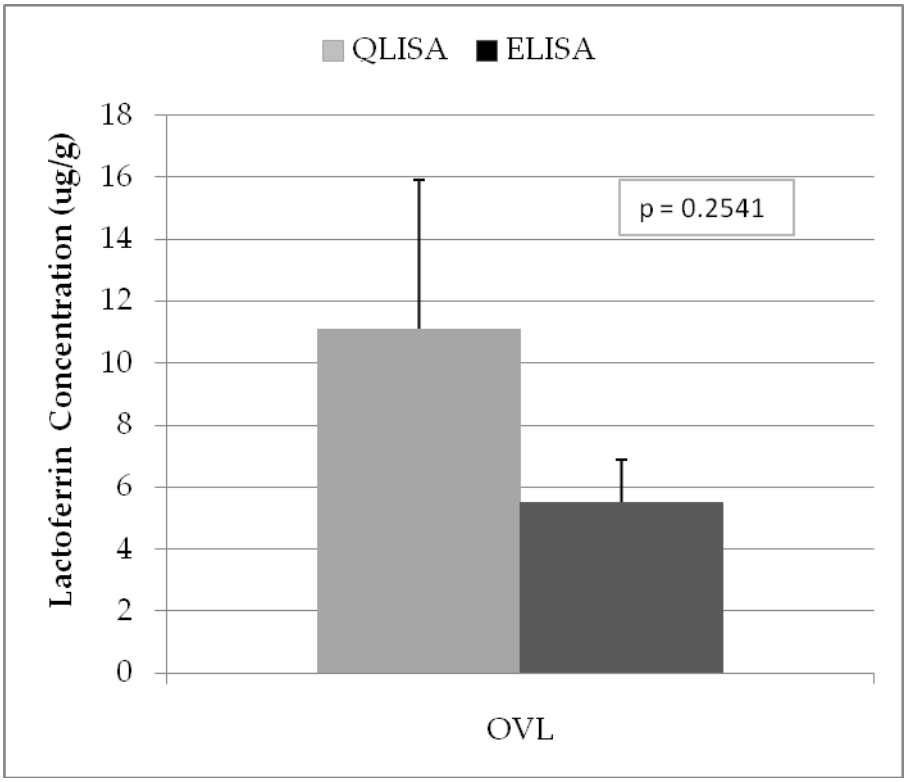

Figure 86: A comparison between lactoferrin levels detected in the stool sample from patient OVL using QLISA and ELISA systems. P-values from a T-test are towards the upper right corner.

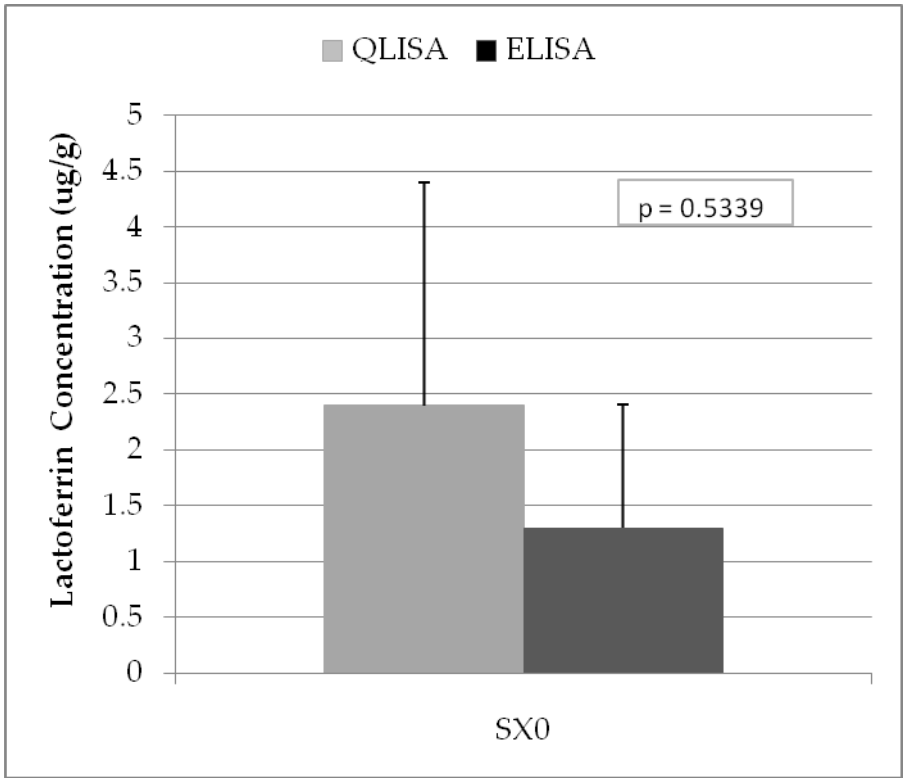

Figure 87: A comparison between lactoferrin levels detected in the stool sample from patient SX0 using QLISA and ELISA systems. P-values from a T-test are towards the upper right corner.

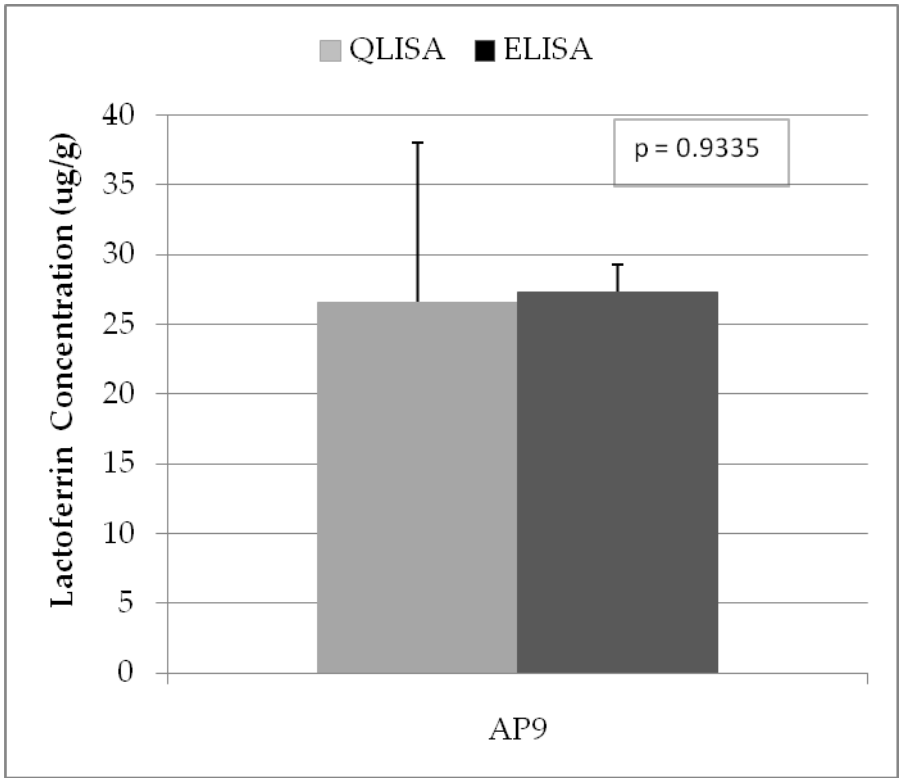

Figure 88: A comparison between lactoferrin levels detected in the stool sample from patient AP9 using QLISA and ELISA systems. P-values from a T-test are towards the upper right corner.

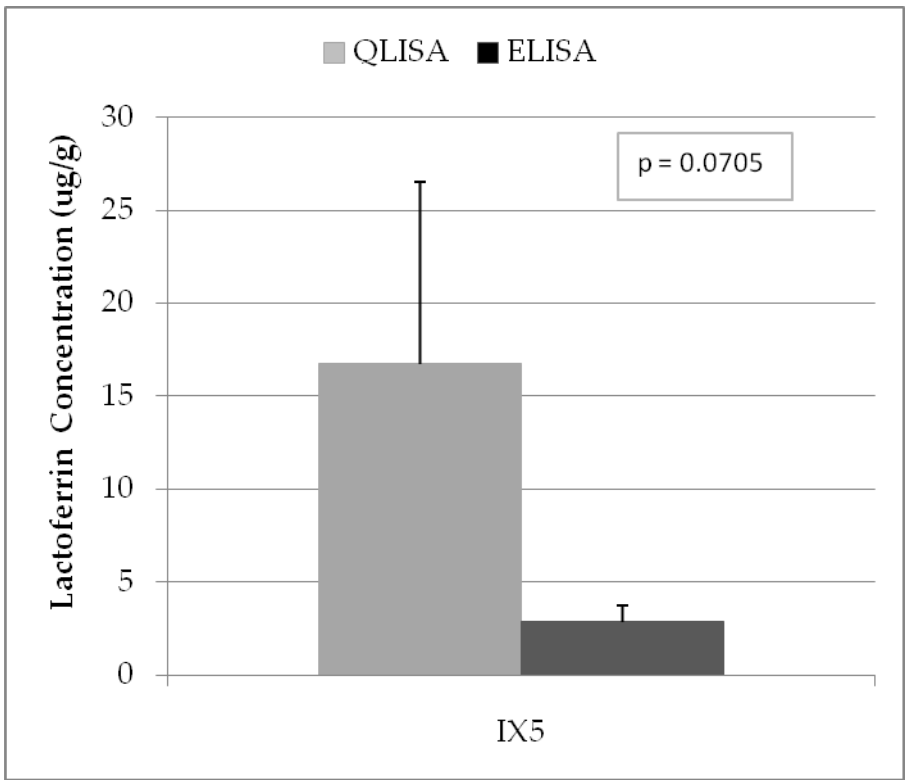

Figure 89: A comparison between lactoferrin levels detected in the stool sample from patient IX5 using QLISA and ELISA systems. P-values from a T-test are towards the upper right corner.

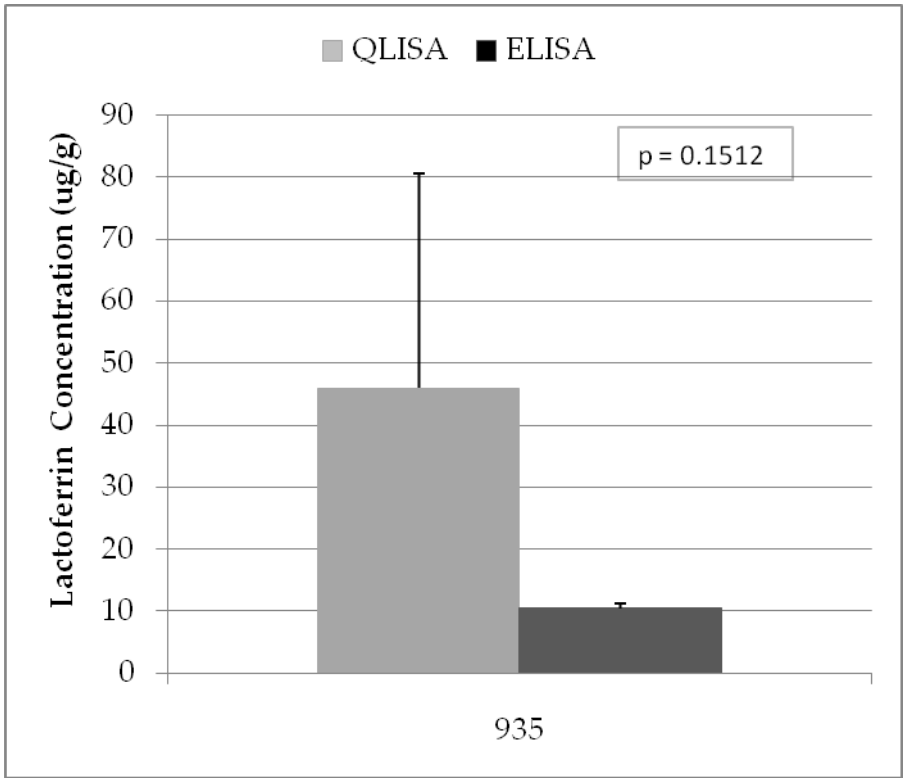

Figure 90: A comparison between lactoferrin levels detected in the stool sample from patient 935 using QLISA and ELISA systems. P-values from a T-test are towards the upper right corner.

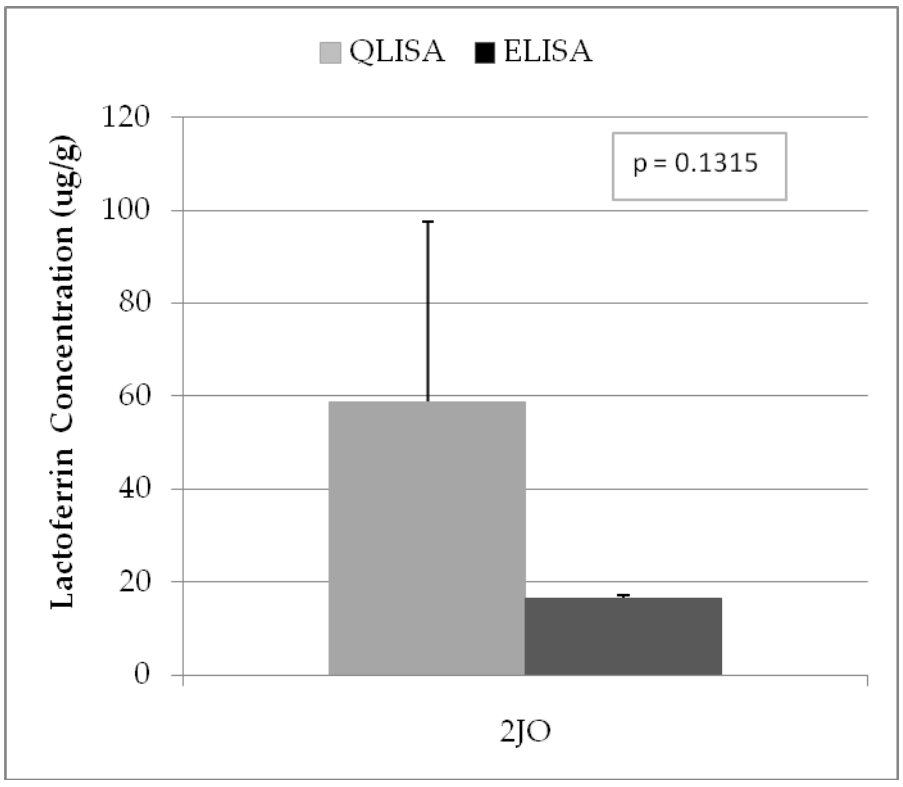

Figure 91: A comparison between lactoferrin levels detected in the stool sample from patient 2JO using QLISA and ELISA systems. P-values from a T-test are towards the upper right corner.

VITA

David Hansberry received his undergraduate degree in biomedical engineering and a minor in physical chemistry from Rutgers University's School of Engineering in New Brunswick, New Jersey. There he did research with Dr. John K-K Li of the Biomedical Engineering Department along with interventional cardiologists at Robert Wood Johnson's Medical School on left ventricular assist devices. Upon graduating in 2005 David entered a Masters program at Drexel University in the Biomedical Engineering Department where he worked with Drs. Ari Brooks and Zach Forbes of the Surgery Department at Drexel University's College of Medicine. Here his researched focused on localized magnetic drug delivery using coronary / vascular stents. This work paralleled his job in industry at Johnson and Johnson's Cordis Corporation. David worked for Dr. Greg Kopia, one of the co-founders and patent holders of the first drug-eluting stent, in a pre-clinical division over a four year period. He defended his Master's thesis in 2007, at which time he joined Dr. Elisabeth Papazoglou's bionanotechnology group as a Ph.D. student where David researched optical biosensors, polymer surface chemistry, bioconjugate techniques, and gastrointestinal disease. Upon defense of his Ph.D., David will return to medical school at the University of Medicine and Dentistry of New Jersey – New Jersey Medical School in Newark, New Jersey where he will graduate with a M.D. in 2014. While a student David has presented at various scientific conferences and published widely in engineering, clinical, and educational journals. He has also contributed to a book chapter and submitted a patent application.